UCRL-16175
c.2 upl.

University of California

Ernest O. Lawrence Radiation Laboratory

ELECTRON SPIN RESONANCE STUDIES
OF TRANSITION METAL ION COMPLEXES

John Brockett Spencer

August 1965

(Ph.D. Thesis)

TWO-WEEK LOAN COPY
This is a Library Circulating Copy
which may be borrowed for two weeks.

Berkeley, California

UCRL-16175 c.2
upl.

DISCLAIMER

This document was prepared as an account of work sponsored by the United States Government. While this document is believed to contain correct information, neither the United States Government nor any agency thereof, nor the Regents of the University of California, nor any of their employees, makes any warranty, express or implied, or assumes any legal responsibility for the accuracy, completeness, or usefulness of any information, apparatus, product, or process disclosed, or represents that its use would not infringe privately owned rights. Reference herein to any specific commercial product, process, or service by its trade name, trademark, manufacturer, or otherwise, does not necessarily constitute or imply its endorsement, recommendation, or favoring by the United States Government or any agency thereof, or the Regents of the University of California. The views and opinions of authors expressed herein do not necessarily state or reflect those of the United States Government or any agency thereof or the Regents of the University of California.

UCRL-16175

UNIVERSITY OF CALIFORNIA

Lawrence Radiation Laboratory
Berkeley, California

AEC Contract No. W-7405-eng-48

ELECTRON SPIN RESONANCE STUDIES OF TRANSITION METAL ION COMPLEXES

John Brockett Spencer

August 1965

(Ph.D. Thesis)

ELECTRON SPIN RESONANCE STUDIES OF TRANSITION METAL ION COMPLEXES

Contents

Abstract v

I. Introduction 1

II. Survey of Previous Work 5

A. $K_3Cr(CN)_5NO$ 5

B. $Cu(H_2O)_6^{+2}$ and $Cu(NH_3)_6^{+2}$ 7

C. $FeCl_4^-$ 10

D. $Cr(H_2O)_6^{+3}$, $CrCl(H_2O)_5^{+2}$ and $CrCl_2(H_2O)_4^+$ 12

III. Experimental Techniques 14

A. $K_3Cr(CN)_5NO$ 14

B. $Cu(H_2O)_6^{+2}$ and $Cu(NH_3)_6^{+2}$ 19

C. $FeCl_4^-$ 23

D. $Cr(H_2O)_6^{+3}$, $CrCl(H_2O)_5^{+2}$ and $CrCl_2(H_2O)_4^+$ 24

IV. Results and Discussion 26

A. $K_3Cr(CN)_5NO$ 26

B. $Cu(H_2O)_6^{2}$ and $Cu(NH_3)_6^{2}$ 60

C. $FeCl_4^-$ 96

D. $Cr(H_2O)_6^{3}$, $CrCl(H_2O)_5^{2}$ and $CrCl_2(H_2O)_4$ 108

Acknowledgements 115

References 116

Line widths for cupric ion in water were measured from -40° to +200°C and in liquid ammonia from -80° to +20°C. The line widths were corrected for unresolved hyperfine structure. Two contributions to the line width were distinguished. One contribution increases with increasing temperature and is the same for all four hyperfine components. The second increases with decreasing temperature and varies with the hyperfine component. A transition region was observed for cupric ion in ammonia between -80° and -100°C. In this region the sample was frozen but an isotropic spectrum was obtained. These results are discussed with regard to several theories of electron spin relaxation.

Glass spectra for ferric chloride in concentrated HCl and concentrated $HClO_4$ have been examined. A sharp resonance at g = 4.24 was observed and assigned to the species $FeCl_4^-$. The theory for high g-value resonances in ferric complexes is reviewed and applied to $FeCl_4^-$.

Glass spectra for the chromic complexes $CrCl(H_2O)_5^{+2}$, cis- and trans-$CrCl_2(H_2O)_4^+$ were examined and compared with the spectrum for $Cr(H_2O)_6^{+3}$. The spectra for the chloro complexes extend from g = 6 to g = 2. The results are discussed in terms of zero field energies and symmetries of the complexes.

I. INTRODUCTION

The field of Electron Spin Resonance (ESR) of transition metal ions has shown considerable development. During the past 15 years a large body of information has been collected for transition metal ions in single crystals.[1,2,3] More recently, there has been a growing interest in the solution spectra of complexes of these ions. Several books have appeared in the last few years dealing with single crystal studies[4] and paramagnetic resonance in general.[5,6,7] The advances in ligand field theory have paralleled those in ESR, which is expected since the two fields are so closely interrelated.[8,9]

It is customary to discuss paramagnetic resonance for transition metal ions in terms of a spin Hamiltonian.[10] The usual form of the spin Hamiltonian for iron group metal ions is

$$\mathcal{H} = g\beta\overline{H}\cdot\overline{S} + D[S_z^2 - 1/3S(S+1)] + E(S_x^2 - S_y^2) + A\overline{I}\cdot\overline{S}$$

where $\overline{S}$, S_x, S_y, and S_z are electron spin operators, $\overline{I}$ is the nuclear spin operator, $\overline{H}$ is the external magnetic field, g is the spectroscopic splitting factor and is a second rank tensor, A is the hyperfine coupling constant and is also a second rank tensor, β is the Bohr magneton, and D and E are scalars derived from the three principal values of the spin-spin interaction tensor. Interactions of higher order in the spin variables have been omitted since they are unimportant for the studies considered in this thesis.

In the most general case, the g- and A-tensors will have three principal values. When the ligand field is axial, the number of independent components is reduced and the spin Hamiltonian takes the particularly convenient form

$$\mathcal{H} = g_{\parallel}\beta H_z S_z + g_{\perp}\beta(H_x S_x + H_y S_y) + D[S_z^2 - 1/3S(S+1)]$$

$$+ E(S_x^2 - S_y^2) + A_{\parallel} I_z S_z + A_{\perp}(I_x S_x + I_y S_y).$$

It should be emphasized that the axis system for the three interactions may not be the same. When one term is particularly large, it may be possible to treat the other terms as perturbations. In less favorable situations, it may be necessary to diagonalize the entire Hamiltonian.

This Hamiltonian has symmetry properties which are useful for the consideration of various complexes. For cubic symmetry, all three crystal axes are equivalent and the spin Hamiltonian reduces to

$$\mathcal{H} = g\beta H_z S_z + A\bar{I}\cdot\bar{S}$$

where g and A are isotropic and the z-axis is defined by the direction of the external magnetic field. For certain symmetries of the ligand field the x and y axes will be equivalent and the value for E will be exactly zero. When S = 1/2, D and E (which give rise to the so called "zero field splitting") both vanish.

In a solution with sufficiently rapid rotation of the complex, one sees only the average values of the spin Hamiltonian components. Thus, one has an effective spin Hamiltonian like that for cubic symmetry, but its g and A values are averages of the principal values for the non-rotating complex

$$A = \frac{A_{\parallel} + 2A_{\perp}}{3} \qquad g = \frac{g_{\parallel} + 2g_{\perp}}{3}$$

while the zero field terms average a zero. Incomplete rotational averaging is one source of line width for complex ions in solution and will depend on the magnitude of the magnetic anisotropies to be averaged, the frequency of rotation of the complex and the Larmor

precision frequency for the electron spin.

There is a second type of averaging that can occur, but it is a spatial rather than a temporal average. Such an average is observed for polycrystalline or glass samples or for solutions with high viscosity. In this case one observes resonances simultaneously from complexes with all possible relative orientations of the magnetic field and the ligand field axis. Such spatially averaged spectra can give detailed g and A value information in favorable conditions, especially for ions with $S = 1/2$. For spins greater than 1/2, there is still information about the zero field terms and the symmetry of the complex which can be obtained.

For an ion with $S = 1/2$ in an axial field, the resonance condition and its angular dependence can be expressed by

$$h\nu = g\beta H + AM_I$$

where

$$g = (g_{\parallel}^2\cos^2\theta + g_{\perp}^2\sin^2\theta)^{1/2}$$

$$A = (A_{\parallel}^2 g_{\parallel}^2\cos^2\theta + A_{\perp}^2 g_{\perp}^2\sin^2\theta)^{1/2}/g \ .$$

The angle between the ligand field axis and the magnetic field is θ, the resonance frequency is ν, and M_I is the nuclear spin quantum number. For a sample with randomly oriented complex ions, the number of complexes having a value of θ between θ and $d\theta$ will be proportional to $\sin\theta d\theta$.[11] One can then introduce a shape function for the resonance of a single ion. Most simply, this is taken to be a delta function, but other shape functions may be used. The result is the intensity of the resonance absorption as a function of the magnetic field and the angle θ.

The explicit evaluation of the total intensity as a function of magnetic field is usually carried out numerically with the aid of a

computer.[12,13] There are two extremes for the spectrum. One is for $\cos\theta = 1$ which corresponds to an abrupt onset of absorption and is termed the parallel spectrum since it occurs for those complexes with the magnetic field and ligand field axis parallel. As $\cos\theta$ approaches zero, the intensity becomes large (infinite for a delta function) and then drops rapidly to zero at $\cos\theta = 0$. This comprises the perpendicular spectrum. In addition, it is found that there may be intermediate values of $\cos\theta$ for which the intensity is also large. Approximate expressions for the position of such "extra" absorptions have been derived.[12,13] Hyperfine interactions with the ligand nuclei may be included in this treatment and have been resolved in some cases.

For spins greater than 1/2, most of the interest in randomly oriented samples has been directed toward organic triplet state molecules and their spectra. Line shape analysis in these systems is well advanced.[14] In principle, the theory could be applied to transition metal ions with $S = 1$ with a few modifications. Such ions are known to have short spin lattice relaxation times so that their spectra could be observed only at very low temperatures.

Only a limited amount of work has been done on randomly oriented species with spins greater than 1. Examples of two different spin states, $S = 3/2$ and 5/2, will be considered later in this paper.

The studies discussed in this thesis were directed toward developing and applying ESR techniques appropriate for identifying transition metal ion complexes in solution and in glasses, and to elucidate some aspects of their structure, bonding, reactions, and interactions with the solvent.

II. SURVEY OF PREVIOUS WORK

A. $K_3Cr(CN)_5NO$

The synthesis of the compound $K_3Cr(CN)_5NO$ was first reported by Griffith, Lewis and Wilkinson in 1959.[15] They measured the magnetic susceptibility of the compound and found it to be consistent with a single unpaired electron. On the basis of the susceptibility, the infra red spectrum and the properties of other similar compounds they characterized the complex as containing Cr^+ (spin-paired $3d^5$ electronic configuration) and NO^+.

The optical and ESR spectra of this complex ion in aqueous solution were first assigned by Bernal and Harrison.[16] They found that the complex had narrow ESR lines in solution (1-2 gauss wide) and assigned the observed hyperfine splittings to interaction of the unpaired electron with the N^{14} nucleus in the NO^+ group and with Cr^{53}. A ligand field bonding scheme and an assignment of the optical transitions were also proposed by them. Several more recent papers[17,18] have offered different interpretations of the optical spectrum.

Hayes[19] also investigated the ESR spectrum of the complex. He corrected Bernal and Harrison's[16] value for the Cr^{53} hyperfine coupling constant and re-assigned one set of lines in the spectrum to hyperfine interaction with C^{13} in the cyanide ligands. Hayes also considered the ESR line width and its temperature dependence in some detail.

The C^{13} assignment was discussed further in two Comments published simultaneously in the Journal of Chemical Physics.[20,21] These two communications were largely concerned with the fact that only a single hyperfine coupling constant was observed for C^{13} although one would expect the interaction of the unpaired electron with the axial and the four equatorial cyanides to be different. They established that the

four equatorial cyanides were responsible for the observed C^{13} splitting. The question remained whether the axial coupling constant was significantly smaller. Bernal and Harrison[16,21] stressed the strength of the Cr-N bond and the consequent weakening of the axial Cr-C bond in comparison with the equatorial Cr-C bonds. For this reason they expected the axial cyanide to exchange more rapidly than the equatorial cyanides. They could not, however, detect any cyanide exchange between the complex and $C^{13}N^-$ in solution over a period of 41 hours at room temperature.

The work on this compound to be considered in this thesis was directed toward resolving the questions of the axial C^{13} hyperfine coupling constant and the relative rates of ligand exchange at the axial and equatorial positions. One approach was to synthesize directly a sample of the complex enriched with $C^{13}N^-$. A second method was to enrich the complex through exchange with $C^{13}N^-$ in solution. The method of exchange has been used previously by Weissman and Cohn[22] in assigning the ESR spectrum of the complex $Mo(CN)_8^{-3}$ in solution. The rates of cyanide exchange for other transition metal cyanide complexes have been studied using radioactive tracer techniques.[23,24,25] Thus, it was also of interest to test the usefulness of ESR for studying the kinetics of such isotropic ligand exchange reactions.

It has been found that the rate of axial exchange in $Cr(CN)_5NO^{-3}$ is accelerated in some non-aqueous solvents.[26] This method for preparing the axially substituted $C^{13}N^-$ complex in N,N-dimethylformamide (DMF) solution was used by us. Our results in DMF solution include values for the isotropic hyperfine coupling constants.

A variation of line width among the Cr^{53} hyperfine components in solution not treated by Hayes[19] was considered in the present work. Anisotropic hyperfine information was obtained from ESR spectra of the

complex in frozen glasses at liquid nitrogen temperature and was used to interpret the variation in line width.

The results of our exchange studies and isotropic hyperfine assignment have been reported briefly in the literature.[27] An independent determination of the axial C^{13} coupling constant has been reported[28] and is in essential agreement with our value.

B. $Cu(H_2O)_6^{+2}$ and $Cu(NH_3)_6^{+2}$

Cupric ion has a $3d^9$ (^2D) electronic configuration. In an octahedral ligand field the ^2D level is split to give a ^2E_g ground state and a $^2T_{2g}$ excited state. One would expect such an orbitally degenerate ground state to be further distorted in compliance with the Jahn-Teller theorem. In fact, most six-coordinated cupric complexes are found to be tetragonally distorted so that they have effective D_{4h} symmetry. The axial bonds may be shorter than those lying in the equatorial plane as is found in $KCuF_3$ and K_2CuF_4. The more usual configuration is that of an elongated octahedron in which there are four equatorial ligands in a square planar arrangement with the two axial ligands at a greater distance. In the limit of very long axial bonds the structure goes over to square planar. For the elongated octahedron the ground electronic state is expected to be the $^2A_{1g}$ state. An excellent survey of the theory and experimental results for cupric complexes is given in Ballhausen's book.[9]

The theory for paramagnetic resonance in such complexes has been given by Abragam and Pryce[29,30] and others.[31,32] A comprehensive listing of results from crystal studies is available in the references given earlier.[2,3,4] The results of such studies and associated optical spectra are generally in satisfactory agreement with the theory if a

value for the spin-orbit coupling parameter, λ, is used which is considerably reduced in magnitude from the value of -828 cm^{-1} for the free Cu^{+2} ion. This apparent reduction in spin orbit coupling was attributed to significant covalent bounding with the ligands.[33,34,35] Maki and McGarvey[35] and Kivelson and Neiman[12] have developed relationships between the ligand field parameters and the Zeeman, Cu-ion hyperfine and ligand hyperfine values obtained from paramagnetic resonance experiments.

The optical spectrum of cupric ion in aqueous solution has been reported by Bjerrum, Ballhausen and Jorgensen.[36] It consists of a single unsymmetrical band which can be resolved into at least two transitions between 9000 cm^{-1} and 13,000 cm^{-1} with the possibility of a third transition[37] abound 14,000 cm^{-1}. As the water ligands were replaced successively with ammonia,[36] the transitions shifted to higher energy. Thus, for cupric ion in liquid ammonia, the transitions were shifted to higher energy by 4,000 cm^{-1} while maintaining the ratio of energies for the transitions. These spectra were interpreted as being consistent with the existence of elongated octahedral complexes in solution, as found in crystals, with the nitrogen ligands giving rise to a stronger ligand field than the oxygen ligands.

Kozyrev[38] studied the paramagnetic resonance of aqueous cupric solutions under varying conditions of concentration and microwave frequency, but could detect neither hyperfine structure nor changes in line width. He did observe an increase in line width as the temperature of the solution was increased from room temperature to 100 °C. Various interpretations of the line width and its temperature dependence have been put forward. Al'tshuler and Valiev[39] proposed that vibrational

modulation of the ligand field was responsible for relaxation of the electron spin. Hayes[19] has discussed this mechanism in detail. Its primary usefulness has been for complexes with small magnetic anisotropies which are effectively averaged out by tumbling of the complex in solution. Since there are three axes for such a complex which can serve as the elongated symmetry axis, it is possible that there is a rapid "inversion" of the complex which leads to a reorientation of the symmetry axis. Avvakumov[40] explicitly treated the dynamic character of this structural inversion process and applied his theory to the variation of line width for cupric ion in solution from 30-130 °C.[41] Hayes[19] was able to observe some hyperfine structure for $Cu(H_2O)_6^{+2}$ in solution by lowering the temperature. From this he concluded that the line width previously reported[38,40] did not represent the relaxation time for the complex and should be corrected for unresolved hyperfine structure contributions. His partially resolved spectrum also showed a definite variation of the line width among the hyperfine components.

All the discussions of electron spin relaxation for $Cu(H_2O)_6^{+2}$ in solution mentioned above have assumed that the chemical lifetime of the complex ion is long in comparison with the rate of electron spin relaxation. Recent studies of the rate of exchange of H_2O^{17} with cupric ions in solution indicate that the rate of ligand exchange is comparable to the rate of electron spin relaxation.[42]

In the work reported here, we have obtained values for the isotropic and anisotropic terms in the spin Hamiltonian for $Cu(H_2O)_6^{+2}$. Using this information we have been able to correct the observed paramagnetic resonance line width in solution for the unresolved hyperfine structure and obtain values for the relaxation time, T_2, as a function of temperature. Knowing this information, one can then

estimate possible contributions to the relaxation from several of the mechanisms mentioned above. The studies of $Cu(NH_3)_6^{+2}$ in liquid ammonia were undertaken for comparison with the aqueous system because the character of the complex should be similar. Liquid ammonia is a convenient solvent for such studies since it is less viscous than water and has a much lower freezing point.

C. $FeCl_4^-$

The characterization and stability of chloro complexes of ferric ion, particularly the higher complexes, have been of continuing interest. In order to avoid complications from hydroxide formation, most of the more recent studies have been carried out in solutions with moderate to high concentrations of acid. Rabinowitch and Stockmayer[43] suggested the existence of a tetrachloroferrate species of some sort on the basis of their studies of the chloride and hydroxide equilibria. In a series of papers Myers, Metzler and Swift[44] investigated the distribution of ferric ion between hydrochloric acid and isopropyl ether. They found that the tetrachloroferrate ion, $FeCl_4^-$, was the predominant species in concentrated HCl and also extracted it into the ether phase. Friedman[45] prepared compounds of the type $KFeCl_4$ and found that their optical spectra were the same as that reported for $FeCl_4^-$.[44] From these and other spectral studies[46] and solution x-ray work,[47,48] it has been generally concluded that the highest chloro complex and predominant species in dilute solutions of ferric ion in concentrated HCl is $FeCl_4^-$. There is also evidence for stabilization of the chloro complexes in perchlorate solutions.[49,50] For example, the stability constant for the monochloro complex increases by a factor of several thousand upon going from 2 F to 8.5 F $HClO_4$.[49] This effect has been attributed to the lowering of the water

activity and possible dehydration of ferric ion and chloride ion in solution.[49] There is also some evidence for the formation of perchlorate complexes of ferric ion in perchloric acid media,[51] but the stability of the corresponding chloride complexes is taken to be much greater.[49,50]

Several salts of the tetrahaloferrate ion have been isolated. Zaslow and Rundle[52] have determined the crystal structure of tetraphenylarsonium tetrachloroferrate (III). They found that the $FeCl_4^-$ unit was a flattened tetrahedron with an Fe-Cl bond distance of 2.19 ± 0.03Å and two Cl-Fe-Cl bond angles, 114.5° and 107.0°. The structure of $NaFeCl_4$ has also been determined[102] and is also found to contain distorted $FeCl_4^-$ tetrahedra. The Fe-Cl bond lengths were found to be 2.18Å for two bonds and 2.20Å and 2.22Å for the other two. The Cl-Fe-Cl bond angles range from 104.9° to 112.7°. The tetraethylammonium salts of $FeCl_4^-$ and $FeBr_4^-$ have been prepared.[53] The magnetic susceptibility, optical and Mossbauer spectra[54] of $(C_2H_5)_4NFeCl_4$, $(CH_3)_4NFeCl_4$, $(PyH)_3Fe_2Cl_9$ and $(PyH)_3Fe_2Br_9$, where Py = pyridine, have all been interpreted in terms of discrete $FeCl_4^-$ or $FeBr_4^-$ tetrahedra. The infra red spectra of such complexes[55] are consistent with the tetrahedral structure. Raman spectra[103] of ether extracts containing $FeCl_4^-$ have indicated that the structure of the complex in such solvents is tetrahedral. Solution ESR spectra for $FeCl_3$ dissolved in non-aqueous solvents[104] have been interpreted in terms of equilibria which give $FeCl_4^-$. In fact, it is only under special circumstances and with difficulty that the higher chloro complexes of ferric ion can be formed.[56]

Much of the paramagnetic resonance work on ferric ion in single crystals has been for ferric coordinated with six oxygens in an approximately octahedral arrangement. This includes environments where

there are six coordinated water molecules,[57,58,59] octahedral oxide sites,[60,61] or chelate oxygens.[62] In all these cases the g values are found to be isotropic and quite close to that of the free electron. The zero field splittings are often fairly large, on the order of 0.2 cm^{-1}.

Of particular interest for us has been the spectrum of ferric ion in polycrystals or glasses. The resonance of hemoglobin[63] in a paste consists of a single peak at g = 6. This was explained[64] in terms of zero field splittings larger than the microwave quantum used for the experiment and was confirmed by single crystal measurement.[63] Slichter et al.[65] observed resonances for ferric ion in glass at g = 6 and g = 4.27. They showed how both of these situations could arise for various relationships between the zero field parameters D and E when these terms were much greater than the interaction with the magnetic field. Wickman and Shirley[66,67] have generalized the treatment by Slichter[65] and applied it to the ferric ion in ferrichrome A. Griffith[68] has given a theoretical discussion of the source of this isotropic resonance at g = 4.27 and has indicated some of the ligand field symmetries under which it may occur.

The present study is directed toward the use of paramagnetic resonance glass spectra for obtaining information about species present in solution. The presence or absence of resonances at g = 2, 4.27 and 6 in the glass spectrum has definite implications for the ferric complexes present in the solution from which the glass was made.

D. $\underline{Cr(H_2O)_6^{+3}}$, $\underline{CrCl(H_2O)_5^{+2}}$ and $\underline{CrCl_2(H_2O)_4^{+}}$

The stability of chromic complexes in solution makes them particularly useful for chemical studies in which a well defined complex is desired.

Thus, hydrated chromic ion has been used for studies of second coordination sphere effects in H_2O^{17} NMR exchange work[69] and chromic complexes have been used to investigate the mechanisms of oxidation-reduction reactions in solution.[70] The chemistry of the chromic chloride complexes has been worked out[71,72,73,74] with the dichloro and monochloro complexes being the major species in most aqueous solutions.

The theory for the paramagnetic resonance of chromic ion ($3d^3$ with $S = 3/2$) has been fully worked out and is presented in several places[4,9,75] along with experimental results for the ion in a variety of environments. The g values observed are isotropic and slightly lower than that of the free electron. The zero field splittings for this ion range from quite small for sites of nearly cubic symmetry to quite large under some conditions of symmetry and bonding. Hyperfine from the 9.54% abundant Cr^{53} ($I = 3/2$) isotope has been observed in some instances where the line width is not too great. Several authors[76,77] have measured the ESR line width of the hydrated chromic ion and the dichloro complex in solution. The greater line width for the dichloro complex has been attributed to its presumably greater zero field splitting.

The present experiments with chromic complexes were undertaken to study the use of glass spectra in characterizing complex ions with spins greater than 1/2, but for complexes with a definite chemical structure. It was hoped that the monochloro and two possible dichloro complexes might be distinguished and compared with the hexaaquo complex.

III. EXPERIMENTAL TECHNIQUES

A. $K_3Cr(CN)_5NO$

The original method of synthesis of the complex[15] was followed using reagent grade chemicals throughout. The product was recrystallized several times from H_2O-EtOH, dried at 80°C in a vacuum oven, pulverized, then dried again for several days. This final product was assumed to be anhydrous. A direct synthesis of the C^{13} enriched complex was carried out using the same procedure scaled down to 0.5 millimoles of the labeled $NaC^{13}N$. The product was recrystallized once from H_2O-EtOH, dried, then dissolved in enough water to give a solution approximately 0.01 F in complex.

A sample of NaCN enriched to approximately 50% C^{13} was purchased from Merck, Sharp and Dohme of Canada. In order to determine the isotropic composition more accurately, a mass spectrographic analysis of the sample was made. Two depressions were made in a section of Pyrex tube which could be attached both to a gas sample bulb for the mass spectrograph and a vacuum system. Several drops of solution 0.2 F in the labeled NaCN were placed in one depression and phosphoric acid in the other. This was then attached to the vacuum system in order to evaporate the solution and de-gas the phosphoric acid. After the evacuation was completed the system was closed off, tilted to mix the acid and cyanide by rotating a ball and socket joint, and then HCN gas collected in the samble bulb. The mass spectral analysis of this gas sample* gave a value of 55.0% C^{13} (+0.2%, -1%). The value of 55% C^{13} has been used in our experiments.

---

* The author wishes to thank Professor B. H. Mahan for the use of his mass spectrograph.

A stock solution of the complex was prepared from a known weight of $K_3Cr(CN)_5NO$ and a stock solution of the NaCN in the same way. Fresh solutions were prepared for subsequent work in order to avoid possible complications from deterioration of the samples over periods of more than a week. Appropriate proportions of the solutions were mixed to obtain samples approximately 0.015 to 0.035 F in complex and 0.1 to 0.2 F in labeled NaCN. For the experiments to determine the effect of added acid, sufficient HCl was added to convert approximately half of the cyanide in solution to HCN. Solutions to investigate the effects of surface and light were prepared in the same way. The DMF used as a solvent in some studies was of commercial purity. The solutions in DMF were saturated in complex and NaCN, and were less than 0.05 F in each.

All ESR spectra of the complex in solution were taken with an X-band balanced bridge spectrometer described elsewhere.[78] The only modification was the replacement of the low frequency modulation components with a Varian Model V-4560 100 kc Field Modulation and Control Unit and a Model V-4531 rectangular cavity. All measurements were made at power levels such that there was no detectable power saturation of the resonance. The amplitude of the 100 kc magnetic field modulation was approximately 1 gauss except for measurements of line widths when a modulation amplitude equal to 1% of the line width was used.

Samples for measuring hyperfine coupling constants were sealed in 5-inch lengths of Pyrex melting point capillary tubing and positioned in the center of the microwave cavity by a sample holder attached to one of the "stacks" of the Varian cavity. In the search for very weak lines in the wings of the 55% C^{13} spectrum a quartz Varian Aqueous Solution Sample Cell was used to provide more sensitivity. All of these spectra were taken at room temperature.

A first derivative presentation of the absorption spectrum was used. For a particular absorption line the points of maximum slope were measured by observing the derivative signal on a voltmeter while sweeping the magnetic field slowly by hand. When one such point of maximum slope was located by progressively increasing the gain of the amplifier and maximizing the derivative signal by slight adjustments in the magnetic field, the value for the magnetic field was measured. This was done by adjusting the frequency of a proton NMR until the proton signal was observed. This frequency was then measured with a Hewlett-Packard 524-C Electronic Counter and printed out. This procedure was repeated five or six times for both peaks of each derivative line. The average magnetic field for the two points of maximum slope was taken to be the center of the absorption line while the difference in magnetic field is the full line width at points of maximum slope. Line positions measured in this way were reproducible to within 0.05 gauss for all but the weakest lines.

For the exchange studies the samples were also sealed in melting point capillaries and suspended in the microwave cavity. An unsilvered quartz dewar extended through the cavity and carried heated air past the sample. A fine copper-constantan thermocouple was glued to the sample tube just at the edge of the microwave cavity, downstream in the air flow and well within the quartz dewar. Gluing the thermocouple to the sample tube provided better thermal contact and reduced noise due to vibrations of the thermocouple in the air stream which arose when it was not fastened securely. Thermocouple voltages were measured with a Leeds and Northrup K-3 potentiometer. Because of temperature fluctuations at the thermocouple and the possibility of thermal gradients

between the thermocouple and the portion of the sample in the cavity, the uncertainty in the temperature was estimated as 2 °C at the highest temperature (100 °C).

The concentration of the unsubstituted complex, $Cr(C^{12}N)_5NO^{-3}$, was followed by observing the intensity of the line at lowest field for the unsubstituted complex containing Cr^{53} and N^{14}. Immediately below this line for $Cr(C^{12}N)_5NO^{-3}$ is a line assigned to the complex containing an equatorial $C^{13}N^-$. This equatorial $C^{13}N^-$ line appears 6.3 gauss below the line assigned to the unsubstituted complex and this pattern is shown in Fig. 2 (in Sec. IV A.1). Relative intensities of these two lines were obtained from the recorder chart whose time base supplied the reference for times of reaction. A response time of 0.3 second was used and the sweep rate adjusted so that there was no noticeable distortion of the line shape.

These two lines were chosen because they are adjacent, which facilitates sweeping through both of them in a reasonable length of time. This provides a direct comparison of their intensities. In addition, these lines are relatively free of interference from other lines during the early part of the exchange. The other lines which could be followed, the C^{13} lines near the center of the spectrum, are distorted by overlapping Cr^{53} hyperfine structure. The lines at the low field end of the spectrum were used because they are slightly narrower than the corresponding lines at the high field end of the spectrum. This difference of several tenths of a gauss in line width provides better resolution of the C^{13} line and a more easily detected signal.

For a particular kinetic run, the temperature of the heated air was adjusted and the dewar allowed to reach a constant temperature.

A sample with the thermocouple attached was then placed in the cavity and this was taken as time t = 0. This assumes that there had been negligible reaction at room temperature. This assumption was substantiated by the fact that no change in the spectrum was found for such samples kept at room temperature for several days.

The intensities of the lines for the unsubstituted complex and the complex with a single equatorial $C^{13}N^-$ were followed until appreciable exchange had taken place. The extent of exchange was indicated by the appearance of additional hyperfine structure at lower fields as well as by the change in intensities of the lines being followed. The initial intensities of the two lines being followed were obtained by extrapolating back to time t = 0. The corresponding initial concentrations of the two species were calculated from the total concentration of the complex present and the natural abundance of C^{13} which is 1.108%.

The solutions used for making glasses were H_2O-MeOH mixtures $1X10^{-3}$ F in complex. Samples were placed in Varian quartz sample tubes (3 mm I.D. thin-wall) and "quick frozen" by rapid immersion in liquid nitrogen. The sample tube was then placed in the cavity and kept cold by passing cold nitrogen gas through the quartz dewar in the cavity. The cold gas was obtained by boiling liquid nitrogen in a storage dewar, the rate of boiling being controlled by the power dissipated in a resistor suspended in the liquid nitrogen. At the highest gas flow rates the temperature of the sample in the cavity was within 10°C of the boiling point of liquid nitrogen.

The glass spectra were taken with a Varian V-4500 X-band spectrometer using 100 kc field modulation and a V-4531 rectangular cavity. The magnetic field was supplied by a Varian 9-inch magnet with

"Fieldial" regulation. Spectra were recorded with an EAI x-y recorder so that measurements of differences in magnetic field could be made directly from the recorder graph paper. Absolute magnetic field could be read directly from settings of the Fieldial to within 10 gauss, but more exact measurements were made using a DPPH reference sample attached to the sample in the cavity. The frequency of the Klystron was measured with a Hewlett-Packard 540B Transfer Oscillator and 524C Electronic Counter. Using that frequency and a g value for DPPH of 2.0036, one could then calculate the magnetic field at which the DPPH signal would occur. Typical spectra taken in this manner employed calibrated sweeps of 250 gauss and provided field measurements estimated to be accurate to within 0.5 gauss.

B. $Cu(H_2O)_6^{+2}$ and $Cu(NH_3)_6^{+2}$

The source of cupric ion for all experiments was G. Fredrick Smith $Cu(ClO_4)_2 \cdot 6H_2O$ which was used without drying or further purification. Perchloric acid solutions were prepared by diluting Baker and Adamson reagent grade 70% $HClO_4$, lot No. W282. Standardization of other samples from this same lot gave a concentration of 11.73 ± 0.03 F $HClO_4$. Stock solutions were prepared from known weights of the hydrated cupric perchlorate and known volumes of the 70% $HClO_4$.

The heavy water used for some experiments was obtained from Stuart Oxygen Company and was specified as containing 99.4% D_2O. Solutions were prepared in the same way as those in regular water. Some isotropic dilution was introduced from the hydrated cupric perchlorate and the 70% $HClO_4$, but all samples contained at least 96% D_2O.

Water-dioxane mixtures were prepared by adding known volumes of Eastman White Lable p-dioxane to solutions of cupric ion in water.

Samples of cupric ion in liquid ammonia were prepared in 3 mm O.D. Pyrex tubing. An aqueous solution of cupric perchlorate containing the desired amount of cupric ion was placed in a 6-inch length of the 3 mm tubing. The sample tube was then attached to a vacuum line and all the solvent removed. Ammonia was then distilled into the sample tube and frozen with liquid nitrogen. When the desired amount had been collected, the sample tube was sealed with a torch and allowed to warm to room temperature. A sample of cupric ion in a mixture of ammonia and tetrahydrofuran (THF) was prepared in a similar way. A solution of cupric perchlorate in THF was placed in a 2 mm Pyrex sample tube and attached to a vacuum line. The solution was frozen with liquid nitrogen and ammonia distilled over on top of it. The tube was then sealed off with a torch and the sample allowed to warm to room temperature. All the sample tubes withstood the pressure of ammonia at room temperature. The solvents used were Matheson reagent grade ammonia and Matheson, Coleman and Bell Chromatoquality tetrahydrofuran.

All measurements were made with the Varian X-band spectrometer and Fieldial magnet as described earlier. Spectra were recorded using the x-y plotter and the calibrated Fieldial sweep ranges. Differences in magnetic field were determined directly from the x-y plots for measurement of line widths and hyperfine coupling constants. The g value measurements were made relative to the signal from a DPPH sample in the cavity as described earlier. Temperature control and measurement were accomplished as before. Particular care was taken to balance the bridge and keep the Klystron frequency adjusted to the resonant frequency of the cavity for measurement of line widths. No power saturation was detected at the power levels used.

Preliminary spectra were recorded displaying the entire spectrum. Line widths were measured by recording only the single line of interest on an appropriately expanded scale. Each line was swept through and recorded at least once in each direction. Line widths measured in this way were reproducible to within 1% for all but the weakest lines. Measurements of field separations for determining hyperfine and g values were carried out in the same way. Each value reported is the average of several determinations.

Varian quartz sample tubes were used for studies of aqueous solution glasses. Some difficulty was encountered from sample tubes breaking, both during quick-freezing to liquid nitrogen temperature and while the sample warmed up after an experiment. Aqueous solution samples used above room temperature were sealed in Pyrex melting point capillary tubes. Allowance of sufficient space for expansion of the solution at elevated temperatures and careful sealing of the sample tubes resulted in samples which could be heated above 200 °C without failing.

Samples of cupric ion in 5.26 F $HClO_4$ solution were found to be unsatisfactory for line width measurements at elevated temperatures. Signal-to-noise ratios were poor and the lines noticeably asymmetric. This was presumably due to the high conductivity loss of these solutions. Solutions 0.1 F in $Cu(ClO_4)_2 \cdot 6H_2O$ and 0.1 F in $HClO_4$ were found to be satisfactory over the temperature range studied (up to 200 °C).

Preliminary glass spectra were taken for aqueous solutions 0.001 to 0.1 F in cupric ion and ranging from no added acid to 70% $HClO_4$. There were marked differences in the sharpness of the spectra. With no added acid only a single, broad, asymmetric resonance could be observed.

With the solution 0.5 F in $HClO_4$, one could start to resolve the parallel hyperfine band edges. Good resolution was obtained with a solution 5.26 F in $HClO_4$ and no improvement was found with 70% $HClO_4$. The sharpness of the spectrum was relatively insensitive to the concentration of cupric ion within the concentration range mentioned above. The g and A values were the same for the spectra where spectra could be resolved, i.e., for acid concentrations greater than 0.5 F. The solution chosen for the aqueous glass studies was 0.0052 F in $Cu(ClO_4)_2 \cdot 6H_2O$ and 5.26 F in $HClO_4$. This particular solution is a water-perchloric acid eutectic which freezes at -56°C,[79] making it useful for solution studies at lower temperatures.

Glass spectra in pure ammonia were poorly resolved. The spectrum of cupric ion in an ammonia-THF glass showed more detail and was used for determining the anisotropic g and A values. The spectrum of cupric ion in ammonia-THF was in good agreement with the features of the spectrum in pure ammonia which could be resolved in the glass. In addition, the isotropic g and A values measured in solution were the same for both the pure and mixed solvents.

At the higher temperatures where only a single line was observed in solution, it was necessary to correct the apparent line width for the unresolved hyperfine structure in order to get the true line width and relaxation time for the complex. In the temperature range where hyperfine structure was discernable, it was necessary to correct the apparent line widths for contributions from partially overlapping lines. These corrections were made with the aid of simulated spectra computed and plotted using D.H. Levy's EPR IV computer program.[80*] Simulated

---

* The author wishes to thank Dr. Levy for the use of his program and computer deck.

first derivative spectra of four equally intense Lorentzian lines spaced a distance A apart were computed and plotted for different values of the component line width, ΔH. For values of the ratio $\Delta H/A$ greater than 1.5 the spectrum consists of a single line whose overall width could be measured. In this way one can correct the overall line width observed to obtain the true line width if the A value is known. Similarly, for values of $\Delta H/A$ less than 1.0 the partially overlapping lines can be corrected to give the true line width. This method is less accurate than comparing experimental and computed spectra and adjusting the input parameters until agreement is obtained. Since the present method depends only on the ratio of the line width to A value and need be computed only once, its use is much less time consuming when many spectra must be analyzed.

C. $FeCl_4^-$

Solutions were prepared using weighed amounts of ferric perchlorate or hydrate ferric chloride and known volumes of concentrated HCl or $HClO_4$. The ferric chloride was Baker and Adamson reagent grade $FeCl_3 \cdot 6H_2O$. Merck reagent HCl, specified as 37.0-38.0% HCl, was used and was assumed to be 12 F in HCl. The ferric perchlorate was G. Fredrick Smith reagent grade, non-yellow, ferric perchlorate in excess $HClO_4$. It was found that this sample of ferric perchlorate contained noticeable amounts of manganous ion. A solution 0.1 F in ferric ion and 1 F in $HClO_4$ gave a room temperature ESR spectrum which consisted of a single broad resonance some 1000 gauss wide with a six-line spectrum superposed. The A value, line width and line width variation with hyperfine component were characteristic of aqueous Mn^{+2}. Approximate intensity comparisons indicated that the Mn^{+2} was

present as a level of approximately 5 parts in 10^5 relative to the Fe^{+3}. No interference from the Mn^{+2} was noted in the glass spectra.

Samples for the glass spectra were placed in Varian quartz sample tubes as in the earlier glass experiments. Spectra and field measurements were taken as before. Apparent g values were estimated to have an accuracy of 1%.

D. $\underline{Cr(H_2O)_6^{+3}}$, $\underline{CrCl(H_2O)_5^{+2}}$ and $\underline{CrCl_2(H_2O)_4^{+}}$

It has been found[70,71] that commercial hydrated chromic chloride, $CrCl_3 \cdot 6H_2O$, is predominantly a mixture of the cis and trans isomers of the dichloro complex, $CrCl_2(H_2O)_4^+$. The original method of purification[71] was to dissolve the complex in 3 F HCl, saturate the solution with additional HCl, and collect the precipitated green crystals. This was found to give a single complex characterized as the trans isomer.[73] The solution from which the trans isomer was precipitated yielded the cis isomer upon further treatment.[73] Both isomers were found to be stable over long periods of time in strong acid.[74] Both isomers were prepared in this way from reagent grade chromic chloride, washed with dry acetone and ether, then dried and stored in a desiccator. Solutions prepared from the compounds were in 5-12 F $HClO_4$.

The monochloro complex was prepared by allowing a solution of the dichloro complex in 0.1 F $HClO_4$ to stand at room temperature for 24 hours. This has been found to give primarily the monochloro complex.[72,74] The complex was then re-precipitated, washed with dry acetone and ether, and stored in a descicator. Solutions of this complex were also in 5-12 F $HClO_4$.

The $Cr(H_2O)_6^{+3}$ solutions were prepared with G. Fredrick Smith reagent grade hydrated chromium perchlorate in 5-12 F $HClO_4$.

Glass measurements were made as before and the apparent g values determined relative to a DPPH reference signal. Concentrations of the complexes used were 10^{-2} - 10^{-3} F.

IV. RESULTS AND DISCUSSION

A. $K_3Cr(CN)_5NO$

1. Isotropic Hyperfine Assignment

The assignment of the hyperfine structure in the ESR spectrum of $Cr(CN)_5NO^{-3}$ in solution without isotropic enrichment is now well established.[20,21] There remains significant variation among the coupling constants reported previously,[16,19-21] as well as between those values and the ones obtained in the present study. Since some determinations of the axial C^{13} coupling constant depend on values for the other coupling constants, it was necessary to check the values for N^{14}, C_e^{13} and Cr^{53}. The existence of sizeable second order shifts in the positions of some lines, as pointed out by Hayes,[19] requires particular care in determining coupling constants. To facilitate the labeling of lines in the spectra, we will employ the usual convention for solution spectra which treats all hyperfine coupling constants as positive in sign.

The dominant central triplet in the solution spectrum, Fig. 1, is assigned to the interaction of the N^{14} (I = 1, 99.6% abundant) nucleus of the NO^+ ligand with the unpaired electron in the complexes containing chromium isotopes of zero nuclear spin. The symmetrically disposed lines of lower intensity are assigned to the same N^{14} splitting in complexes also containing Cr^{53} (I = 3/2, 9.54% abundant). The lines indicated by arrows in Fig. 1, however, were first assigned by Hayes[19] to interaction with C^{13} in the cyanide ligands in complexes with zero spin chromium isotopes. This assignment is supported by our observation of the corresponding lines expected for the naturally abundant $C^{13}N^-$ in complexes containing Cr^{53} as indicated by the arrows in Fig. 2. Further confirmation

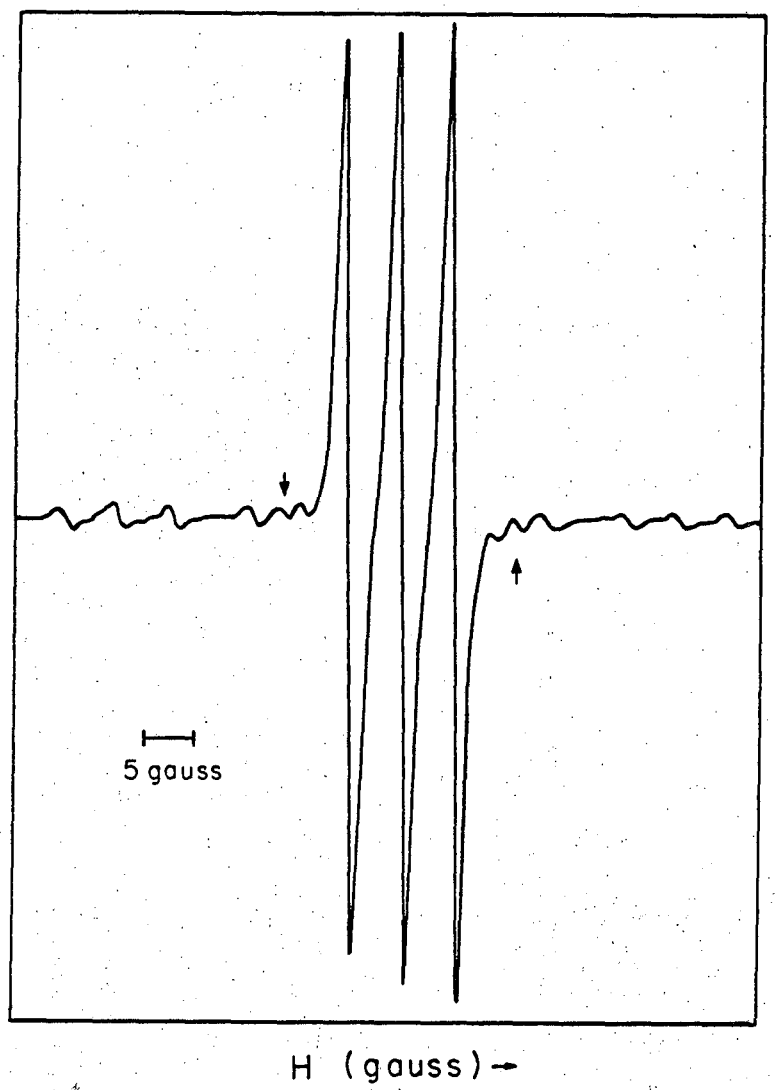

MU-36079

Fig. 1

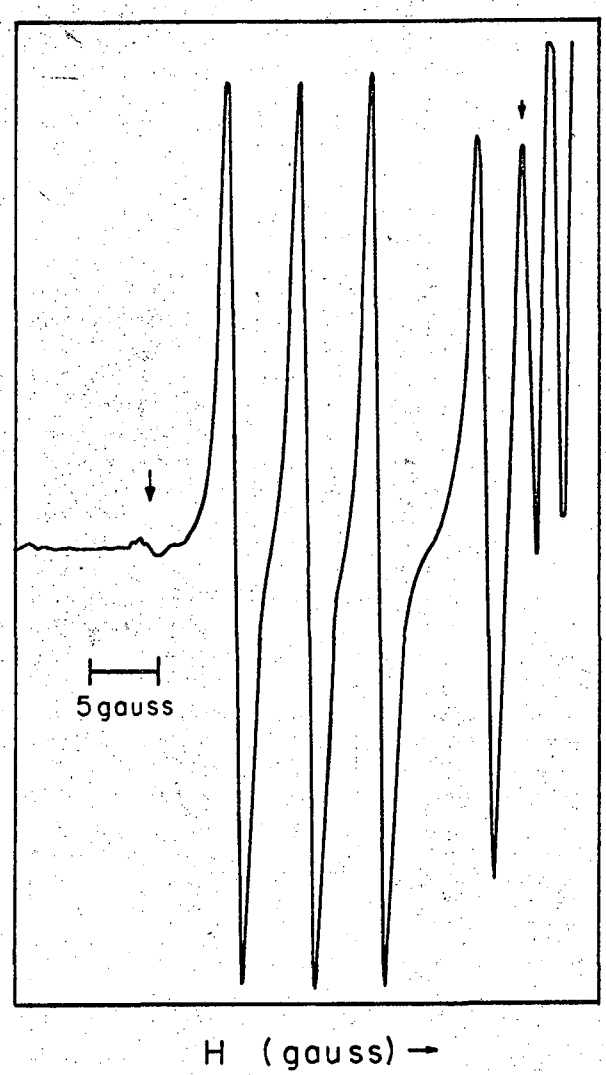

MU-36081

Fig. 2

of this assignment was obtained by exchanging cyanide in the complex with $C^{13}N^-$ in solution. The result of partial exchange in a solution 0.02 F in complex and 0.1 F in 55% C^{13} NaCN is shown in Fig. 3. The only alteration in the spectrum compared with that in Fig. 1 is an increase in the intensity of the lines assigned to the C^{13} interaction as indicated by the arrows. Similarly, the spectrum in Fig. 4 shows the increase in intensity of the C^{13} line for complexes containing Cr^{53} as compared with the spectrum before exchange shown in Fig. 2. In the spectra for naturally abundant C^{13} (I = 1/2, 1.108% abundant) one would expect the intensities of the lines due to C^{13} relative to those for C^{12} to be different depending on the number of equivalent positions for the $C^{13}N^-$. If one were observing only C^{13} in the axial position, that line should have 0.56% of the intensity of the C^{12} line next to it. If only the four equivalent equatorial positions are being observed, the intensity should be 2.2%. If the axial and equatorial positions have the same C^{13} coupling constant, then the intensity would be 2.8%. Although it is possible to rule out the first alternative on the basis of the observed relative intensities, it was impossible to choose between the latter two situations because the intensities could not be measured that accurately.

Table I lists the positions of the lines in Figs. 1 and 2 as the proton resonance frequencies observed for the corresponding magnetic field. The lines are identified by the M_I values for the particular isotopes present in the complex, assuming positive values for A in every case. Line widths are given for the principal lines. The average uncertainty in the line positions was estimated to be 0.2 kc. (0.05 gauss). Within the experimental uncertainty of ±0.4 kc. (0.1 gauss) in the measured line widths, it is apparent that the low field Cr^{53} lines and

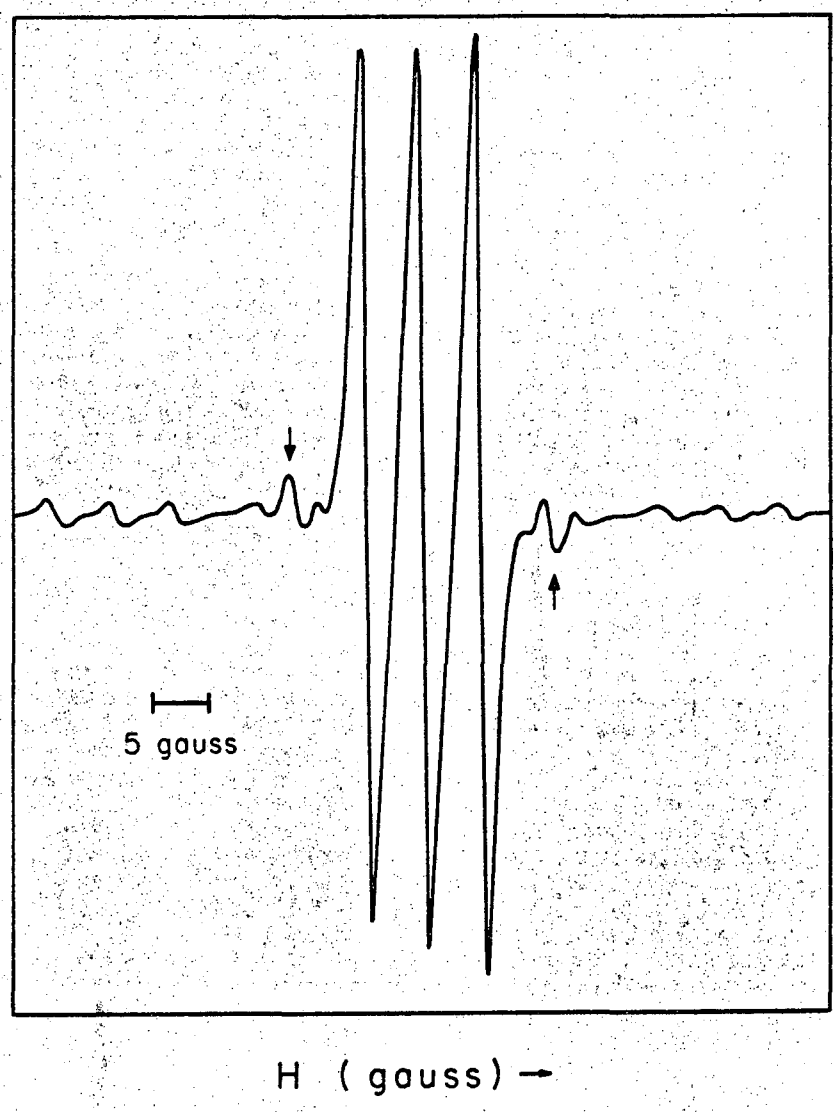

MU-36082

Fig. 3

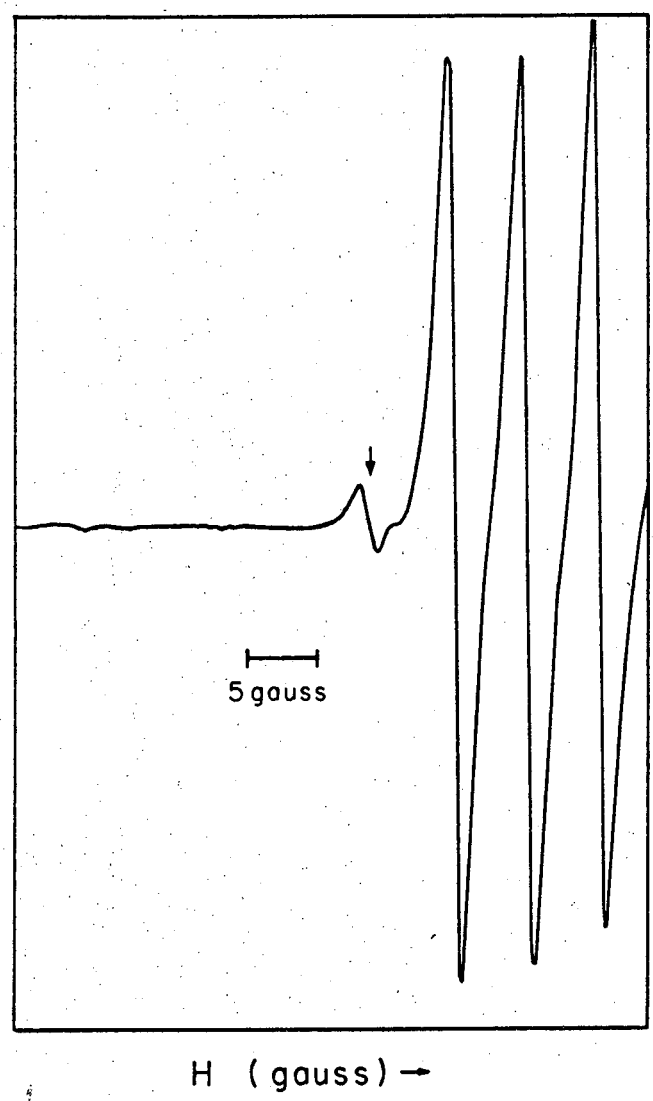

MU-36080

Fig. 4

Table I. Spectrum of $Cr(CN)_5NO^{-3}$ in H_2O

M_{Cr}^{53}	M_N^{14}	$M_{C_e}^{13}$	Line center (proton mc.)	Line width (proton kc.)
+3/2	+1	+1/2	13.7173	
+3/2	+1		13.7442	6.0
+3/2	0		13.7666	5.9
+3/2	-1		13.7891	5.9
+1/2	+1		13.8220	
	+1	+1/2	13.8352	
+1/2	0		13.8441	
	+1		13.8620	6.1
	0		13.8845	6.3
	-1		13.9069	6.0
	-1	-1/2	13.9333	
-1/2	-1		13.9452	
-3/2	+1		13.9791	7.0
-3/2	0		14.0014	6.8
-3/2	-1		14.0240	6.8
-3/2	-1	-1/2	14.0510	

the central triplet have the same line width of 5.9 kc. or 1.4 gauss. The Cr^{53} triplet at high field is composed of lines whose average width is 6.9 kc. or 1.6 gauss. This variation in line width can be observed in the spectrum in Fig. 1. It appears as a difference in derivative amplitude for the high and low field triplets. Since, for a constant concentration, the amplitude of the derivative of a Lorentzian line varies inversely with the square of the line width, small variations in line width are easily detected by observing the variation in derivative peak heights. The probable source of this line width variation will be discussed later.

From the line positions listed in Table I, it is now possible to calculate values for the isotropic hyperfine coupling constants $A(N^{14})$, $A(Cr^{53})$ and $A(C_e^{13})$. The separation between the $M_N{}^{14} = \pm 1$ components for each of the three resolved triplets is exactly $2A(N^{14})$ since the second order terms cancel. All three sets of lines give a value for $A(N^{14})$ of 5.27 gauss while the estimated uncertainty in each is 0.05 gauss. In a similar manner, the difference between the position of the $M_N{}^{14} = +1$ line in the low and high field triplets for $M_{Cr} = \pm 3/2$ is exactly $3A(Cr^{53})$ since the second order terms again cancel. The difference for the $M_N{}^{14} = 0, -1$ components was also checked. The three values obtained for $A(Cr^{53})$ were 18.39, 18.38 and 18.39 gauss, so we have taken an average value of 18.39 gauss with an estimated uncertainty of 0.05 gauss. Two methods for calculating $A(C_e^{13})$ were used. The difference between the positions of the first and last lines listed in Table I is exactly $3A(Cr^{53}) + 2A(N^{14}) + A(C_e^{13})$. Using the values for $A(Cr^{53})$ and $A(N^{14})$, one then calculates a value for $A(C_e^{13})$ of 12.66 gauss with an estimated uncertainty of 0.2 gauss. The second method of calculation is to use the extreme lines of the spectrum and those immediately adjacent which

are not split by C^{13}. This splitting is close to $(1/2)A(C_e^{13})$, but must be corrected slightly for the second order shifts in line positions. The corrected values for $A(C_e^{13})$ obtained from the low and high field ends of the spectrum are 12.61 and 12.66 gauss, each with an estimated uncertainty of 0.2 gauss. We have taken an average of all three values for $A(C_e^{13})$ and gotten a final result of $A(C_e^{13}) = 12.64 \pm 0.2$ gauss.

The first method used to distinguish between the axial and equatorial C^{13} coupling constants was to record the solution spectrum of $Cr(CN)_5NO^{-3}$ which had been synthesized using 55% C^{13} enriched NaCN. The central portion of this spectrum is shown in Fig. 5. The high and low field ends of the spectrum were observed with very high sensitivity and the positions of the first and last lines in the spectrum measured. These lines were found to be 124.8 ± 0.2 gauss apart. These lines would be for the species $Cr^{53}(C_a^{13}N)(C_e^{13}N)_4NO^{-3}$ and their separation should be exactly $3A(Cr^{53}) + 2A(N^{14}) + 4A(C_e^{13}) + A(C_a^{13})$. Using the coupling constants determined previously, one calculates that $A(C_a^{13}) = 8.55 \pm 0.4$ gauss. Moving in from the outermost lines one would expect to find next a line due to the species with four C_e^{13} located 4.3 gauss in from the outermost line and with an intensity 1.6 times that of the outermost line. Two gauss further in should be a line for the species with three C_e^{13} and one C_a^{13} having an intensity 6.4 times that of the outermost line. Just such a pattern was observed at both ends of the spectrum. The measured intensities relative to the outermost line for the lines due to three C_e^{13} and one C_a^{13} were 5.6 at the low field end of the spectrum and 7.2 at the high field end. This is in satisfactory agreement with the ratio of 6.4 predicted for 55% C^{13}.

As will be discussed in Sec. IV.A.3., exchange experiments in

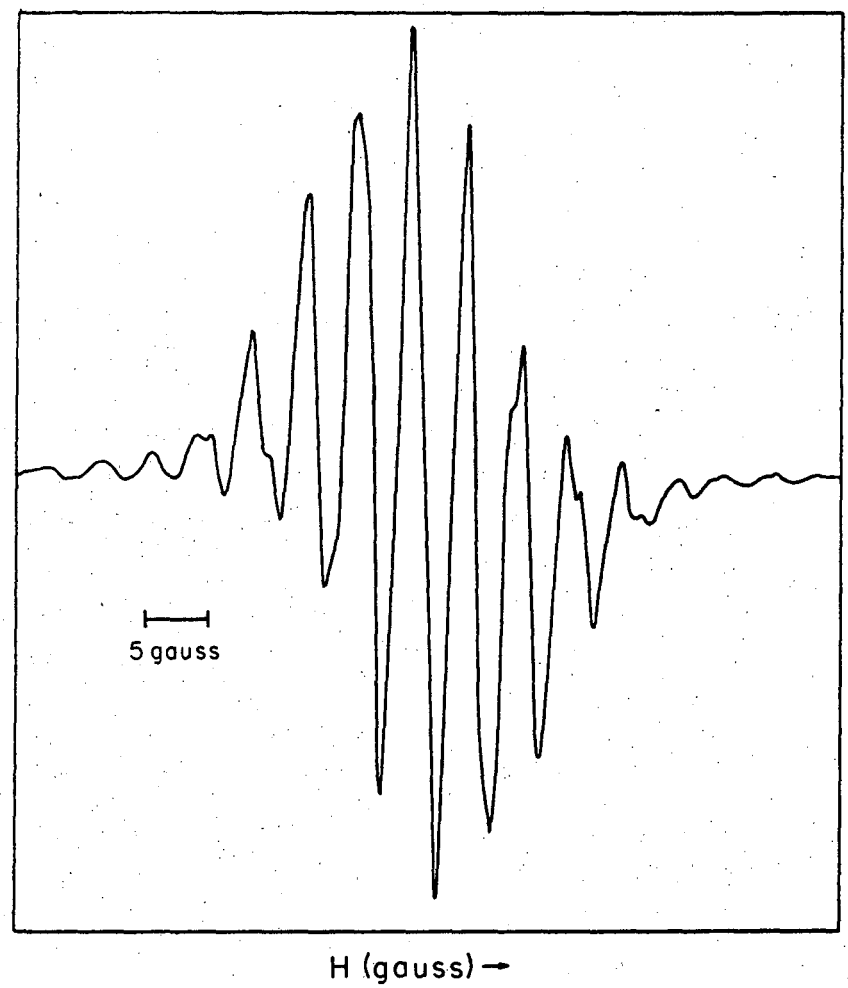

MU-36077

Fig. 5

solutions with added acid exhibited accelerated rates of exchange for the axial cyanide position. A spectrum of the complex resulting from partial exchange in such a solution is shown in Fig. 6. This is the low field part of the spectrum showing the hyperfine structure for complexes containing both Cr^{53} and C^{13} as is shown in Figs. 2 and 4. The line due to C^{13} in the axial position (line no. 3 in Fig. 6) is now quite prominent and can be used to obtain a value for $A(C_a^{13})$ directly. Using the position of this line and the one for the unsubstituted complex (line no. 4 in Fig. 6), one can again calculate the corrected value for $A(C_a^{13})$ as was done for the complex with a single C_e^{13}. In this way a value of 8.93 ± 0.2 gauss was obtained for $A(C_a^{13})$. Combining this value with the value of 9.55 ± 0.4 gauss obtained from the resolution of the fully substituted complex, we have assigned the axial coupling constant a value of 8.80 ± 0.3 gauss.

A summary of our coupling constants and those reported previously is given in Table II, as well as the recently published values of Kuska and Rogers.[28]

Early in our attempts to obtain predominantly axial substitution we learned[26] that axial exchange is more rapid in some non-aqueous solvents than in water. Since some difficulties had been encountered in dimethylsulfoxide,[26] we carried out the exchange in N,N-dimethylformamide (DMF) and found almost complete axial exchange of $C^{13}N^-$ in 40 hours at room temperature. The hyperfine coupling constants for the complex in DMF were measured and found to be within a few percent of those obtained in water. It was found that upon diluting the DMF solution 50% with water, the coupling constants were again the same as in aqueous solution. It was also observed in DMF that the widths of the low field lines and those

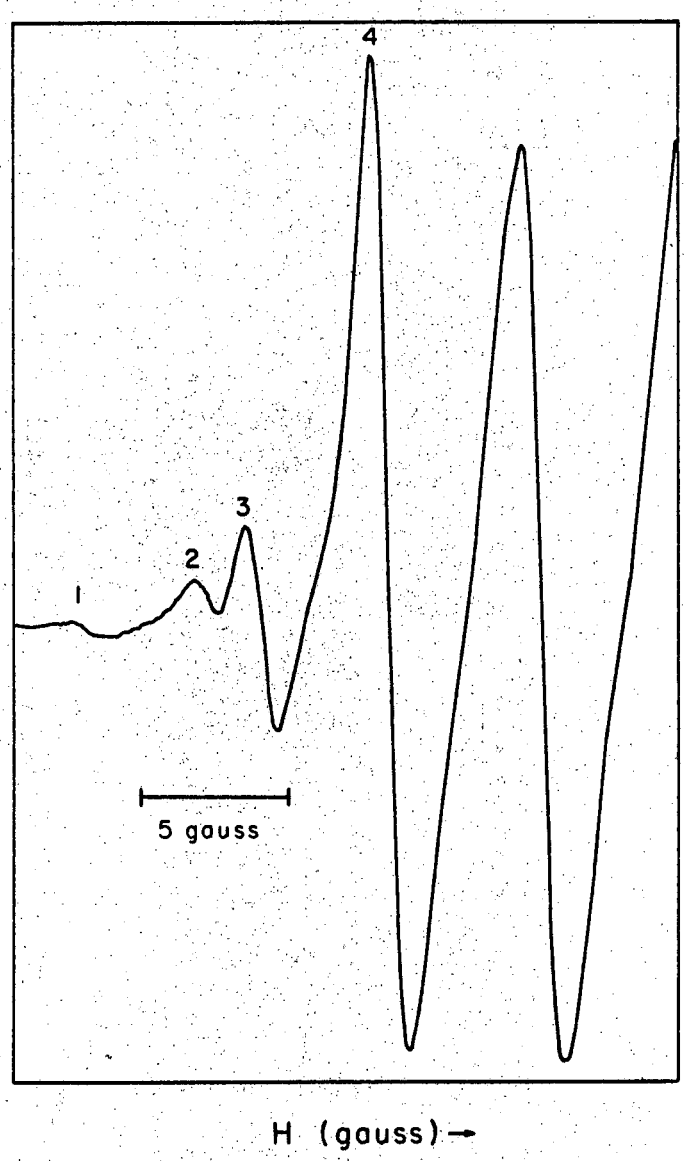

MU-36085

Fig. 6

Table II. Isotropic Hyperfine Coupling Constants for $Cr(CN)_5NO^{-3}$ in H_2O

Quantity	This work[27] (gauss)	Kuska & Rogers[28] (gauss)	Previous work (gauss)
$A(N^{14})$	5.27±0.05	5.26±0.05	5.4[20], 5.45[21]
$A(Cr^{53})$	18.39±0.05	18.49±0.05	18.5[20,21]
$A(C_e^{13})$	12.64±0.2	12.49±0.10	11.9[20,21]
$A(C_a^{13})$	8.80±0.3	8.43±0.20	
g		1.99454±0.00005	1.9950[16]

in the central triplet were the same (1.3 gauss) while the widths of the high field lines were greater (1.9 gauss) as had been the case in aqueous solution. The coupling constants in DMF are given in Table III.

Table III. Isotropic Hyperfine Coupling Constants for $Cr(CN)_5NO^{-3}$ in DMF.

$A(N^{14})$	5.54±0.05 gauss
$A(Cr^{53})$	18.69±0.05
$A(C_e^{13})$	12.73±0.2
$A(C_a^{13})$	8.93±0.2

The general features of the ESR parameters for the $Cr(CN)_5NO^{-3}$ complex ion are consistent with the proposed bonding schemes.[18,81] These place the four spin-paired electrons in the $e(d_{xz,yz})$ orbital, while the single unpaired electron occupies the non-bonding $b_2(d_{xy})$ orbital which is directed in the equatorial plane. If the axial and equatorial metal-carbon

bond lengths are virtually the same as in the related $Fe(CN)_5NO^{-2}$ complex,[82] one would expect the directional characteristics of the orbital for the unpaired electron to be reflected in the axial and equatorial coupling constants. As Kuska and Rogers[28] point out, however, there is also the effect of the mixing of ligand orbitals with the $b_1(d_{x^2-y^2})$ and $a_1(d_{z^2})$ excited states. The b_1 state can mix with orbitals on the equatorial ligands while the a_1 state mixes with orbitals on axial ligands. If the b_1 excited state lies lower as predicted, then this could also contribute to the larger equatorial ligand hyperfine interaction. Thus, from the hyperfine and bond length information at hand, it is not possible to decide whether the axial Cr-C bond is necessarily weaker than the equatorial Cr-C bonds as suggested by Bernal and Harrison.[16,21]

2. Anisotropic Assignment

In order to explain the variation of line width for different hyperfine components in the solution spectrum of $Cr(CN)_5NO^{-3}$, it was necessary to obtain estimates for the anisotropies in the hyperfine interaction and g value. Although single crystal studies are more accurate and can potentially yield more information and resolution, spectra of randomly oriented species are much more readily obtained. The theory for such spectra in the case of S = 1/2 was discussed in the Introduction. When applied to the present case, the treatment will give a parallel spectrum at higher field than the perpendicular spectrum. Assuming axial symmetry for the complex, we can describe the spectrum in terms of parallel and perpendicular components for each quantity whose isotropic value is given in Table II.

The spectrum of $Cr(CN)_5NO^{-3}$ in a frozen H_2O-MeOH glass is shown in

Fig. 7. The positive band edges at the low field end of the spectrum are assigned to the onset of absorption for complexes whose principal axis is aligned perpendicular to the external magnetic field and comprise the perpendicular spectrum. The dominant three line spectrum is assigned to the interaction of the unpaired electron with N^{14} of the NO^{+} ligand. The spacing between these lines gives a value for $A_{\perp}(N^{14})$ and the three lines are centered about the magnetic field corresponding to $g_{\perp}$. The lines of lesser intensity appearing at lower field are assigned to Cr^{53}. Since no lines are observed below these in the spectrum, this group of lines is assigned to the $M_{Cr} = +3/2$ component. The spacing between the line appearing at lowest field and the low field component of the intense triplet is then equal to $(3/2)A(Cr^{53})$. It will be convenient for later discussion if we convert these coupling constants from gauss to cm^{-1} using the appropriate g value. In these terms the values obtained thus far are $g_{\perp} = 2.006$, $A_{\perp}(N^{14}) = 6.3X10^{-4}$ cm^{-1}, and $A_{\perp}(Cr^{53}) = 11.6X10^{-4} cm^{-1}$. The single negative derivative at higher field is the parallel spectrum. Its position corresponds to a value of $g = 1.973$. If the isotropic and anisotropic hyperfine for Cr^{53} are both positive as expected, then one would predict from the values for $A(Cr^{53})$ and $A_{\perp}(Cr^{53})$ that $A_{\parallel}(Cr^{53})$ is approximately $30X10^{-4}$ cm^{-1}. Under higher gain as shown in Fig. 7, an additional peak is observed at higher field. This is assigned to the $M_{Cr}53 = -3/2$ splitting of the parallel peak and yields a value for $A_{\parallel}(Cr^{53}) = 30.9X10^{-4}$ cm^{-1}. The width of these peaks and the fact that no triplet structure is observed indicate that $A_{\parallel}(N^{14})$ is no greater than approximately $2X10^{-4}$ cm^{-1}.

When a sample of the complex synthesized with 55% C^{13} NaCN was dissolved in an H_2O-MeOH solution and frozen, the spectrum in Fig. 8 was obtained.

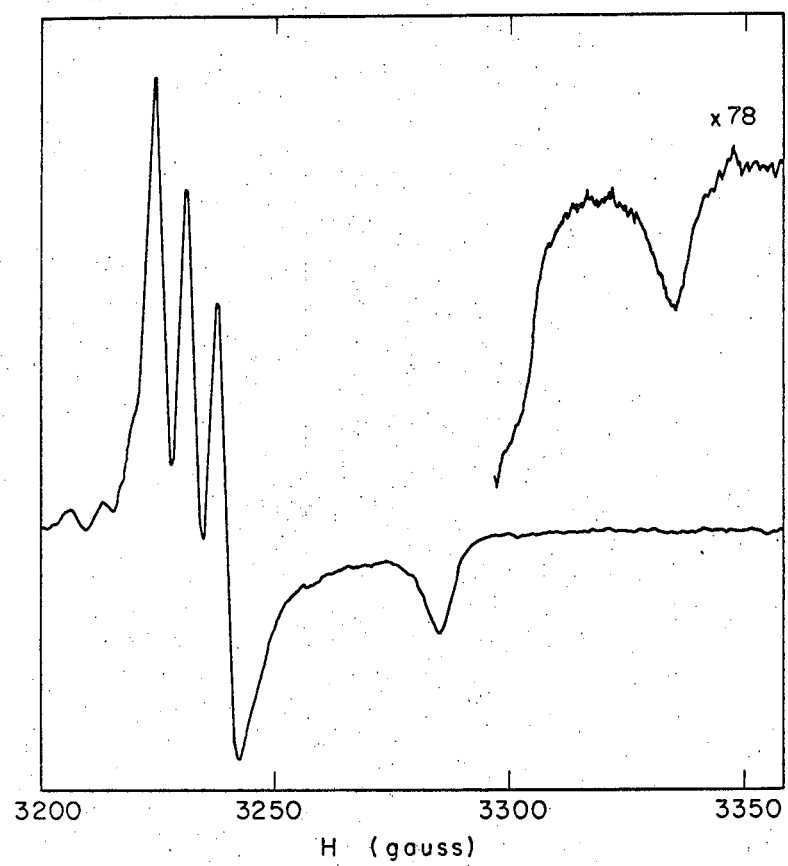

MU-36089

Fig. 7

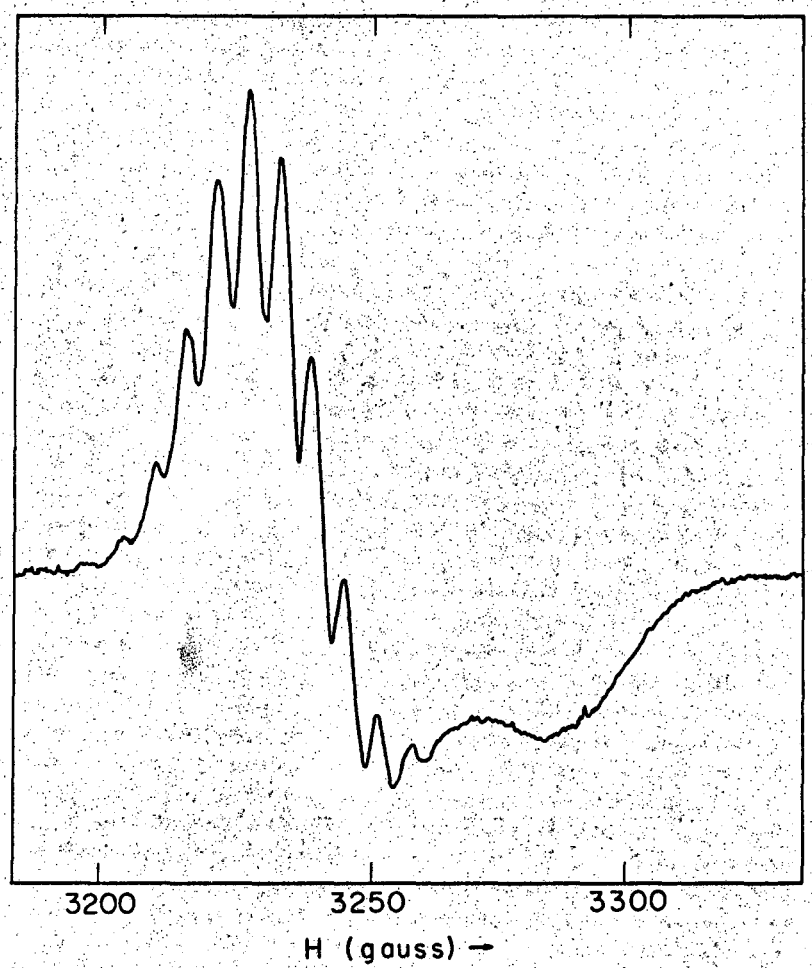

MU-36083

Fig. 8

This spectrum shows extensive splitting of the perpendicular structure and a broadening of the parallel peak. Since the value for $A_{\perp}(N^{14})$ had already been determined, it was possible to fit the 11-line perpendicular hyperfine structure with a value for $A_{\perp}(C_e^{13})$ of approximately 13×10^{-4} cm^{-1}. A more exact assignment was made by comparing solution and glass spectra for samples in which varying amounts of $C^{13}N^-$ exchange had taken place. The same procedure was carried out for solutions to which acid had been added in order to assign the axial C^{13} coupling. In both cases partially resolved perpendicular hyperfine structure was obtained while the parallel peak was only broadened and not split. Values of $A_{\perp}(C_e^{13}) = 11.0 \times 10^{-4}$ cm^{-1} and $A_{\perp}(C_a^{13}) = 9.2 \times 10^{-4}$ cm^{-1} were obtained.

Even though the parallel hyperfine structure was not observed, it was possible to estimate the values for the remaining coupling constants. If one assumes that the magnetic interactions for the complex in solution and in a glass are approximately the same, then the isotropic g and A values measured in solution should be averages of the anisotropic values in the glass as discussed in the Introduction. Using the values for $g_{\parallel}$ and $g_{\perp}$ given above, one calculates that the isotropic g value in solution should be 1.995, while the observed value of 1.99454 is in good agreement. Such a calculation for the isotropic Cr^{53} coupling constant in solution yields a value of 18.0×10^{-4} cm^{-1}, while the value observed is 17.1×10^{-4} cm^{-1}. Although we can only measure the absolute magnitude of the coupling constants and cannot determine their sign, it is necessary to distinguish between two cases. In the first, the isotropic and both anisotropic coupling constants are all of the same sign. This was assumed for the Cr^{53} coupling constants and was seen to give reasonable results. The second case is when $A_{\parallel}$ and $A_{\perp}$ are of opposite signs. When using values for A and $A_{\perp}$

to estimate $A_{\parallel}$, we must keep these two possibilities in mind. Thus, if all three coupling constants for N^{14} are of the same sign, one would predict that $A_{\parallel}(N^{14}) = 2X10^{-4}$ cm^{-1}. If the signs of $A_{\parallel}$ and $A_{\perp}$ are opposite, the value predicted is $27X10^{-4}$ cm^{-1}. The smaller value is consistent with the observation that there is no resolved triplet splitting of the parallel peak. Applying the same argument to the C^{13} coupling constants, one concludes that A, $A_{\parallel}$, and $A_{\perp}$ are all of the same sign both for the axial and equatorial positions (although this in no way implies that the axial coupling constants are of the same sign as the equatorial coupling constants). The values obtained are $A_{\parallel}$ $(C_e^{13}) = 13X10^{-4}$ cm^{-1} and $A_{\parallel}(C_a^{13}) = 6X10^{-4}$ cm^{-1}. These results are summarized in Table IV with the values obtained using isotropic coupling constants from the solution spectra enclosed in parentheses. The indicated uncertainties were estimated by comparing values obtained from several spectra and are due primarily to the uncertainty in locating line centers. A detailed analysis of the magnetic anisotropies and bonding for this complex on the basis of single crystal ESR spectra is the subject of a forthcoming publication by Hayes[26] and will not be discussed here.

It is apparent from the results in Table IV that the largest magnetic anisotropies are to be expected for the Cr^{53} hyperfine components. In the aqueous solution spectrum we found that the widths of the lines due to complexes containing chromium isotopes of zero nuclear spin and the widths of the Cr^{53} hyperfine components with $M_{Cr^{53}} = +3/2$ were identical within experimental error. This is taken as an indication that the rotational averaging of the magnetic anisotropy for the $M_{Cr^{53}} = +3/2$ hyperfine component is sufficiently complete that there is no measurable contribution to the observed line width from this mechanism.

Table IV. Anisotropic Hyperfine Coupling Constants for $Cr(CN)_5NO^{-3}$ in an H_2O-MeOH Glass

Coupling constants in units of 10^{-4} cm^{-1}	
$A_\perp(N^{14}) = 6.3\pm0.3$	$A_\parallel(N^{14}) = (2\pm1)$
$A_\perp(Cr^{53}) = 11.6\pm1$	$A_\parallel(Cr^{53}) = 30.9\pm1$
$A_\perp(C_e^{13}) = 11.0\pm1$	$A_\parallel(C_e^{13}) = (13\pm1)$
$A_\perp(C_a^{13}) = 9.2\pm1$	$A_\parallel(C_a^{13}) = (6\pm1)$
$g_\perp = 2.006\pm0.002$	$g_\parallel = 1.973\pm0.002$

The theory of rotational averaging in ESR as a source of line width was first presented by McConnell. It has been further developed by Kivelson[84] and applied to vanadyl complexes in solution by Rogers and Pake.[85] A discussion of this theory will be taken up in Sec. IV.B. For our present purposes we will use the theory as derived by Kivelson.[84] Values for the appropriate anisotropies can be obtained from Table IV. They are

$$\Delta g = g_\parallel - g_\perp = -0.033$$

$$b' = 2(A_\parallel - A_\perp)/3$$

$$= 12.9\times10^{-4}\ cm^{-1} \text{ for } Cr^{53}$$

The reciprocal of the relaxation time, $1/T_2$, is then given in terms of these anisotropies, the value of M_I and the correlation time for tumbling of the complex. Treating the complex as a rigid sphere of radius a_o rotating in a medium of viscosity η, Kivelson[84] uses the usual approximation for the tumbling correlation time, τ_t,

$$\tau_t = \frac{4\pi a_o^3 \eta}{3kT} .$$

Assuming a radius of 3.7 Å for the complex on the basis of the structure of similar complexes,[82] one estimates a correlation time of 5×10^{-11} sec for aqueous solutions of $Cr(CN)_5NO^{-3}$ at 25°C. The peak to peak derivative line width for a Lorentzian line is related to $1/T_2$ by

$$\Delta H = \frac{h}{g\beta} \frac{1}{\pi\sqrt{3}} \frac{1}{T_2} .$$

Using Kivelson's theory we are now in a position to calculate the tumbling contribution to the line width. When the calculation is carried through for the Cr^{53} hyperfine components it is found that this mechanism should contribute 0.08 gauss to the width of the narrowest line and 0.80 gauss to the widest line. The experimental results mentioned previously were that the narrowest line for Cr^{53} had no detectable contribution from this sort of mechanism while the widest Cr^{53} line had a contribution of 0.2 gauss. If the correlation time were shortened to 1×10^{-11} sec., however, the contribution to the line width predicted for the tumbling mechanism would be 0.2 gauss as found. A similar calculation for the N^{14} components of the central triplet indicates that the variation in line width should be less than 0.05 gauss as is observed experimentally.

The line width variation is in fair agreement with that predicted for rotational averaging. Exact agreement is lacking as has been the result of previous work.[76,85] If one assumes that the theory for tumbling and the model for the tumbling correlation time are correct, there still remain two sources of difficulty. In order to calculate a tumbling correlation time it is necessary to estimate an "effective ionic radius" for the complex. Since this radius enters the expression for the correlation time as a_o^3, the times calculated are quite sensitive to the choice of radius. The second difficulty is in the use of crystal or

glass g and A anisotropies. It is possible that the distortions of the complex in a crystal or glass cause significant changes in the magnetic anisotropies. In this particular case, a smaller anisotropy in the g value for the complex in solution would give better agreement between predicted and observed line widths.

3. Kinetic Studies

The exchange reactions under consideration are

$$Cr(C^{12}N)_5NO^{-3} + C^{13}N^- \xrightarrow{k_a} Cr(C^{12}N)_4(C^{13}N_a)NO^{-3} + C^{12}N^- \quad (1)$$

$$Cr(C^{12}N)_5NO^{-3} + C^{13}N^- \xrightarrow{4k_e} Cr(C^{12}N)_4(C^{13}N_e)NO^{-3} + C^{12}N^- \quad (2)$$

where a and e refer to axial and equatorial positions. There are, of course, exchange reactions subsequent to these, but they involve the same two rate constants and neither these nor the back reactions contribute appreciably to changes in concentrations of any of the species in Eqs. (1) and (2) during the early part of the exchange. It is also necessary to follow only the early part of the exchange because overlapping hyperfine lines make it difficult to follow the reaction for more than one half-life for a single exchange.

For the general class of ligand exchange or replacement reactions, techniques have been developed to fit data with two rate laws, both of which are first order in the concentration of the complex. They differ only in whether the rate of exchange is independent of the concentration of the free ligand or depends upon that concentration to the first power.[86,87] Attempts to distinguish between these two situations were made in this case by working with both the initial rates of reaction and the integrated rate equations. On the basis of our data no definite

differentiation could be made since the variation in concentration of the reactants was small and the uncertainties in the data too great. Since information from other studies[23] showed that the rates of cyanide exchange are independent of the free cyanide concentration for the complexes $K_4Fe(CN)_6$, $K_3Cr(CN)_6$, $K_3Co(CN)_6$ and $K_3Mn(CN)_6$, the same condition is assumed to prevail for $K_3Cr(CN)_5NO$. Making this assumption and the further assumption mentioned above, that only reactions (1) and (2) contribute appreciably, the rates of disappearance of the unsubstituted complex and appearance of the mono-substituted complexes would be given by Eqs. (3-5). In these equations $f_{C^{13}}$ is the fraction of the free

$$\frac{d}{dt}[Cr(C^{12}N)_5NO^{-3}] = -(k_a + 4k_e)(f_{C^{13}})[Cr(C^{12}N)_5NO^{-3}] \qquad (3)$$

$$\frac{d}{dt}[Cr(C^{12}N)_4(C^{13}N_a)NO^{-3}] = k_a(f_{C^{13}})[Cr(C^{12}N)_5NO^{-3}] \qquad (4)$$

$$\frac{d}{dt}[Cr(C^{12}N)_4(C^{13}N_e)NO^{-3}] = 4k_e(f_{C^{13}})[Cr(C^{12}N)_5NO^{-3}] \qquad (5)$$

cyanide in solution containing C^{13}. The rate constant k_e corresponds to the process in which there is exchange of one of the four equivalent equatorial cyanide ligands.

By following the concentrations of the unsubstituted complex and the complex containing a single equatorial $C^{13}N^-$ as described in the experimental section, the initial rates of reaction for Eqs. (3) and (5) were obtained. From the known initial concentrations it is then possible to estimate the quantity $(k_a + 4k_e)$ from Eq. (3) and k_e from Eq. (5). Thus, approximate values for k_a, k_e and the ratio $k_a/4k_e$ were obtained.

Within the assumption of dealing only with those species appearing in reactions (1) and (2), the following quantities can be defined.

$$\Delta[Cr(C^{12}N)_5NO^{-3}] = [Cr(C^{12}N)_5NO^{-3}]_0 - [Cr(C^{12}N)_5NO^{-3}] \tag{6a}$$

$$\Delta[Cr(C^{12}N)_4(C^{13}N_a)NO^{-3}] = [Cr(C^{12}N)_4(C^{13}N_a)NO^{-3}] - [Cr(C^{12}N)_4(C^{13}N_a)NO^{-3}]_0 \tag{6b}$$

$$\Delta[Cr(C^{12}N)_4(C^{13}N_e)NO^{-3}] = [Cr(C^{12}N)_4(C^{13}N_e)NO^{-3}] - [Cr(C^{12}N)_4(C^{13}N_e)NO^{-3}]_0 \tag{6c}$$

In addition, there are several useful relationships which are readily derived and are given in Eqs. (7a-d).

$$[C^{12}N^-] + [C^{13}N^-] = [C^{12}N^-]_0 + [C^{13}N^-]_0 \tag{7a}$$

$$f_{C^{13}} = \frac{[C^{13}N^-]}{[C^{12}N^-] + [C^{13}N^-]} = \frac{[C^{13}N^-]_0 - \Delta[Cr(C^{12}N)_5NO^{-3}]}{[C^{12}N^-]_0 + [C^{13}N^-]_0} \tag{7b}$$

$$\Delta[Cr(C^{12}N)_5NO^{-3}] = \Delta[Cr(C^{12}N)_4(C^{13}N_a)NO^{-3}] + \Delta[Cr(C^{12}N)_4(C^{13}N_e)NO^{-3}] \tag{7c}$$

$$\frac{k_a}{4k_e} = \frac{\Delta[Cr(C^{12}N)_4(C^{13}N_a)NO^{-3}]}{\Delta[Cr(C^{12}N)_4(C^{13}N_e)NO^{-3}]} \tag{7d}$$

The relationships given in Eqs. (7a-c) can be substituted into the rate expressions for the disappearance of the unsubstitued complex, Eq. (3), and the result then integrated to give Eq. (8).

$$\log\left|\frac{[Cr(C^{12}N)_5NO^{-3}]}{[C^{13}N^-]_0 - \Delta\,[Cr(C^{12}N)_5NO^{-3}]}\right| = -\frac{(k_a + 4k_e)\{[C^{13}N^-]_0 - [Cr(C^{12}N)_5NO^{-3}]_0\}}{2.3\,\{[C^{12}N^-]_0 + [C^{13}N^-]_0\}}\,t + \log\frac{[Cr(C^{12}N)_5NO^{-3}]_0}{[C^{13}N^-]_0} \tag{8}$$

Using the experimentally determined concentration of the unsubstituted complex as a function of time, a plot of the first quantity in Eq. (8) versus time (t) should give a straight line whose slope is directly related to the sum of the axial and equatorial rate constants ($k_a + 4k_e$). It was observed that for approximately the first third of the reaction such a plot was linear, but as the reaction progressed, some curvature was noticeable. This curvature was in the direction corresponding to an apparent slowing down of the reaction as would be expected both from increasing overlap of hyperfine lines and from increasing contributions from the back reactions.

The other species followed during the reaction was the complex with a single labeled cyanide in an equatorial position. Again using the relationships in Eqs. (7a-d) and substituting into the rate equation for equatorial exchange and integrating, one obtains the integrated rate expression in Eq. (9).

$$\log \left| \frac{[Cr(C^{12}N)_5NO^{-3}]_0 - (1 + \frac{k_a}{4k_e})\Delta[Cr(C^{12}N)_4(C^{13}N_e)NO^{-3}]}{[C^{13}N^-]_0 - (1 + \frac{k_a}{4k_e})\Delta[Cr(C^{12}N)_4(C^{13}N_e)NO^{-3}]} \right|$$

$$= \frac{(k_a + 4k_e)\{[Cr(C^{12}N)_5NO^{-3}]_0 - [C^{13}N^-]_0\}}{2.3\{[C^{12}N^-]_0 + [C^{13}N^-]_0\}} t$$

$$+ \log \frac{[Cr(C^{12}N)_5NO^{-3}]_0}{[C^{13}N^-]_0} \qquad (9)$$

Since the quantity ($k_a + 4k_e$) has already been evaluated for a given kinetic run, it remains to determine the ratio $k_a/4k_e$ which

appears in the first term of Eq. (9). This is accomplished by first using the value for that ratio determined from initial rates of reaction in order to plot the first term in Eq. (9) versus time. From the slope of such a plot a value for $(k_a + 4k_e)$ can be calculated and compared with that found from the disappearance of the unsubstituted complex. Successive approximations for the ratio $k_a/4ke$ can then be made until the proper value for $(k_a + 4k_e)$ is obtained. In practice, this required two or three successive approximations.

Once values for $(k_a + 4k_e)$ and $k_a/4k_e$ have been obtained, the separate rate constants can be calculated. The rate constants at various temperatures from 60° to 100°C and the total concentrations of complex and cyanide are listed in Table V. The concentrations quoted are not corrected for changes in the densities of the solutions at different temperatures, but are the concentrations of the solutions at room temperature. In a separate blank experiment with unlabeled cyanide, it was found that there was no apparent decomposition of the complex below 100°C in the length of time typically used in these kinetic runs. It was assumed that any decomposition of the cyanide in solution was much slower than the reactions being studied. The extent of exchange attained for reactions allowed to go almost completely to equilibrium supports this assumption.

The rate constants given in Table V are shown plotted as log k vs. $10^3/T$ in Figs. 9 and 10. The straight lines were drawn to give a best fit to the data by the method of Least Squares. Assuming that the first order rate constants are given by Eq. (10), values for the enthalpy of

$$k_r = \frac{kT}{h} \exp\left(\frac{\Delta S^{\ddagger}}{R}\right)\exp\left(-\frac{\Delta H^{\ddagger}}{RT}\right) \qquad (10)$$

Table V. Rate Constants for Axial and Equatorial Exchange of CN^- with $Cr(CN)_5NO^{-3}$ in H_2O.

Temp. °C	$[Cr(CN)_5NO^{-3}]$ F	$[CN^-]$ F	k_a sec^{-1}	k_e sec^{-1}
62.2	0.0344	0.096	2.0×10^{-5}	6.9×10^{-7}
71.6	0.0344	0.096	3.6×10^{-5}	2.7×10^{-6}
71.8	0.0260	0.143	1.5×10^{-5}	5.0×10^{-6}
72.0	0.0174	0.190	2.0×10^{-5}	2.6×10^{-6}
79.8	0.0344	0.096	5.3×10^{-5}	1.9×10^{-5}
80.2	0.0260	0.143	1.4×10^{-4}	1.0×10^{-5}
80.2	0.0174	0.190	1.3×10^{-4}	1.0×10^{-5}
87.6	0.0344	0.096	2.8×10^{-4}	2.5×10^{-5}
87.6	0.0174	0.190	3.0×10^{-4}	2.3×10^{-5}
87.8	0.0260	0.143	3.3×10^{-4}	3.3×10^{-5}
99.4	0.0344	0.096	1.3×10^{-3}	9.7×10^{-5}
99.6	0.0260	0.143	1.8×10^{-3}	7.5×10^{-5}
100.0	0.0174	0.190	1.6×10^{-3}	9.4×10^{-5}

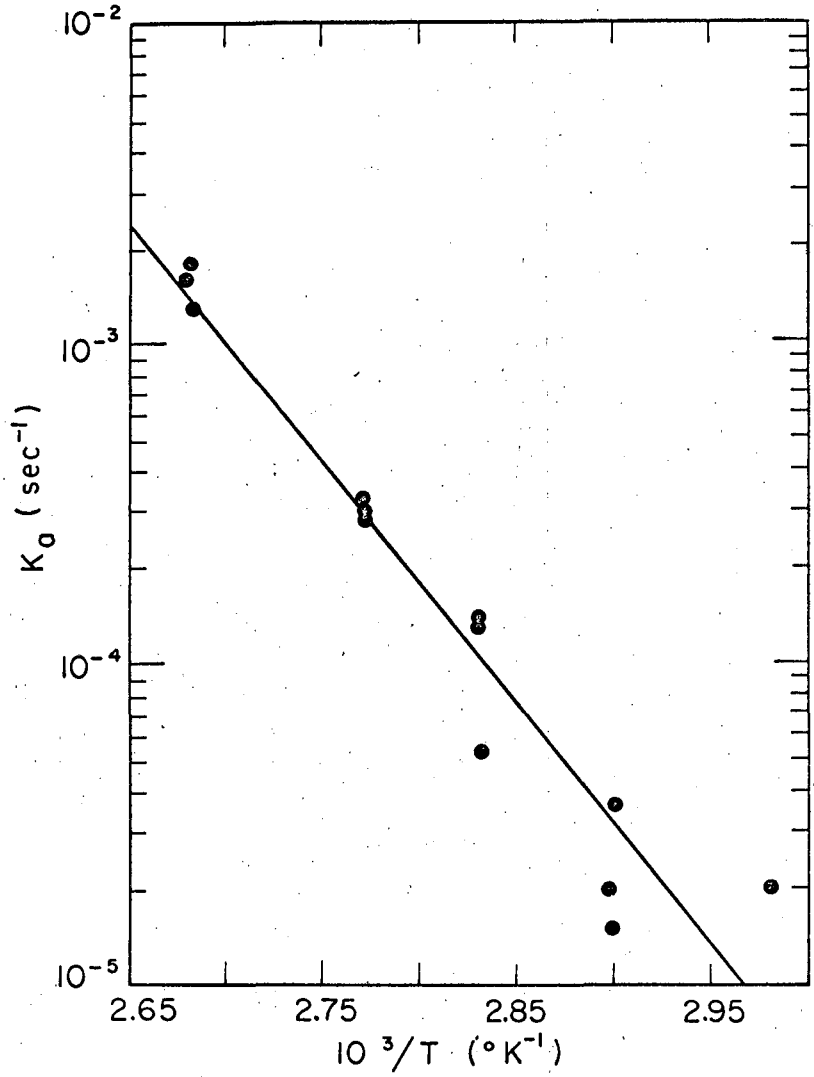

MU-36076

Fig. 9

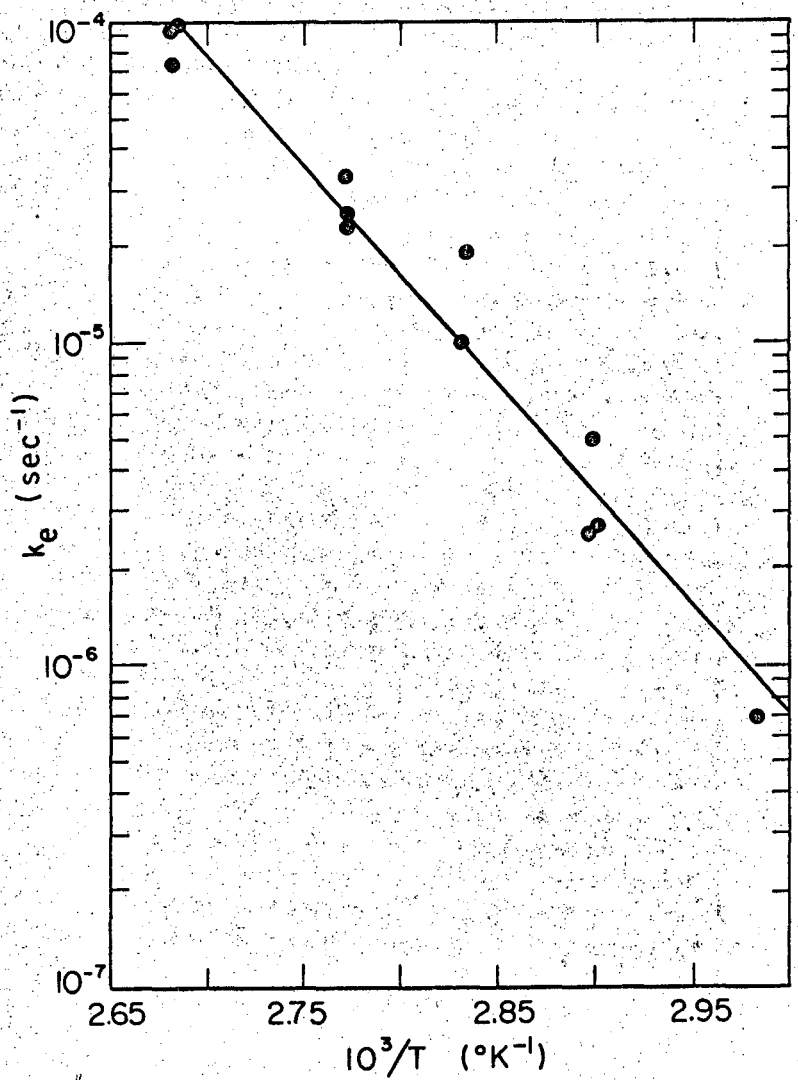

MU-36075

Fig. 10

activation, $\Delta H^{\ddagger}$, and the entropy of activation, $\Delta S^{\ddagger}$, were calculated and are listed in Table VI. The indicated uncertainties were estimated by ignoring each set of three points at a given temperature, recalculating the enthalpy and entropy of activation and observing the changes in the values of those quantities. The rate constants at 75°C as calculated from Eq. (10) and the thermodynamic quantities are included in Table VI. It was observed that the ratio $k_a/4k_e = 3 \pm 2$ throughout the temperature range studied.

Table VI. Enthalpies and Entropies of Activation for Exchange

Axial Exchange	Equatorial Exchange
$\Delta H_a^{\ddagger} = 33.5 \pm 4$ kcal/mole	$\Delta H_e^{\ddagger} = 30.5 \pm 4$ kcal/mole
$\Delta S_a^{\ddagger} = 18 \pm 8$ e.u.	$\Delta S_e^{\ddagger} = 5 \pm 8$ e.u.
$k_a = 6 \times 10^{-5} sec^{-1}$ at 75°C	$k_e = 6 \times 10^{-6} sec^{-1}$ at 75°C

In an attempt to obtain primarily axial exchange for the purpose of confirming the assignment of the axial coupling constant as well as to determine the effect of pH changes, a solution was prepared in which sufficient acid was added to convert approximately half the free cyanide in solution to HCN. First a blank was run using unlabeled cyanide and sufficient HCl to give a solution 0.08 F in both CN^- and HCN with a concentration of the complex of 0.025 F. This sample was kept at 75°C for several hours and no decomposition was detected during this time. An identical sample was then prepared using 55% C^{13} enriched NaCN and the reaction was followed for 30 minutes at 70.2°C. The reaction was then quenched by cooling the sample to room temperature and the spectrum

again taken. As the line from the complex with an axial $C^{13}N^-$ was now quite prominent in comparison with that from equatorial substitution, a situation different from that encountered in the earlier spectra, it was apparent that the rate of axial exchange relative to equatorial exchange had been enchanced. The relative intensities of the two peaks gave $k_a/4k_e = 5.1$ while the rate of disappearance of the unsubstituted complex was also determined. These two quantities gave values for the rate constants of $k_a = 1.3\times10^{-4}\,sec^{-1}$ and k_e $6.7\times10^{-6}\,sec^{-1}$. These are to be compared with the rates of exchange taken from the graphs in Figs. 9 and 10 of $k_a = 2.7\times10^{-5}\,sec^{-1}$ and $k_e = 2.9\times10^{-6}\,sec^{-1}$. This corresponds to increases of approximately a factor of 5 in the axial rate and 2 in the equatorial rate. If one assumes that the complex is a stronger acid than HCN, the solutions used for the kinetic studies summarized in Tables V and VI had a hydrolysis pH of around 11 while, for the samples with added acid, the pH would be around 9 at room temperature.

Another attempt to get exchange preferentially in the axial position was made by carrying out the reaction in DMF solution.[26] A solution of DMF approximately saturated in both complex and NaCN was allowed to stand at room temperature for 40 hours. At the end of that time the spectrum was taken and it was apparent that extensive exchange had taken place primarily in the axial position. This is in contrast with the situation in water where, after a week at room temperature, only very slight exchange had taken place.

In order to check for possible surface effects a solution 0.0145 F in complex and 0.174 F in labeled cyanide was prepared. Samples were sealed in Pyrex melting point capillaries as usual and in a quartz tube

of approximately equal diameter. After 30 minutes at 85°C, the samples were cooled to room temperature and their spectra taken. The rates of reaction were found to be within 20% of each other and the ratios of axial to equatorial exchange approximately the same. This indicates no pronounced differences between quartz and Pyrex surfaces for the reactions.

Other cyanide exchange studies[23] have shown pronounced light catalysis in some instances. Our kinetic experiments were carried out in the semi-darkness of the microwave cavity. Samples at room temperature in direct and diffuse light showed no exchange after several days. Another sample of the solution used to check the effect of glass and quartz was placed within 5 cm of the front of an AH-4 lamp for a rather drastic test for light catalysis. After 30 minutes there had been a slight increase in the relative intensity of the equatorial C^{13} line, and after an hour of irradiation the relative intensity of that line was about twice that for naturally abundant C^{13}. Although some exchange was noted, it is not at all certain how much was due to the direct effect of irradiation and how much to heating of the sample. In any case, there should have been no light catalysis in our normal kinetic experiments.

The rate of cyanide exchange in this complex is slow, but it is reasonable in comparison both with exchange of cyanide in some other cyanide complexes[23] and with some other ligand exchange reactions.[86,87] Unfortunately, there has been only one temperature study[24] in the previous cyanide exchange work so that it is not possible to compare entropies and enthalpies of activation.

There are, however, interesting comparisons which can be made between the exchange processes for the axial and equatorial positions in the

case of $Cr(CN)_5NO^{-3}$. In light of the fact that the enthalpies of activation for the two positions are quite similar, it is apparent that the different entropies of activation are responsible for the more rapid exchange at the axial position. The apparent large positive entropy of activation for the axial position is consistent with the activated complex for axial exchange being a protinated species.* Such a rapid equilibrium in shown in Eq. (11). The entropy change associated with the transfer

$$Cr(CN)_5NO^{-3} + HCN = HCr(CN)_5NO^{-2} + CN^- \qquad (11)$$

of a proton from HCN to a tri-anion base can be estimated by considering the analagous protination of PO_4^{-3} by HCN. The thermodynamic data for the aqueous phosphate-cyanide system[88] give an entropy change of +40 e.u. for such a proton transfer. If a subsequent reaction is the rate determining step, such as for the dissociation mechanism in Eq. (12), then

$$HCr(CN)_5NO^{-2} \xrightarrow{k} Cr(CN)_4NO^{-2} + HCN \qquad (12a)$$

$$Cr(CN)_4NO^{-2} + CN^- \xrightarrow{fast} Cr(CN)_5NO^{-3} \qquad (12b)$$

the entropy associated with the protination of the complex will be included in the apparent entropy of activation for the rate determining reaction. In at least one case[24] it has been suggested that cyanide exchange involves displacement by solvent water molecules rather than a dissociation mechanism of the type in Eq. (12a). The participation of water was suggested because of the large negative entropy of activation (-44 e.u.) for the reaction. Judging from the large positive entropy of activation we observe for the axial exchange, it is apparent that the solvent water molecules do not participate significantly in the rate

*The author is indebted to Prof. Robert E. Connick for suggesting this possibility.

determining step. The small entropy change for equatorial exchange is consistent both with a dissociation mechanism for the unprotinated complex and with a displacement by water for the protinated complex.

Acid catalysis has been observed for other cyanide complexes, although not in all cases.[23] Isolation of the compound $H_2Fe(CN)_5NO$ indicates that such protinated species do exist.[89] The observation that the axial rate of exchange is increased relative to the equatorial rate when half the cyanide is present as HCN lends support to the argument, although some acid catalysis for the equitorial exchange is also possible from the data. A plausible explanation for such behavior is that the formal charge of +1 on the NO group favors protination of the axial CN^- rather than the closer equatorial position.

The rate of axial exchange is faster than that at the equatorial position as predicted by Bernal and Harrison.[16,21] It is doubtful, however, that this is due to a relative weakening of the axial Cr-C bond as they suggest, since the enthalpies of activation are virtually the same for both positions. It appears more likely that the greater protination of the axial position is responsible for the more rapid rate of exchange.

Possible modes of decomposition for pentacyanonitrosyl complexes are suggested by Addison and Lewis.[89] They cite evidence for the reaction of $Fe(CN)_5NO^{-3}$ with hydroxide ion to form $Fe(CN)_5NO_2^{-4}$ as well as for formation of the aquopentacyano complex. At least for the conditions of concentration, pH, illumination and temperature under which the behavior of $Cr(CN)_5NO^{-3}$ was studied, we found such decomposition to be unimportant.

The enhanced rate of exchange and apparent specificity for axial

exchange in DMF solution is interesting, but cannot be of particular use in the interpretation of the exchange mechanism in water because of the drastic change in solvent properties. Similar behavior has been noted for solutions of the complex in dimethylsulfoxide with the added complication of apparent reaction with the solvent to form some other, as yet uncharacterized, complex.[26]

B. $Cu(H_2O)_6^{+2}$ and $Cu(NH_3)_6^{+2}$

1. Assignment

The analysis of polycrystalline or glass ESR line shapes to obtain spin Hamiltonian parameters was introduced by Sands[11] and developed further for cupric complexes for which it has been used most successfully.[12,13] Using these methods one can analyze the glass spectrum of cupric ion in $HClO_4$ at liquid nitrogen temperature shown in Fig. 11. The four positive band edges in this derivative presentation correspond to the onset of resonance for complexes with their symmetry axis parallel to the magnetic field and with the four possible M_I values. Note that the band edge at lowest field is sufficiently sharp that structure due to both Cu^{63} ($I = 3/2$, $\mu = 2.2206$, 69.06% abundant) and Cu^{65} ($I = 3/2$, $\mu = 2.3790$, 30.91% abundant) can be observed. The spacing between these components and the position of the center of the hyperfine pattern, after correction for second order terms, give values for $g_{\parallel}$ and $A_{\parallel}$. The perpendicular spectrum at higher field shows only a small splitting. These two peaks could be partially resolved perpendicular hyperfine structure, but one would expect to see evidence of two more hyperfine lines. Also, the value for $A_{\perp}$ would be larger than usual.[13] A second possibility is that the complex has lower symmetry than tetragonal in which case there could

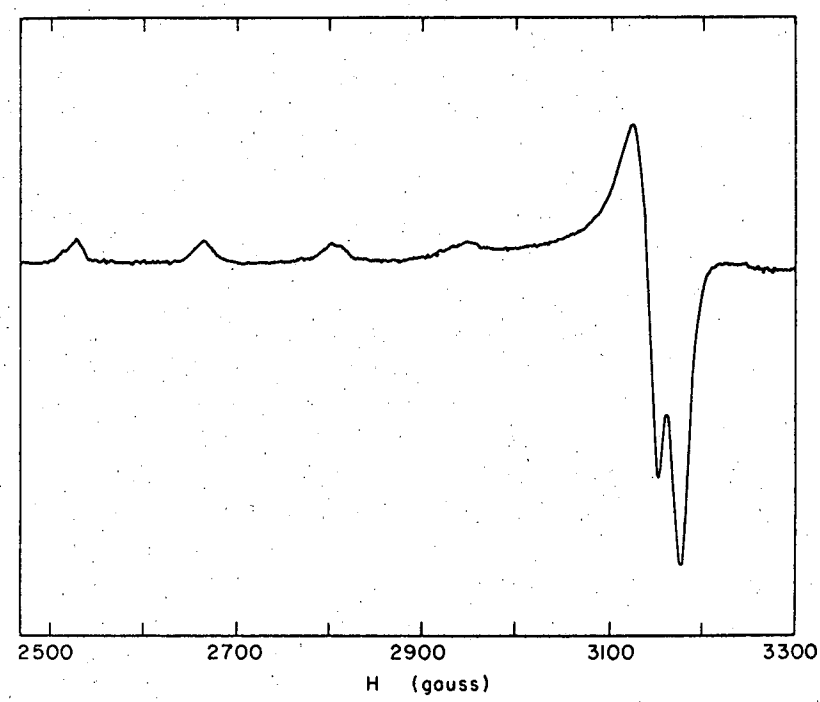

MU-36088

Fig. 11

be two slightly different g values around $g_\perp$. Although the possibility of lower symmetry cannot be eliminated, it seems unlikely that such a distortion would occur with sufficient regularity in the glass to give two distinct $g_\perp$ values rather than a distribution of values. A final possibility is that one of the two peaks in an "extra" absorption of the type discussed in the introduction. One can calculate where the four "extra" absorptions should occur for a given set of spin Hamiltonian parameters using the approximate expressions available.[12,13] Taking the peak at lower field to be $g_\perp$(2.076), one calculates that the "extra" absorptions should be centered at 2.08 and 2.10, which would be at still lower fields. Taking the peak at higher field to be $g_\perp$(2.057), one calculates that the "extra" absorptions should be centered 2.06 and 2.08. Qualitatively, this second alternative gives a better fit. In order to settle the point for certain it would be necessary to compute the entire spectrum using a line shape function with a finite width which was different for each component (see the variation in line width for the parallel spectrum). Within the accuracy needed for our later discussions we will take the average of the two values for $g_\perp$. An upper limit can be set on the value for $A_\perp$ from the widths of these two peaks. The spin Hamiltonian parameters determined in this way are listed in Table VII later in the section.

The spectrum of cupric ion in frozen D_2O 0.1 F in $HClO_4$ was considerably less well resolved as mentioned earlier. From the position of the parallel component at lowest field, however, it was apparent that the splittings were essentially the same as in regular water.

Cupric ion in aqueous solution gives a broad symmetric line whose g value is 2.199. As the temperature is lowered the line becomes

progressively more asymmetric until indications of hyperfine structure become apparent around 0°C. Such a spectrum for cupric ion in D_2O is shown in Fig. 12. Similar, but more asymmetric, spectra were obtained for the H_2O-$HClO_4$ eutectic solution cooled to near its freezing point. For the spectra with the best resolution the apparent A value approached the value of 52 gauss estimated from the glass spectrum.

Although the spectrum of copper in an ammonia glass was poorly resolved, it was possible to estimate values for $A_{\parallel}$ and $g_{\parallel}$. Somewhat better resolution was obtained when the solution used consisted of equal volumes of ammonia and THF. That spectrum is shown in Fig. 13. The parallel features of this spectrum were analyzed as for the aqueous glass spectrum. A value for $g_{\perp}$ can be obtained, but the greater width of the perpendicular peak may be due to a poor glass as suggested by the widths of the parallel band edges, to unresolved copper and ligand hyperfine structure, or to a combination of these effects.

Solution spectra were taken both for cupric ion in pure ammonia and in the ammonia-THF mixture over a range of temperatures. The isotropic g value was found to be the same in both solvents and independent of temperature in the range covered from +20° to -80°C. Hyperfine structure was resolved below -20° C in both solvents and gave an A value which was the same in both solvents and independent of temperature. One such solution spectrum is shown in Fig. 14. The g and A values are listed in Table VII. In the solution spectrum of cupric ion in liquid ammonia shown in Fig. 14, the high field line was compared with Gaussian (dashes) and Lorentzian (dots) line shapes computed for a line of that width and amplitude. The line shape is seen to be Lorentzian to a good approximation. This indicates that the line does not contain significant

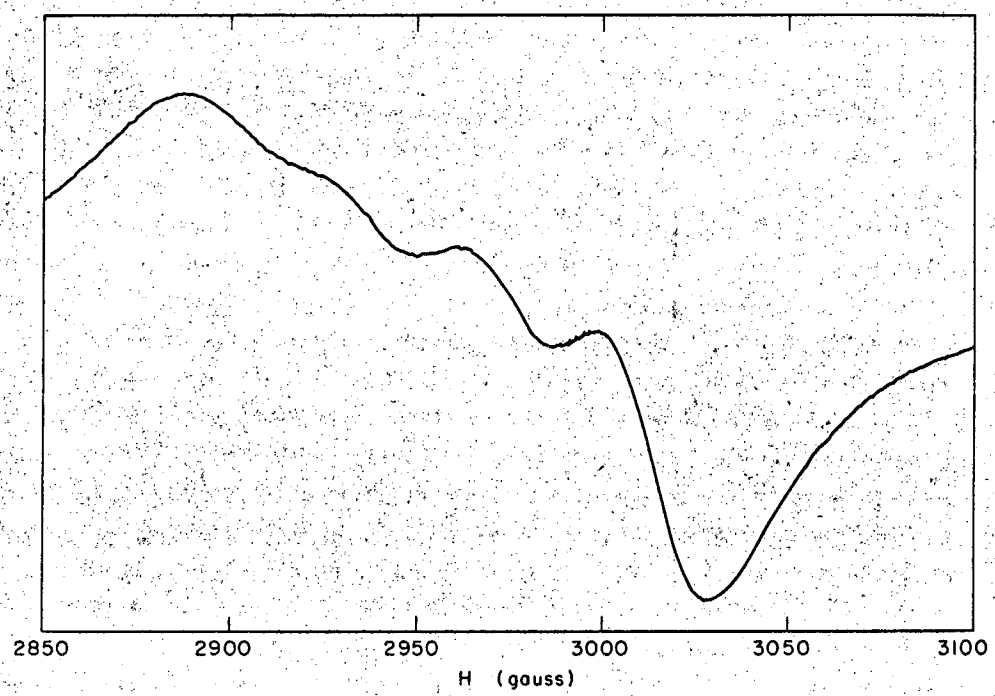

MU-36095

Fig. 12

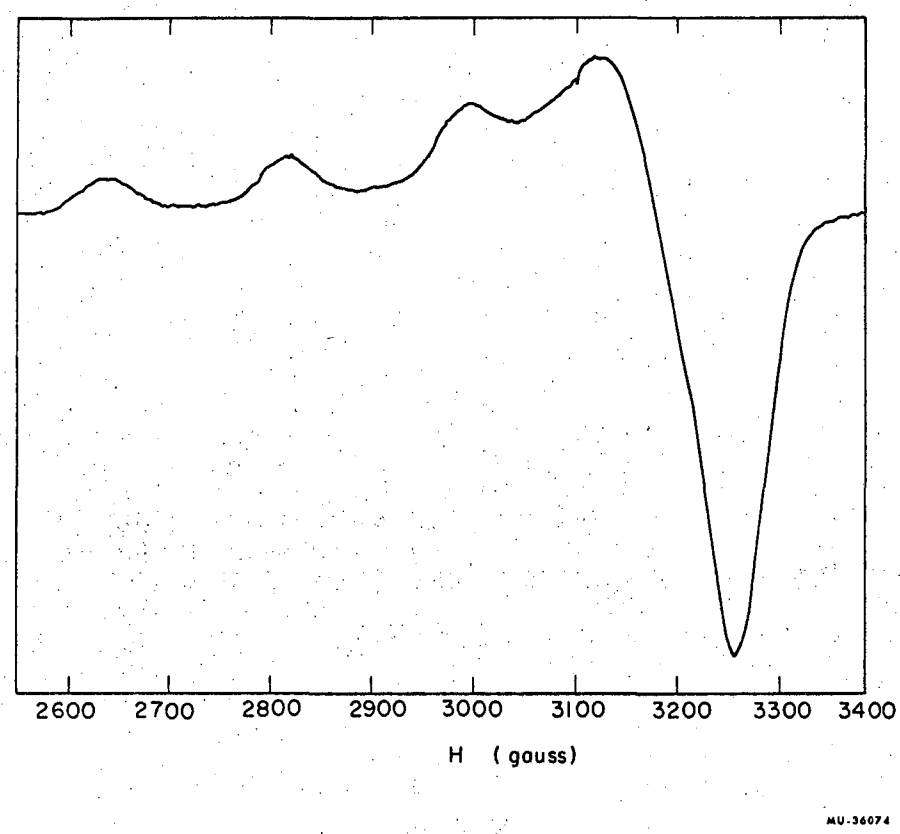

Fig. 13

Table VII. CuL_6^{+2} Spin Hamiltonian Parameters

	$Cu(H_2O)_6^{+2}$	$Cu(NH_3)_6^{+2}$
	Glass Spectra	
$g_{\parallel}$	2.379 ± .005	2.228 ± .005
$g_{\perp}$	2.066* ± .02	2.055 ± .02
$A_{\parallel} \times 10^4$ cm^{-1}	155 ± 2	192 ± 5
$A_{\perp} \times 10^4$ cm^{-1}	(≤7)	(8)
	Solution Spectra	
g	2.199 ± .005	2.124 ± .003
$A \times 10^4$ cm^{-1}	(52-56)	69 ± 2

* Average of two components: 2.076 and 2.057
Values enclosed in parentheses are estimates as discussed in the text.

contributions from unresolved hyperfine structure. By combining the isotropic A value in solution and the value of $A_{\parallel}$ from the glass spectrum, we have estimated the value for $A_{\perp}$ given in Table VII.

Neiman and Kivelson[12] have discussed the bonding for cupric complexes in considerable detail. Although they considered primarily square planar complexes, they pointed out that the addition of two axial ligands at a distance greater than that of the equatorial ligands should have little effect on the spin Hamiltonian parameters. In particular, the values for $g_{\parallel}$, $A_{\parallel}$, and $A_{\perp}$ should be unaffected while the value for $g_{\perp}$ should increase slightly. Their method is to set up linear combinations of ligand and metal ion orbitals of the proper symmetry, apply the usual spin Hamiltonian to these wave functions and obtain relationships for the observable magnetic parameters, the coefficients of the wave functions used, and the energy separation between various levels.

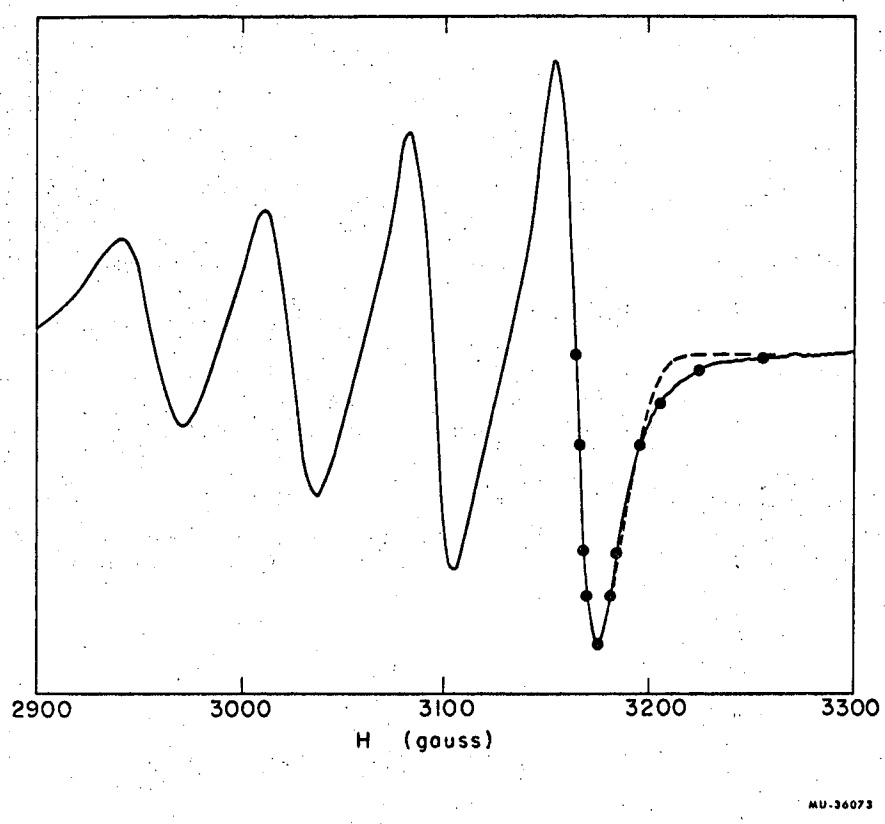

Fig. 14

Qualitatively, their results indicate that increasing covalent character for the metal-ligand bonds should be expected to lead to g values which are closer to that of the free electron and increases in the hyperfine interaction with the copper nucleus. Quantitative calculations of the ligand field coefficients from paramagnetic resonance data have been made for a variety of cupric complexes with sulfur, nitrogen and oxygen ligand atoms.[12,13] These results show significant contributions to the bonding from the ligand orbitals.

The magnetic properties of hydrated cupric ion in a glass can be compared with the same ion in similar environments. The paramagnetic resonance of cupric ion has been studied in a variety of single crystals. In the case of Tutton's salts, copper is coordinated with six water molecules in the usual elongated octahedral structure. The results of these studies have been tabulated.[2] The general behavior of cupric ion in such a series of crystal lattices is consistent, but with definite small variations when the dimensions of the site are changed. The g and A components listed in Table VII for the aquo complex are typical of those found in single crystals. It is interesting to note that the ESR results for $Cu(H_2O)_4SO_4 \cdot H_2O$, in which there is a square planar arrangement of water ligands with two axial sulfate oxygens at a greater distance, are the same as one might expect for complexes with six waters of coordination.[90] This is in agreement with the conclusion mentioned earlier[12] that the axial ligands should have little effect on the spectrum. The same situation exists for ammonia complexes of cupric ion. Gersman and Swalen[13] looked at $CuCl_2$ with excess added ammonia in organic solvents, the precise complex being unknown. The spectrum of single crystals of $Cu(NH_3)_4SO_4 \cdot H_2O$, in which there is a

square planar arrangement of ammonias and two axial sulfate oxygens, has also been assigned.[90,91] In both of these cases the g and A values are quite close to those listed for cupric ion in liquid ammonia in Table VII. This would again indicate that the equatorial ligands are primarily responsible for the magnetic properties of such complexes.

In order to compare the bonding in the water and ammonia complexes it is necessary to estimate the energies of the excited states. The optical transitions for these complexes in water and liquid ammonia have been reported,[36] but the assignments of the spectra are not certain. It is apparent from the spectra, however, that the transitions for the complex in liquid ammonia occur at higher energy than the corresponding ones for the complex in water. Polarized crystal spectra for $CuSO_4 \cdot 5H_2O$ indicate[37] that there may be at least three components for the broad spectrum observed. This broad band is centered in the region of 13,000-15,000 cm^{-1} for the aquo complex in aqueous solution while the corresponding band for the ammonia complex in liquid ammonia is centered in the region of 16,000-18,000 cm^{-1}. The spectrum of cupric ion in liquid ammonia[36] is attributed to the complex with four equatorial and two more distant axial ammonia ligands by comparison with the spectra for complexes containing four and five ammonia in concentrated aqueous ammonia solutions. Gersmann and Swalen[13] place some excited states as high as 30,000 cm^{-1} in addition to others as low as 14,000 cm^{-1} on the basis of their optical spectra which were neither presented nor discussed.

Lacking good assignments of the energies of the excited states for $Cu(H_2O)_6^{+2}$ and $Cu(NH_3)_6^{+2}$, one can still make qualitative comparisons of the bonding in the two complexes from their spin Hamiltonian parameters

and the increase in the energy of a given excited state upon going from $Cu(H_2O)_6^{+2}$ to $Cu(NH_3)_6^{+2}$. On this basis, the change in $g_{\parallel}$ and $A_{\parallel}$ for the ammonia complex relative to the aquo complex is partly due to the greater energies for the excited states in the ammonia complex. If one uses energies like those used by Gersman and Swalen,[13] one must also conclude that there is slightly larger contribution of the ligand orbitals to the bonding for the ammonia complex than for the aquo complex.

A variation of g and A values with temperature for cupric ion in various crystals has been noted.[2] For crystals with sites of high symmetry occupied by the cupric ions, the effect is most pronounced. At room temperature the spectrum may be isotropic, while at liquid nitrogen and liquid helium temperatures the spectrum becomes progressively more anisotropic. This effect was first explained by Abragam and Pryce[29] as being due to the dynamic nature of the distortion of the complex in sites of high symmetry. Avvakumov[40] has discussed the degenerate vibrations responsible for this pseudo-rotation of the complex in an attempt to treat the temperature dependence quantitatively. In our studies of the aqueous system we observed only an abrupt change from the isotropic solution spectrum to the anistropic glass spectrum at the melting point of the solution being used. For cupric ion in pure liquid ammonia, however, different behavior was observed. As spectra of cupric ion in liquid ammonia were taken at progressively lower temperatures, the line widths of the hyperfine components changed, but the g and A values did not. At a temperature of -83 °C the sample froze as indicated by an abrupt change in the dielectric loss of the sample and consequent change in the balance of the microwave bridge. As subsequent spectra were taken at lower temperatures the spectrum

remained like that for cupric ion in solution. The low field hyperfine component line width was changing more rapidly with temperature than it had in solution, but the g and A values remained the same. This behavior continued until the temperature had been lowered to around -105°C. At this temperature the high field hyperfine component had also broadened considerably and the parallel structure was starting to appear. A spectrum taken in this intermediate range is shown in Fig. 15. This behavior was reproducible upon raising the temperature for samples which had been frozen at liquid nitrogen temperatures. The reasons for this behavior will be discussed in more detail in the next section.

2. Relaxation

In order to determine electron spin relaxation times, T_2, it is necessary to correct the observed line widths for unresolved or overlapping hyperfine structure as discussed in the experimental section. The procedure was straightforward for cupric ion in liquid ammonia since the isotropic A value could be obtained directly from spectra such as the one shown in Fig. 14. For cupric ion in aqueous solutions, however, the situation is more complicated. As one can see from the spectrum in Fig. 12, the poor resolution of the hyperfine structure leads to highly approximate A values. In the 5.26 F $HClO_4$ solutions the apparent separation between the hyperfine component at highest field (M_{Cu} = +3/2 for a negative A value) and the adjacent one (M_{Cu} = +1/2) approached a value of 50 gauss as the temperature was lowered and the resolution improved. This corresponds to $A=51\times10^{-4}$ cm^{-1}. Assuming that the g and A values for the complex are approximately the same in the glass and in solution, one can estimate the isotropic A value in solution from $A_{\parallel}$ and $A_{\perp}$ in the glass. Using the values listed in Table VII, one calculates an

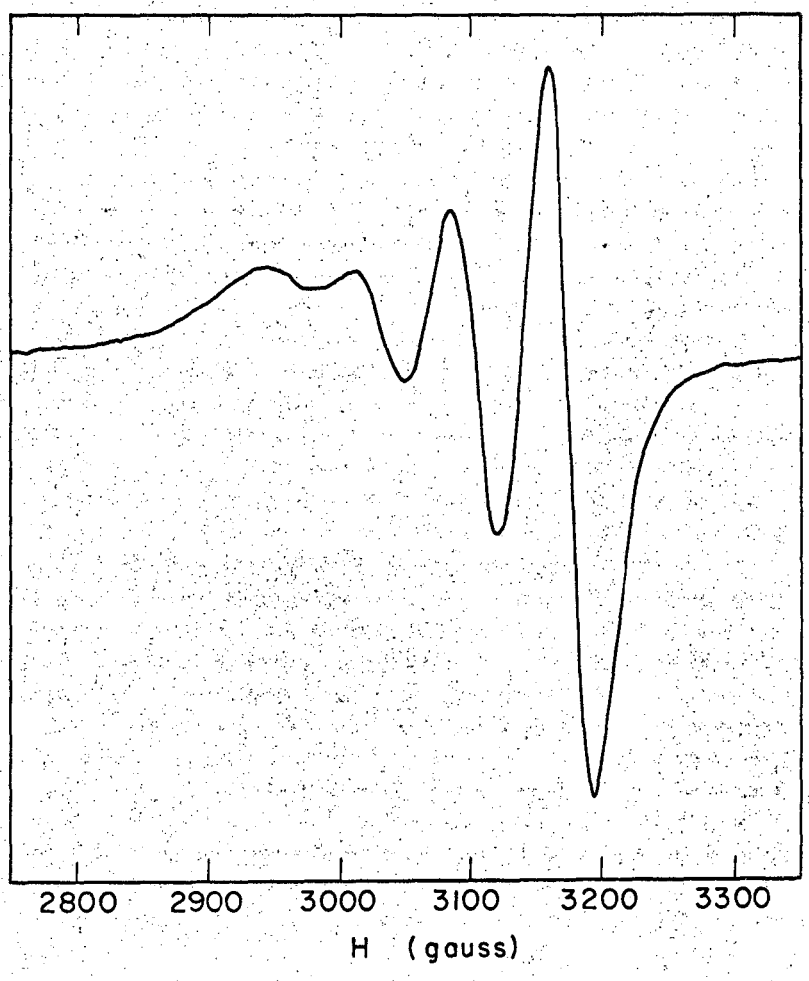

MU-36072

Fig. 15

upper limit for A of 56×10^{-4} cm^{-1}. If the value for A were reduced to zero, the resulting value for A would be 52×10^{-4} cm^{-1}. The procedure to be followed will be to use a value for A = 53×10^{-4} cm^{-1} when correcting the line width for hyperfine structure and carry through the estimated uncertainty of $\pm3\times10^{-4}$ cm^{-1} in order to indicate the uncertainty in relaxation times. The same value for A will be used for the D_2O complex since the parallel portion of the spectrum in the glass, which was all that could be resolved for D_2O, was the same for both D_2O and H_2O and the solution g values are identical.

The results for 0.1 F cupric ion in 0.1 F $HClO_4$ are shown in Table VIII. The experimental line width is the distance between the maxima and minima of the first derivative presentation taken directly from the spectrum. The corrected line width represents the width of each of the four unresolved hyperfine components obtained from the experimental line width using A = 53×10^{-4} cm^{-1}.

Table VIII. Line width for 0.1 F $Cu(H_2O)_6^{+2}$ in 0.1 F $HClO_4$

Temp. °C	ΔH (experimental) gauss	ΔH (corrected) gauss
21.4	143	
36.4	147	
51.5	159	
62.2	165	
86.4	212	
104.0	263	199
123.8	303	256
140.0	347	315
161.6	410	393
187.7	533	530
208.6	608	608

The total uncertainty in the corrected line widths due to uncertainties in the experimental line width and the A value is estimated to be 5%. The data for cupric ion in D_2O were treated in the same way and are listed in Table IX.

Table IX. Line widths for 0.05 F $Cu(D_2O)_6^{++}$ in 96.7% D_2O with 0.1 F $HClO_4$

Temp. °C	ΔH (experimental) gauss	ΔH (corrected) gauss
24.1	140	
37.7	144	
64.4	161	
89.7	204	
124.0	278	220
137.0	298	249
149.0	332	295
160.8	367	340
175.7	401	382
187.5	483	478
203.0	522	518

The spectrum of cupric ion in 5.26 F $HClO_4$ for the temperature range of -40° to 0°C is sufficiently resolved to obtain estimates for the line width of the high field (M_{Cu} = +3/2) component. The experimentally observed line width was corrected for interference due to the adjacent hyperfine component using $A = 53 \times 10^{-4}$ cm^{-1} as before. The line widths obtained from these experiments are tabulated in Table X.

The corrected line widths in Tables VIII, IX and X are shown plotted as log ΔH vs T^{-1} in Fig. 16. The solid points are for $Cu(H_2O)_6^{+2}$ in 0.1 F $HClO_4$ at temperatures above ambient (Table VIII) and are based on the assumption that the four lines are all of equal width

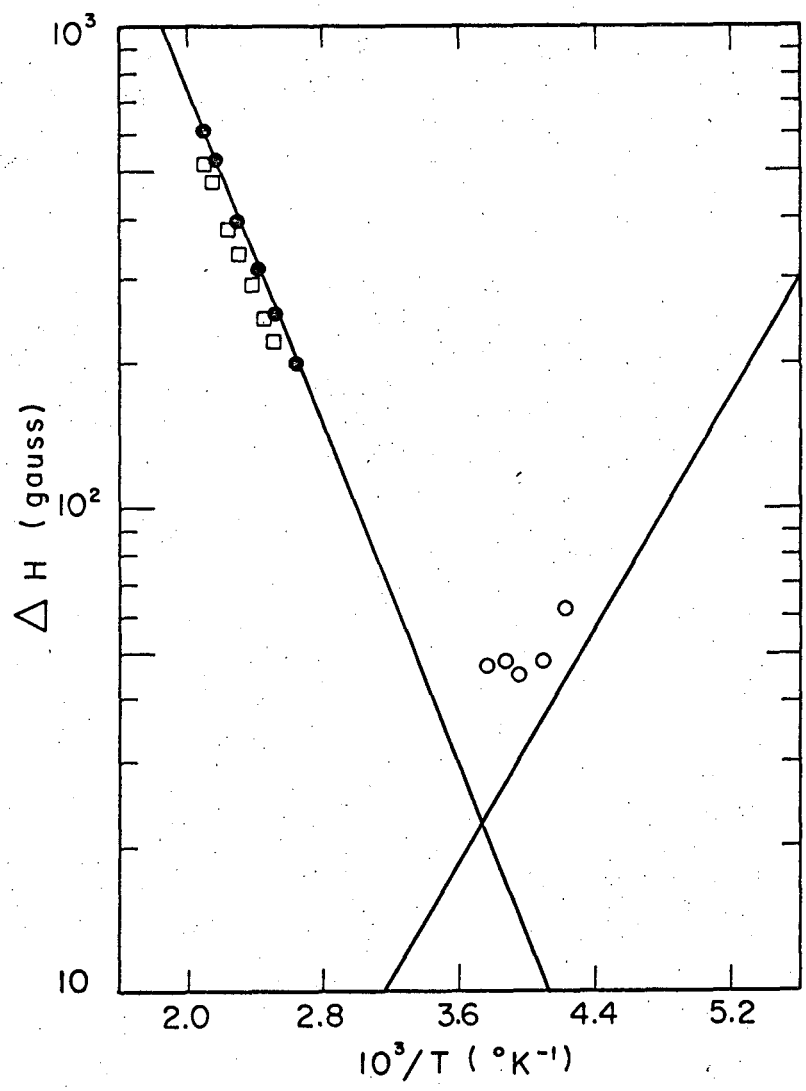

MU36084

Fig. 16

Table X. Line width for the $M_I = +3/2$ (high field) hyperfine component of 0.05 F $Cu(H_2O)_6^{++}$ in a 5.26 F $HClO_4$ solution

Temp. °C	ΔH ($M_I = +3/2$, high field) Experimental gauss	Corrected gauss
-8.0	37.0	47.3
-14.2	37.5	48.0
-19.1	36.0	45.2
-28.0	37.5	48.0
-36.0	44.7	62.1

at these temperatures. The open squares represent the D_2O data from Table IX. The open circles are for the low temperature data in Table X. The line of negative slope was drawn to give a best fit to the high temperature H_2O data. Since the ESR lines were seen to be symmetric above room temperature and asymmetric below room temperature, it was assumed that at lower temperatures significant contributions were being made to the line width from a different mechanism which has a dependence on M_I. Since contributions to the line width are additive, the contribution from the mechanism dominant at high temperatures was subtracted from the $M_{Cu} = +3/2$ line width observed at low temperature. In this way, the contribution to the line width of the $M_{Cu} = +3/2$ component by the low temperature mechanism was estimated and is represented by the line of positive slope in Fig. 16. Possible explanations for these two mechanisms will be discussed shortly. The enthalpies of activation for these two processes are given in Table XI along with their respective contributions to the total relaxation at 25°C.

Table XI. Enthalpy of activation and contribution to relaxation for high and low temperature processes for cupric ion in aqueous solution

High Temperature Mechanism	
$Cu(H_2O)_6^{+2}$ in 0.1 F $HClO_4$ at 25°C	$\Delta H^{\ddagger}$ = +3.3 kcal/mole
	contribution to line width = 48 ± 6 gauss
	contribution to T_2 = 1.2×10^{-9} sec
$Cu(D_2O)_6^{+2}$ in D_2O at 25°C	$\Delta H^{\ddagger}$ = +3.6 kcal/mole
	contribution to line width = 36 ± 5 gauss
	contribution to T_2 = 1.7×10^{-9} sec
Low Temperature Mechanism	
$Cu(H_2O)_6^{+2}$ in 5.26 F $HClO_4$ at 25°C	$\Delta H^{\ddagger}$ = -3.7 kcal/mole
	contribution to line width = 13 gauss
	contribution to T_2 = 4.5×10^{-9} sec for M_I = +3/2

The line width data for cupric ion in liquid ammonia could be handled in a more straightforward manner since the resolution was much better over a wider temperature range. Line width measurements were made on both the M_{Cu} = +3/2 (high field) and M_{Cu} = -3/2 (low field) hyperfine components and the experimental widths corrected for overlapping lines using the isotropic A value measured in solution. The experimental and corrected line widths are tabulated in Table XII. In addition, the line widths are given for the transition region where the sample was frozen but the spectrum remained isotropic in character. The line width results for cupric ion in the ammonia-THF mixture are given in Table XIII.

The data from Table XII for the variation of line width with temperature for cupric ion in liquid ammonia are shown plotted in Fig. 17.

Table XII. Line widths for 0.03 F $Cu(NH_3)_6^{++}$ in liquid ammonia

	$M_I = -3/2$ (low field)		$M_I = +3/2$ (high field)	
Temp. °C	Experimental gauss	Corrected gauss	Experimental gauss	Corrected gauss
-20.1			42.0	50.0
-21.0	43.0	51.6		
-27.6			38.8	45.2
-27.8	40.4	47.7		
-36.1			35.8	40.7
-36.2	37.3	42.8		
-45.9			31.8	35.0
-46.0	34.8	39.1		
-52.4			29.5	31.9
-53.2	33.0	36.6		
-61.5	31.8	34.8		
-62.4			26.1	27.4
-70.4	30.6	33.4		
-70.8			23.5	24.3
-75.4			21.8	22.4
-76.0	31.0	34.0		
-78.2			21.2	21.6
-80.7			21.0	21.4
-81.0	30.8	33.6		
Transition Spectra				
-89.2	43	51	31	34
-91.6	~70		35	40
-96.2			~54	
-102.4			~93	

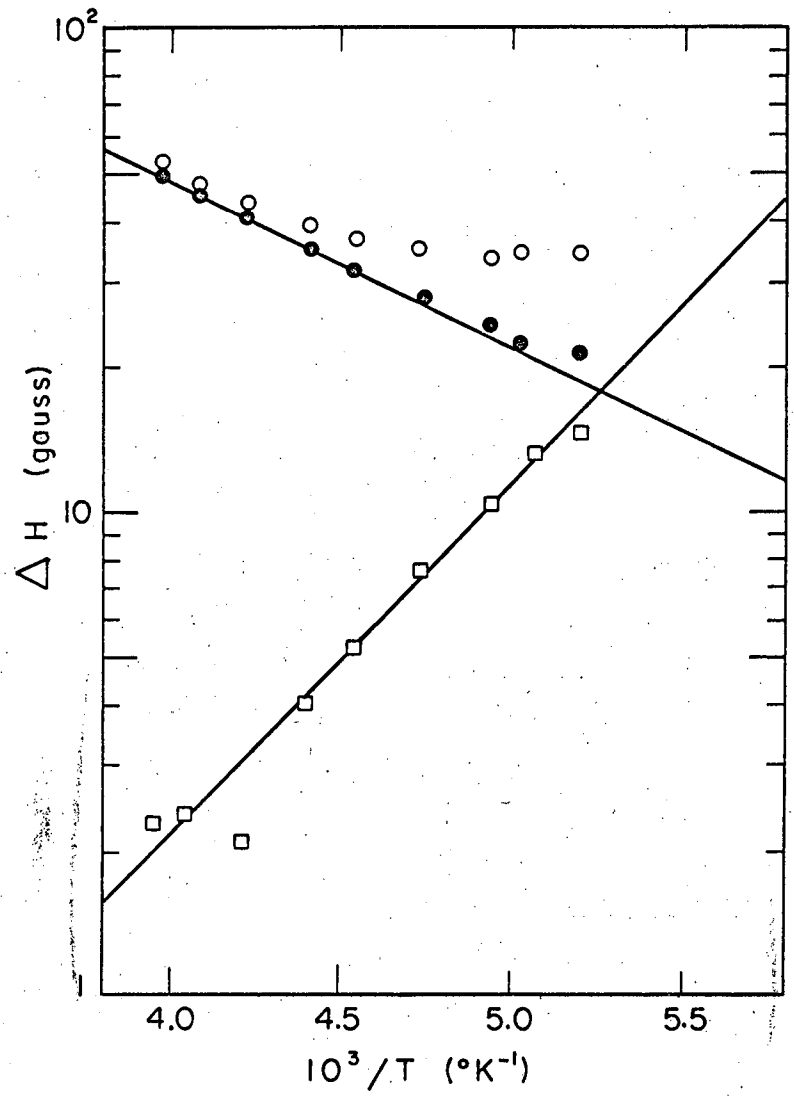

MU-36071

Fig. 17

The solid circles are the corrected line widths for the $M_{Cu} = +3/2$ hyperfine component while the open circles are for the $M_{Cu} = -3/2$ component. The line of negative slope was drawn to give a best fit to the five data points at highest temperature. These points were used because they represent a temperature range in which the low temperature mechanism contribution to the line width is unimportant. If one assumes that the high temperature mechanism contribution to the line width is the same for all the hyperfine components, then that contribution derived from the $M_{Cu} = +3/2$ component line width can be subtracted from the line width of the $M_{Cu} = -3/2$ component. The residual line width obtained in this way, indicated by the squares in Fig. 17, should be the contribution from the low temperature mechanism to the line width of the $M_{Cu} = +3/2$ component.

Table XIII. Line widths for 0.05 F $Cu(NH_3)_6^{++}$ in ammonia/THF

	$M_I = -3/2$ (low field)		$M_I = +3/2$ (high field)	
Temp. °C	Experimental gauss	Corrected gauss	Experimental gauss	Corrected gauss
-21.4	36.7	41.9	36.7	41.9
-50.1	35.0	39.3	29.0	31.2
-76.5	37.0	42.3	23.0	23.7

The enthalpies of activation for the high and low temperature mechanisms are given in Table XIV. The contribution of the high temperature mechanism to all the component line widths is included as well as the contribution of the low temperature mechanism to the line width of the $M_{Cu} = -3/2$ component at temperatures of 25° and -50 °C.

Table XIV. Enthalpies of activation and line width contributions for high temperature and low temperature relaxation mechanisms for $Cu(NH_3)_6^{++}$ in liquid ammonia.

High Temperature Mechanism	
	$\Delta H^{\ddagger}$ = 1.1 kcal/mole
contribution to line width	= 80.9 gauss at 25 °C 33.1 gauss at -50 °C
contribution to T_2	= 0.76×10^{-9} sec at 25 °C 1.9×10^{-9} sec at -50 °C
Low Temperature Mechanism	
	$\Delta H^{\ddagger}$ = -3.4 kcal/mole
contribution to line width for M_{Cu} = -3/2	= 0.72 gauss at 25 °C 4.7 gauss at -50 °C
contribution to T_2 for M_{Cu} = -3/2	= 8.6×10^{-8} sec at 25 °C 1.3×10^{-8} sec at -50 °C

Let us first consider the relaxation mechanism which is dominant at low temperatures. It is characterized by a line width which depends on the value of M_I and which decreases as the temperature is increased. Such behavior is typical for many complex ions in solution[19,76,85] and was first explained by McConnell[83] as being due to rotational averaging of the magnetic anisotropies of the complex. His treatment was for complexes with S = 1/2, which is the situation here. It is apparent that an inversion of the complex can have qualitatively the same net result as rotating the complex through an angle of 90°. The result in both bases is that if the symmetry axis of the complex was initially parallel to the magnetic field, it will now be perpendicular to it. The normal coordinates for this inversion process have been

discussed in detail by Avvakumov.[40] As will be shown shortly, the path followed in getting from the initial to the final state has a definite bearing on the relaxation time involved.

In order to compare the processes of inversion and tumbling we shall adopt a model for the inversion process in which the complex "jumps" from one of its three equivalent orientations to another. This model would be applicable if, for example, the complex remained in one orientation until a diffusional process in the second coordination sphere caused a transition to another orientation. This is to be compared with the tumbling model in which the complex retains its symmetry, but rotates continuously to a new position. The inversion process requires a displacement of the ligands along their respective metal-ligand axes while the tumbling process requires a rotational displacement of the ligands about the center of the complex. Thus, one can speak of the rotation of the "ligand-fixed" axis system for tumbling and the discontinuous change in orientation for the "ligand field-fixed" axis system for inversion.

The relaxation effects in terms of averaging magnetic anisotropies for such an inversion "jump" process can be derived in a manner strictly analagous to that used by McConnell[83] for tumbling. One starts by defining a "ligand-fixed" axis system p, q, r and a "ligand field-fixed" axis system x,y,z in which the z-axis is the unique or symmetry axis of the complex. The relationship between these two axis systems can then be defined. For this purpose we construct a set of special delta functions, δ_1, δ_2, δ_3. These delta functions have the property that $\delta_1 = 1$ when the r and z axes coincide and is zero otherwise. Similarly, $\delta_2 = 1$ when z and q coincide, $\delta_3 = 1$ when z and p coincide and both are zero otherwise. These delta functions have the properties

indicated in Eq.(13).

$$\delta_1 + \delta_2 + \delta_3 = 1 \tag{13a}$$

$$\delta_i \cdot \delta_i = \delta_i \tag{13b}$$

$$\delta_i \cdot \delta_j = 0 \tag{13c}$$

It is now possible to define H_z in terms of H_r, H_q and H_p using the delta functions and the same is true for the other operators in the usual axial spin Hamiltonian. An example is given in Eq.(14).

$$H_z = H_r\delta_1 + H_q\delta_2 + H_p\delta_3 \tag{14a}$$

$$S_z = S_r\delta_1 + S_q\delta_2 + S_p\delta_3 \tag{14b}$$

Making these substitutions into the usual Hamiltonian as given in Eq. (15),

$$\begin{aligned} \mathcal{H} = {} & \beta g_{\parallel} H_z S_z + \beta g_{\perp}(H_x S_x + H_y S_y) \\ & + A_{\parallel} I_z S_z + A_{\perp}(I_x S_x + I_y S_y) \end{aligned} \tag{15}$$

one obtains the Hamiltonian in terms of the delta functions as shown in Eq. (16).

$$\begin{aligned} \mathcal{H} = {} & g\beta H_o S_r + A I_r S_r + (\Delta g \beta H_o + b I_r)(\delta_1 - 1/3) S_r \\ & - \frac{b}{4}(I_+ S_- + I_- S_+)(\delta_1 - 1/3) - \frac{b}{4}(I_+ S_+ + I_- S_-)(\delta_2 - \delta_3) \end{aligned} \tag{16}$$

where

$$g = (g_{\parallel} + 2g_{\perp})/3 \qquad A = (A_{\parallel} + 2A_{\perp})/3$$

$$\Delta g = g_{\parallel} - g_{\perp} \qquad b = A_{\parallel} - A_{\perp}$$

The first two terms of the Hamiltonian in Eq. (16) will give rise to the usual isotropic solution spectrum. The third term, which is also constant in the spin operators, will give rise to modulation of the resonance and dephasing of the electron spin (contribute to $1/T_2$).

The final terms include simultaneous electron spin and nucelar spin transitions, giving rise to spin-lattice (T_1) relaxation. At this point in the derivation for tumbling,[83] the Hamiltonian contains terms analagous to those in Eq. (16) with the exception of two additional terms,

$$1/2(\Delta g\beta Ho + bI_r)(\sin\theta\cos\theta)(S_+e^{-i\phi} + S_-e^{+i\phi})$$
$$+ (1/2)b(\sin\theta\cos\theta)(I_+e^{-i\phi} + I_-e^{+i\phi})S_r.$$

The first of these terms, involving the electron spin raising and lowering operator, gives rise to electron spin-lattice relaxation while the second does the same for the nuclear spins. On this basis, it would appear likely that the tumbling mechanism should be more effective in inducing electron spin-lattice relaxation than the inversion mechanism.

To facilitate solution of the problem at this point, McConnell[83] introduces the approximation, $\Delta g\beta H \gg b$, so that the terms in the Hamiltonian having only b as a coefficient may be ignored. At this level of approximation, then, the two Hamiltonia are given in Eqs. (17) and (18).

Tumbling:
$$\begin{aligned}\mathcal{H}_t &= g\beta H_o S_r + AI_rS_r \\ &+ (\Delta g\beta H_o + bI_r)(\cos^2\theta - 1/3)S_r \\ &+ 1/2(\Delta g\beta H_o + bI_r)(\sin\theta\cos\theta)(S_+e^{-i\phi} + S_-e^{+i\phi})\end{aligned} \tag{17}$$

Inversion:
$$\begin{aligned}\mathcal{H}_i &= g\beta H_o S_r + AI_rS_r \\ &+ (\Delta g\beta H_o + bI_r)(\delta_1 - 1/3)S_r\end{aligned} \tag{18}$$

Inspection of Eqs. (17) and (18) shows that the process of dephasing of the spins will be the same for the two mechanisms except for the averaging over the time-dependent orientation functions. The more

striking difference is that the inversion should be much less effective than tumbling for spin-lattice relaxation. Using the time averages of the orientation functions given in Eq. (19),

$$\langle |\cos^2\theta - 1/3|^2 \rangle = \frac{4}{45} \tag{19a}$$

$$\langle |\delta_1 - 1/3|^2 \rangle = \frac{2}{9} \tag{19b}$$

one can carry through the McConnell derivation. The result for inversion is given in Eq. (20) and can be compared with the result for tumbling in Eq. (21).

$$\text{Inversion: } \left(\frac{1}{T_2'}\right)^2 = \frac{16\pi}{9h^2} (\Delta g\beta H_o + bM_I)^2 \tan^{-1}\left(\frac{2\tau_i}{T_2'}\right) \tag{20}$$

$$\text{Tumbling: } \left(\frac{1}{T_2'}\right)^2 = \frac{32\pi}{45h^2} (\Delta g\beta H_o + bM_I)^2 \tan^{-1}\left(\frac{2\tau_t}{T_2'}\right) \tag{21}$$

In these equations τ_i and τ_t are the characteristic times associated with the inversion and tumbling processes respectively. $1/T_2'$ is the contribution of that mechanism to the overall line width. In the event that $1/T_1$, the spin-lattice contribution, does not contribute appreciably to the line width as is assumed in this case, then $T_2' = T_2$. An additional simplification is obtained when $\tau/T_2 \ll 1$, as is generally true in these studies. The $\tan^{-1}$ dependence can then be approximated to give the relationships in Eqs. (22) and (23) for relaxation.

$$\text{Inversion: } \frac{1}{T_2'} = \frac{32\pi}{9h^2} (\Delta g\beta H_o + bM_I)^2 \tau_i \tag{22}$$

$$\text{Tumbling: } \frac{1}{T_2'} = \frac{64\pi}{45h^2} (\Delta g\beta H_o + bM_I)^2 \tau_t \tag{23}$$

One can see from comparing Eqs. (22) and (23) that the tumbling mechanism should give line widths which are 2-1/2 times smaller for a given anisotropy and correlation time. The magnetic field and M_I

dependence for the two should be the same. Looking back at Eqs. (17) and (18), we can see that at this level of approximation the inversion mechanism should introduce no spin-lattice relaxation while tumbling definitely does. It must be remembered, however, that we have neglected terms of the order b^2 relative to those of the order $(\Delta g\beta H_o)^2$ or $b(\Delta g\beta H_o)$ in both derivations. For the cupric complexes we have seen that b can close to the magnitude of $\Delta g\beta H_o$, indicating that our approximation may not be too good. We can at least say that spin-lattice relaxation should be more effective for tumbling by virtue of the differences in the Hamiltonian for the two cases as discussed following Eq. (16). One can also predict that spin-lattice relaxation should be independent of magnetic field for the inversion mechanism as seen from Eq. (16) while tumbling contributions to spin-lattice relaxation should show a magnetic field dependence.

It is now desirable to use the experimentally determined relaxation times and magnetic anisotropies to estimate correlation times for tumbling or inversion. The correlation times obtained in this way can then be compared with the correlation time for tumbling calculated from viscosity data and also with the rate of water exchange. It should be kept in mind that the characteristic times for tumbling or inversion calculated from Eqs. (22) and (23) represent lower limits for those times since we are treating each process separately and assuming that the other does not contribute to the averaging. The results of these calculations for $Cu(H_2O)_6^{+2}$ in aqueous solutions are presented in Table XV. The magnetic anisotropies were calculated from the values in Table VII assuming that both $A_{\parallel}$ and $A_{\perp}$ are negative,[12] and using a value for H_o = 2943 gauss. Correlation times for tumbling

Table XV. Contributions to the low temperature relaxation of $Cu(H_2O)_6^{++}$ in solution at 25°C (M_I = +3/2 component)

$\frac{\Delta g \beta H_o}{h} = 1.29 \times 10^9 \text{ sec}^{-1}$ $\qquad$ $\frac{b}{h} = -0.444 \times 10^9 \text{ sec}^{-1}$

From Eq. (8) $\tau_i \geq 5.2 \times 10^{-11}$ sec

From Eq. (9) $\tau_t \geq 1.3 \times 10^{-10}$ sec

From Eq. (10) $\tau_t = 7.4 \times 10^{-11}$ sec for 5.26 F $HClO_4$

$\tau_t = 4.9 \times 10^{-11}$ sec for pure H_2O

Rate of exchange of water*

$\frac{1}{k_r} = 6.7 \times 10^{-10}$ sec for 5.26 F $HClO_4$

$= 1.2 \times 10^{-10}$ sec for 0.1 F $HClO_4$

*Reference 19

were calculated for comparison using Eq. (24),[83] for the tumbling of a spherical ion of radius a_o in a medium viscosity η

$$\tau_t = \frac{4\pi a_o^3 \eta}{3kT} \tag{24}$$

Merideth[42] used a value of 3.65Å for the ionic radius, a_o, based on an average Cu-O bond distance of 2.25Å taken from crystal structures of cupric hydrates and the van der Waals radius for oxygen. The viscosity of water is readily available[92] and the viscosity of the $HClO_4$ solution was taken from the work of Brickweddie.[79] Values for the low temperature contribution to T_2 were taken from Table XI.

If one assumes that the entire low temperature contribution to the line width is from the inversion process, then one obtains a minimum value for the characteristic time for inversion of 5.2×10^{-11} sec.

Regardless of any other processes occurring, we know that the characteristic time for inversion cannot be shorter than this value since that would lead to a longer T_2 than observed. Merideth[42] has interpreted his H_2O^{17} exchange studies to mean that the exchange of water from the axial position in the complex into the bulk solution is the rate determining step whose rate is given by k_r. He also concludes that the rate of inversion of the complex is faster than k_r, i.e., that a particular water molecule will see both an axial and an equitorial environment before being expelled back into solution. Thus, $1/k_r$ sets an upper limit on the inversion lifetime of the complex. The combination of these limits requires that the inversion lifetime lie in the range of 7×10^{-10} to 5×10^{-11} sec.

If one assumes that the entire low temperature contribution is due to tumbling of the complex, one calculates a correlation time for tumbling of 1.3×10^{-10} sec. For comparison, the tumbling correlation time calculated from the ionic radius and viscosity is around 6×10^{-11} sec, a factor of two shorter. The uncertainty in the choice of ionic radius could probably account for this sort of discrepancy.

Since the rates of inversion, exchange and tumbling for the complex all lie within a narrow time interval it is simplest to consider them as all controlled by a common mechanism. Such a mechanism would involve the motion or diffusion of water molecules into and out of the second coordination sphere as well as the direct exchange process in the first coordination sphere. The result would be that almost every inversion would be accompanied by the loss of an axial water molecule from the complex. Support for such a conclusion is found in the similarity of the enthalpies of activation for relaxation, exchange and viscosity.

Using the viscosity of water[92] or perchloric acid solutions[79] from room temperature to -50°C, one obtains an enthalpy of activation of -5 kcal/mole. The enthalpy of activation for the low temperature contribution to the line width is -4 kcal/mole and the enthalpy of activation for water exchange[42] is +4 kcal/mole, of the opposite sign and the same absolute magnitude as expected.

For cupric ion in liquid ammonia the separation of the high and low temperature contributions is much more clear cut. Unfortunately, all that is known about the rate of ammonia exchange is that the rate constant is greater than 10^6 sec^{-1} at 25°C.[93] It is still possible to set limits on the characteristic times for tumbling and inversion for $Cu(NH_3)_6^{+2}$ in liquid ammonia from the data in Tables VII and XIV using Eqs. (22) and (23). The results of these calculations along with the estimated tumbling correlation time using Eq. (24) are listed in Table XVI.

Table XVI. Contributions to the low temperature relaxation of $Cu(NH_3)_6^{++}$ in liquid ammonia (M_I = -3/2 component)

$\frac{\Delta g \beta H_o}{h} = 8.15\times10^8$ sec^{-1}	$\frac{b}{h} = -5.51\times10^8$ sec^{-1}
At 25°C	
From Eq. (8)	$\tau_i \geq 3.9\times10^{-13}$ sec
From Eq. (9)	$\tau_t \geq 9.7\times10^{-13}$ sec
From Eq. (10)	$\tau_t = 5.9\times10^{-12}$ sec
At -50°C	
From Eq. (8)	$\tau_i \geq 2.6\times10^{-12}$ sec
From Eq. (9)	$\tau_t \geq 6.4\times10^{-12}$ sec
From Eq. (10)	$\tau_t = 1.9\times10^{-11}$ sec

The ionic radius was taken to be the sum of an average Cu-N bond distance for ammine complexes[94] (2.0Å) and the van der Waals radius for nitrogen[95] (1.5Å), or 3.5Å. The viscosity data for liquid ammonia show a good deal of scatter so the average of several sets of data was used.[96,97,98] The tumbling correlation times calculated from the ionic radius and viscosity are approximately a factor of 10 longer than the tumbling correlation times derived from the T_2 contributions both at 25° and -50°C. Even though the tumbling correlation time derived from the viscosity and ionic radius is subject to uncertainty as is the correlation time calculated from the McConnell mechanism due to the approximations involved, this factor of ten discrepancy suggests that tumbling is not responsible for the rotational averaging of the magnetic anisotropies. The enthalpy of activation for the low temperature contribution to the relaxation (-3 kcal/mole) and the enthalpy of activation for the viscosity (-2 kcal/mole), however, still suggest the possibility of related mechanisms for averaging and viscosity. The larger contribution of the low temperature mechanism for cupric ion in the ammonia-THF mixture would be consistent with an increased viscosity for the mixture relative to that of pure ammonia.

The existence of the transition region in which the sample is frozen, but there is still averaging of the anisotropies, gives strong support to the model of inversion of the complex strongly influenced by its local environment as the source of averaging for cupric ion in pure ammonia. First, comparison of the line width contributions in this transition region with those plotted in Fig. 17 for liquid ammonia shows that the extent of averaging is changing much more rapidly with temperature for the frozen sample. This is in accord with the more

restricted motion in the solid than in the solution. Although there is undoubtedly movement of the ammonia molecules in the solid at these temperatures, it is easier to visualize the $Cu(NH_3)_6^{+2}$ complex undergoing inversion with the cooperation of the surrounding ammonia molecules than rotation of the complex as a whole. Using the model for the inversion set up earlier, one can calculate from Eq. (22) the characteristic time for inversion from the line widths in this transition region. At a temperature of -80°C where the sample is still liquid, the time for inversion is calculated to be 8×10^{-12} sec from the low temperature contribution to the line width of the $M_I = -3/2$ hyperfine component. The calculated inversion time changes continuously (but with a greater temperature dependence than in solution) throughout the transition region. At -92°C the same calculation gives an inversion time of 1×10^{-11} sec. When the temperature has been lowered another 10 degrees, the spectrum has almost completed its transition to that for a glass at low temperatures. The Larmor precession frequency, ω_o, is 5.6×10^{-10} sec in these experiments so that $1/\omega_o$ is 2×10^{-11} sec. This means that an averaging process with a characteristic time shorter than 2×10^{-11} sec should give a partially averaged spectrum, while for a characteristic time longer than 2×10^{-11} sec, the spectrum should start to show anisotropic structure. Thus the characteristic times calculated from the inversion model and found directly by comparison with the Larmor frequency are in good agreement.

The high temperature contribution to the line width of cupric ion in solution has been of major interest in the past. It is apparent that the source of line width is not an averaging mechanism such as has just been discussed. Such a mechanism would be expected to show a

a temperature dependence for the line width opposite that observed at high temperatures. In addition, it should show a marked dependence on the Larmor frequency for the experiment. Kozyrev[38] has shown that there is no dependence on the Larmor frequency in the range of 10^8-10^{10} sec^{-1}. We have also established that the rates of inversion and exchange at 25°C are approximately a factor of 10 more rapid than the rate of electron spin relaxation. It is not surprising that the process of exchange of water in the axial position should be ineffective for relaxing the electron spin since the magnetic properties of the complex are quite insensitive to the axial substituent.

Another possible source of relaxation is vibronic modulation of the ligand field as suggested by Al'tshuler and Valiev.[39] Their treament is concerned with relaxation through the low-lying $^2B_{1g}$ excited state lying approximately 1000 cm^{-1} above the ground state. According to the treatment by Avvakumov,[40] one would expect the degenerate vibrations leading to inversion of the complex to be most effective in producing this sort of relaxation. Al'tshuler and Valiev[39] predict that the line width for $Cu(H_2O)_6^{+2}$ should be proportional to the quantity $\tau/(1 + \omega_{ab}^2 \tau^2)$ where ω_{ab} is the frequency interval characteristic of the separation between the $^2A_{1g}$ gound state and the $^2B_{1g}$ excited state and τ is the correlation time for the vibration responsible for the relaxation. In this case, τ should be identified with the characteristic time for inversion, τ_i, discussed earlier. They estimate for cupric complexes that $\omega_{ab}^2\tau^2 \gg 1$ so that the line width would be expected to be proportional to $1/(\omega_{ab}^2\tau)$. This predicts that as the correlation time decreases, the line width increases as is observed for the high temperature region for cupric ion in water and liquid ammonia.

The results for cupric ion in D_2O follow this same trend. At a given temperature the viscosity of D_2O is approximately 15% greater than that of H_2O.[99] This would be expected to result in a corresponding increase in the vibrational correlation time and a decrease in the line width. Comparison of line widths for cupric ion in H_2O and D_2O at the same temperature shown in Fig. 16 do show the expected 15% decrease in line width upon going to D_2O. Experiments in aqueous cupric solutions containing 20 mole % p-dioxane show similar behavior. Although the exact viscosity of such solutions is not known at temperatures above 60°C, the 10% decrease in line width for the p-dioxane/water mixture at 140°C is approximately what one would expect from the data available at lower temperatures.[100] This suggests that the change in width for D_2O is primarily due to the change in solvent viscosity rather than a specific change in the complex. Rivkind[101] has observed similar behavior for copper-ammonia complexes in solution. He found that the line width depended primarily on the viscosity of the solvent when he added glycol or polystyrene to the aqueous solutions at room temperature. The situation in liquid ammonia is similar. Presumably the ammonia/THF mixture is more viscous than pure ammonia. At the higher temperatures this leads to narrower lines in the mixed solvent while in the low temperature region the line widths are greater in the mixed solvent due to less complete averaging.

When one attempts to rationalize the exact temperature dependence the agreement is only qualitative. If inversion is responsible for both the high and low temperature relaxation mechanisms, then the two mechanisms should have approximately equal and opposite enthalpies of activation. This is seen to be so to within a kilocalorie for the

aqueous solutions. In addition, the enthalpies of activation for viscosity of H_2O and D_2O in the appropriate temperature ranges are also close. For cupric ion in liquid ammonia the enthalpy of activation for the low temperature relaxation mechanism is -3 kcal/mole while that for the high temperature mechanism is +1 kcal/mole. For viscosity the enthalpy of activation is -2 kcal/mole in the range -20° to -60°C.[96,97,98] Since the uncertainties in the ammonia line width data are much smaller than those for water, we must conclude that the enthalpies of activation for the two relaxation mechanisms need not be identical. Hayes[19] has reconsidered the mechanism proposed by Al'tshuler and Valiev[39] for vibrational modulation of the ligand field and has concluded that the increase in line width with temperature should be approximately linear. Thus, the Al'tshuler and Valiev theory must be considered only a qualitative description of a possible relaxation mechanism.

The possibility that the electron spin relaxation is controlled by chemical processes should also be considered. We have already seen that the rate of axial exchange of waters is more rapid than the rate of spin relaxation. It is possible that equatorial exchange at a rate on the order of ten to one hundred times slower than axial exchange could account for the observed relaxation. The electronic structure of the complex is certainly more sensitive to the equatorial ligands than to the axial ones so that exchange of an equatorial ligand would be expected to cause relaxation of the electron spin. For such a mechanism the enthalpy of activation would be that observed for the variation of the line width at high temperatures. Taking the rate constant for the exchange of the ligand at only one of the four equivalent positions, one calculates that the entropy of activation for equatorial water

exchange would be -9 e.u. while that for ammonia exchange would be -16 e.u. Negative entropies of activation in this size could be attributed to significant participation by the solvent in the activated complex.

A more interesting test of these possible relaxation mechanisms would be to determine the electronic spin-lattice relaxation time, T_1. Al'tshuler and Valiev[39] predict that T_1 should be significantly longer than T_2 and that T_1 should increase as the temperature is raised. Chemical exchange of an equatorial ligand should cause spin-lattice relaxation to occur giving $T_1 = T_2$ with T_1 decreasing as the temperature is raised. Merideth[42] interpreted the chemical shift for H_2O^{17} due to cupric ion as indicating that the electronic T_1 was significantly longer than the electronic T_2, but that their temperature dependence was the same. A direct measurement of the electronic T_1 should help to clarify the situation.

In conclusion, we have corrected the line width of cupric ion in aqueous and ammoniacal solution for overlapping hyperfine structure and have separated the observed line width into contributions from two mechanisms. At low temperatures the relaxation is dominated by incomplete averaging of the magnetic anisotropies of the complex. The averaging process is taken to be inversion of the complex rather than rotation. This view is substantiated by the observation of averaging in frozen samples where the process of inversion could still occur while rotation of the complex as a whole should not. The source of the relaxation process dominant at higher temperatures is less certain. Arguments are given supporting the theory that vibronic modulation of the ligand field is responsible for relaxation. In addition, a possible

mechanism for chemical exchange controlled relaxation is suggested. A means for distinguishing between these two mechanisms by measurement of the electronic T_1 is proposed.

C. $FeCl_4^-$

In order to discuss the spectra of ferric ion in glasses, it will be necessary to summarize the theory of paramagnetic resonance for the case where $S = 5/2$. It is customary to describe the pertinent interactions in terms of the spin Hamiltonian given in Eq. (25) and as discussed in the Introduction. The x-y-z axis system is molecule-fixed

$$\mathcal{H} = g\beta\bar{H}\cdot\bar{S} + D[S_z^2 - (1/3)S(S+1)] + E(S_x^2 - S_y^2) \qquad (25)$$

with the z-axis usually taken along the symmetry axis for the complex in single crystal studies. There may be additional terms involving higher order electron spin operators, but they are smaller than the D and E terms, the interaction with the magnetic field, or both as in the present case. Their inclusion would not add to the argument and the small effects to which they give rise could not be resolved in glass spectra. For ferric ion with its $3d^5$ electronic configuration and $^6S_{5/2}$ ground state, the g value is found to be isotropic and close to that of the free electron. For the rest of our discussion we will assume that $g = 2.00$. Since the bulk of naturally abundant iron has no nuclear spin and no hyperfine is observed from the ligands, we have not included the hyperfine interaction in the spin Hamiltonian.

First, let us consider the case when the interaction of the electron spin with the external magnetic field is the largest term in the Hamiltonian. Treating the D and E terms as perturbations, one sees that although the energies of the M_s states vary with the relative

orientation of the magnetic field and crystal z-axis, the energy of separation between the $M_s = \pm 1/2$ levels remains the same. This means that so long as D and E are smaller than $g\beta H$, there will be an isotropic transition at $g = 2.00$. In second order, this transition is slightly broadened, but unaltered otherwise. In addition, the other transitions should be symmetrically disposed about $g = 2$. Thus, absence of an isotropic line at $g = 2$ for ferric glasses indicates that the zero field splittings must be sizeable.

Slichter[65] has considered the case when the zero field energies are much larger than the magnetic field interaction. He treats the system using the molecule-fixed axis system in which the z-axis is the symmetry axis of the complex. In this representation he deals with two extreme possibilities. In one case he takes D large and $E = 0$, and in the other, E larger and $D = 0$. The first possibility corresponds to a complex in which the x and y axes are equivalent. He then discusses the conditions under which the second possibility could arise. Wickman[66] has shown that by a transformation of the coordinate system one can always work in a representation in which $0 \leq |E/D| \leq 1/3$. The zero field Hamiltonian in this representation is given in Eq. (26).

$$\mathcal{H} = D[S_{z'}^2 - (1/3)S(S+1)] + \lambda(S_{x'}^2 - S_{y'}^2) \qquad (26)$$

where $\lambda = E/D$, $|\lambda| \leq 1/3$. It is apparent that when $\lambda = 0$ this is equivalent to Slichter's[65] case with $E = 0$. Wickman[66] shows that $|\lambda| = 1/3$ corresponds to Slichter's[65] case for $D = 0$ with large E. In this transformed representation, E is always positive while D has the same sign as λ. The treatment is analagous to the nuclear quadrupole interaction and its asymmetry parameter, η.

This transformed zero field Hamiltonian can then be diagonalized for various values of λ and the eigenvalues and eigenfunctions obtained. There are three energy levels each with a two-fold ($\pm M_s$) degeneracy in zero field. The ordering of the energy levels, but not their spacing, depends on the sign of λ. Thus, only positive values for λ need be considered. One can now introduce as a perturbation the interaction of the magnetic field with the new spin functions which are linear combinations of the old $M_s = \pm 1/2$, $\pm 3/2$ and $\pm 5/2$ spin states. Since we have assumed that D is large, the separation between the energy levels in zero field is greater than the energy of the microwave quantum being used and transitions between those levels will not be observed. Those levels which were degenerate in zero magnetic field will now be split and it will be possible to observe transitions between such levels. The separation between these initially degenerate levels will be linear in the applied magnetic field with a slope, m, which depends on the value of λ and the angle between the axis of spin quantization and the external magnetic field. The resonance condition for transitions between such levels is just

$$h\nu = mg\beta H \tag{27}$$

where ν is the microwave frequency and g is taken to be 2.00. Thus, one can define an effective g value, g_{eff}, which describes such a transition. Wickman[66,67] lists these g_{eff} values for each of the three zero field levels as a function of λ. Since these g_{eff} values are different for different orientations of the magnetic field, he gives principal values for them with the magnetic field parallel to the axis of quantization (g_z) and perpendicular to it (g_x and g_y).

In the limit of $\lambda = 0$, the lower level gives $g_z = 2$, $g_x = g_y = 6$. This was discussed by Slichter[65] and is expected to give a resonance peaked at $g_{eff} = 6$ and ending at $g_{eff} = 2$ since all orientations are present in a glass. In the limit of $\lambda = 1/3$, an interesting result is obtained for the middle level where $g_x = g_y = g_z = 30/7 = 4.286$. This indicates that there is an isotropic transition at $g_{eff} = 4.286$. The other two levels have principal g_{eff} values of 0.607, 0.857 and 9.678. Thus, one might expect band edges to occur at those g_{eff} values. As one moves away from $\lambda = 1/3$, one would expect the width of the $g_{eff} = 4.286$ peak to increase. Wickman[66,67] observed a rather broad resonance for ferrichrome A at $g_{eff} = 4.3$ and estimated from its width that $\lambda = 0.25 \pm 0.04$. At 1°K he observed the band edges appropriate to that value of λ. Slichter[65] observed a much sharper resonance for ferric ion in samples of plate glass at $g_{eff} = 4.27$ indicating that λ was close to 1/3. Under favorable conditions, variation of relative intensities for lines arising from different zero field levels as the temperature is lowered makes it possible to estimate the size and sign of D.

Slichter[65] advanced several suggestions for ligand field symmetries which could give rise to the situation with $\lambda = 1/3$ and a large D. Griffith[68] considers the two environments suggested by Slichter[65] and adds one other possibility. He shows from group theoretical arguments that these symmetries could easily give rise to a situation in which D is large and λ approaches 1/3, but he finds that λ could be exactly 1/3 only accidentally. The three symmetries considered are a regular tetrahedron with two different groups, MA_2B_2; a distorted octahedron, MA_6, for which the equatorial groups are at the corners of a rectangle;

and an octahedral complex of the type MA_3B_3 with C_{2v} symmetry. As Griffith[68] points out, however, there may be other possibilities.

We now have several useful relationships between glass or polycrystalline ferric spectra and the properties of the complex giving rise to the spectrum. When the symmetry of the complex is close to cubic and/or the zero field terms small relative to the microwave frequency, an isotropic line at $g_{eff} = 2$ is expected. The absence of a line at $g_{eff} = 2$, if other lines are observed, indicates that the zero field terms are large. The appearance of lines in the higher g_{eff} value region of the spectrum can then be interpreted in terms of the value for λ derived from the spectrum.

The glass spectrum for 1×10^{-2} F $FeCl_3 \cdot 6H_2O$ in concentrated HCl is shown in Fig. 18. The most prominent feature is the sharp, relatively isotropic resonance at $g_{eff} = 4.24\pm0.06$ with a width of 47 ± 5 gauss. There is also seen to be an onset of resonance between $g_{eff} = 9$ and 10 and an inflection at $g_{eff} = 6$. The spectrum did not change noticeably with the ferric concentration was reduced by a factor of 10. The width of the $g_{eff} = 4.24$ line gives a value for $|\lambda| = 0.322\pm0.005$ which is quite close to the limiting value of 0.333. This calculation assumes that the observed line width is due entirely to the anisotropy of the transition. If the anisotropy is less than the line width, then the value for λ would be even closer to 1/3. Using Wickman's[66] table of principal g_{eff} values, one obtains the following principal g_{eff} values when $\lambda = 0.322$:

Upper level	0.79,	0.57,	9.71
Middle level	4.28,	4.22,	4.35
Lower level	0.93,	9.65,	0.65.

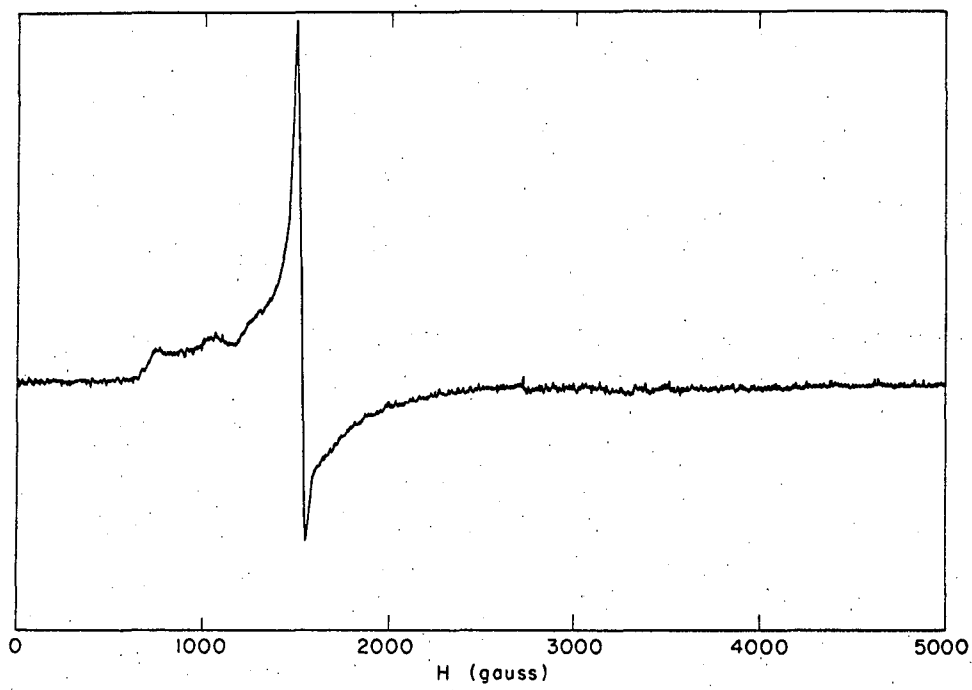

MU-36092

Fig. 18

These results predict an onset of resonance around $g_{eff} = 9.7$ as is observed. Band edges which could also be observed with the magnetic field strength available are expected at $g_{eff} = 0.93$ and 0.79 (7 and 8 kilogauss). The fact that they are not observed under present conditions is probably due to their width. These low g_{eff} values are changing more rapidly with λ than are those at $g_{eff} = 9.7$ so they would be expected to be more sensitive to stresses in the glass. In addition, there are two transitions occurring close together around $g_{eff} = 9.7$ and only one at each of the higher g_{eff} values.

It is now necessary to assign this resonance to the appropriate ferric complex. As discussed in the introduction, it seems well established that the predominant species in concentrated HCl is a complex with 4 chloride ligands. In non-aqueous systems[103,104] there is evidence that the complex is $FeCl_4^-$ with a regular tetrahedral structure. The two crystal structure determinations for salts of the complex[52,102] again show discrete $FeCl_4^-$ units, but with distorted tetrahedral structures. The question remains whether the tetrachloro complex in aqueous solution is tetrahedral, or whether it contains additional water ligands. The radial distribution functions of the solution x-ray studies[47,48] have been the center of some controversy, but there seems to be agreement that the primary species present in concentrated HCl is the tetrahedral $FeCl_4^-$. The strongest evidence for the tetrahedral $FeCl_4^-$ structure in solution comes from electronic spectra. The similar electronic spectra for the concentrated HCl solutions,[45] ether extracts,[44] solutions of $(CH_3)_4NFeCl_4$ in acetone,[47] and for the crystalline salts,[45] have all been assigned to the common component, $FeCl_4^-$.

If we accept the premise that the predominant species in concentrated

HCl solution is the tetrahedral $FeCl_4^-$ and that the chemical composition of this species does not change during rapid freezing to make the glass, then the ESR spectrum of the glass has definite implications for the structure of the $FeCl_4^-$ complex in the glass. Since there is no line observed at $g_{eff} = 2$, we can rule out the possibility that $FeCl_4^-$ exists in the glass with a regular tetrahedral structure. The line at $g_{eff} = 4.24$ requires that the complex have a large D value and be of an appropriate symmetry. The distorted tetrahedral structures found for $FeCl_4^-$ in its salts[52,102] approximate the case of a 4-coordinated complex with C_{2v} symmetry suggested by Slichter[65] and Griffith[68] as being capable of giving a resonance at $g_{eff} = 4.3$. Thus, there is evidence favoring distortions of this sort in the solid state which could give rise to a $g_{eff} = 4.3$ resonance for $FeCl_4^-$ in a glass. On the basis of the ESR spectrum alone it is not possible to rule out species such as trans-$FeCl_4(H_2O)_2^-$ with the equatorial chlorides at the corners of a rectangle (but not a square), or possibly even the cis-$FeCl_4(H_2O)_2^-$ which also has C_{2v} symmetry. Considering the weight of evidence for a tetrahedral $FeCl_4^-$ in solution, however, we have assigned the spectrum in Fig. 18 to a tetrahedral $FeCl_4^-$ which is sufficiently distorted in the glass to have a large D value and λ close to 1/3.

Clearly, the small absorption observed at $g_{eff} = 6$ cannot be due to the complex responsible for the rest of the spectrum since the $g_{eff} = 6$ transition requires that λ be close to zero. Since it has been observed[45] that the intensity of the optical absorption of $FeCl_4^-$ still increases as the HCl concentration is increased from 12 to 16 F, the existence of a second species in 12 F HCl is likely. Two complexes which would meet these requirements are a tetrahedral $FeCl_3(H_2O)$ complex or the 6-coordinated

$FeCl_3(H_2O)_3$ complex with a three-fold axis. One further possibility is that the second species is trans-$FeCl_4(H_2O)_2^-$ with a regular four-fold axis. This final possibility would require that the effect of adding further HCl be to dehydrate the complex to give additional $FeCl_4^-$.

A second set of experiments was performed with $FeCl_3 \cdot 6H_2O$ dissolved in 10 F $HClO_4$. Figure 19 is the spectrum obtained from such a glass. The main features of this spectrum are quite similar to those for ferric chloride in HCl. The only additional feature is the presence of a line at $g_{eff} = 2$. It was found that the line width was slightly greater for 0.05 F ferric solutions than for 0.01 F, so the measurements were made at the lower concentration. The width of the line at $g_{eff} = 4.24 \pm 0.08$ was found to be 55±3 gauss. If all the line width were due to anisotropy in the g_{eff} value, the appropriate value for $|\lambda|$ would be 0.330±0.005. This is quite close to the value found for λ in concentrated HCl, and the principal g_{eff} values are almost identical with those listed previously. It has been suggested[47] that $FeCl_4^-$ is formed when ferric chloride is dissolved in strong perchloric acid solutions. An equilibrium[104] of the type in Eq. (28), which results

$$2\ FeCl_3(H_2O)_3 = FeCl_4^- + FeCl_2(H_2O)_4^+ + 2H_2O \qquad (28)$$

in the reduction of the water coordinated with ferric ions, should be favored in strong perchloric acid media. Thus, the sharp resonance at $g = 4.24$ is again taken to be due to the presence of $FeCl_4^-$.

An equilibrium of the type in Eq. (28) also provides a second species responsible for the 130 gauss wide resonance appearing at $g_{eff} = 2$. Of course further equilibria could be involved to give other complexes with even fewer coordinated chlorides. As will be explained shortly, there is

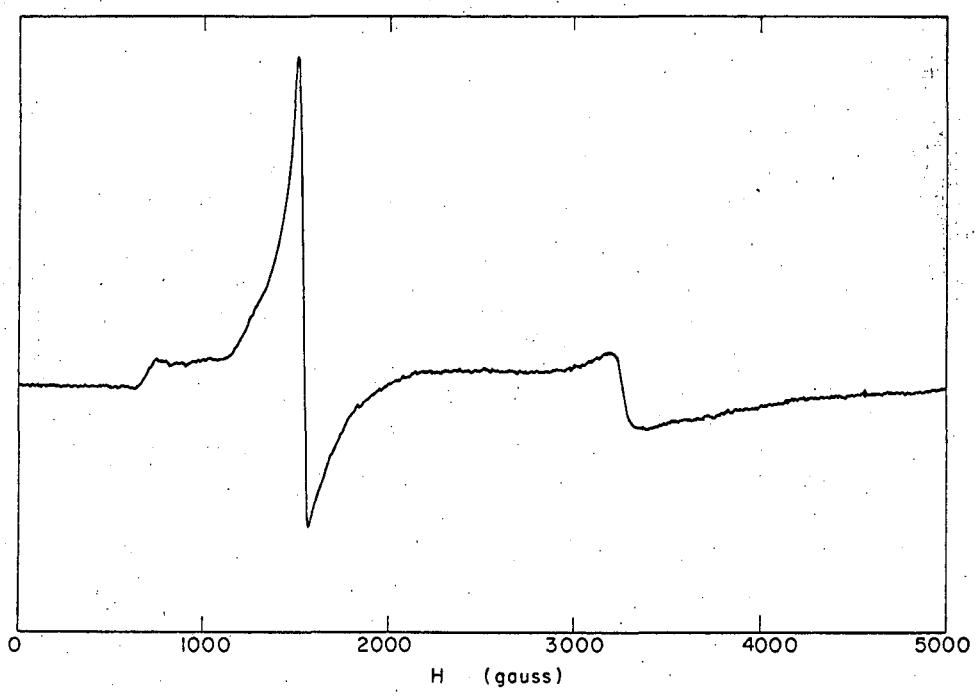

MU-36094

Fig. 19

reason to believe that there is some chloride associated with the predominant species responsible for the line at $g_{eff} = 2$. We know from our previous analysis that the existence of a line at $g_{eff} = 2$ (without an accompanying line at $g_{eff} = 6$) indicates that the zero field terms are smaller than the microwave quantum, in this case 0.3 cm^{-1}. If the D value is small, then the width of the resonance should be indicative of the magnitude of the zero field splitting. The line width of 130 gauss corresponds to zero field terms of approximately 0.01 cm^{-1}. It is entirely possible that the zero field terms lie between this value and 0.3 cm^{-1}, and that the resulting spectrum is due to the $M_s = \pm 1/2$ transition while the other transitions are too broad to be seen.

The final spectrum, Fig. 20, is of a frozen 10 F $HClO_4$ solution containing 0.01 F $Fe(ClO_4)_3$. Variation of ferric concentration and temperature left this spectrum unchanged. Once again there are lines centered at $g_{eff} = 4.3$ and $g_{eff} = 2$, but they are now much broader. The 207 gauss width of the line at $g_{eff} = 4.3$ gives a value for $|\lambda| = 0.28$ which is farther removed from the limit of 1/3 than we have found previously. The 334 gauss width of the line at $g_{eff} = 2$ is 2.5 times larger than was found for ferric chloride in $HClO_4$ of the same concentration. This suggests that the stresses in the glass should be approximately the same in both cases so that differences in line width are due to differences in the specific ferric complex present. This was the reason for the earlier statement that the $g_{eff} = 2$ line for ferric chloride in $HClO_4$ was not due to complexes without chloride ligands.

The shape of the spectrum is different from that observed in the chloride complexes and suggests that the zero field terms and the Zeeman interaction may be of the same magnitude. Particularly if there is some

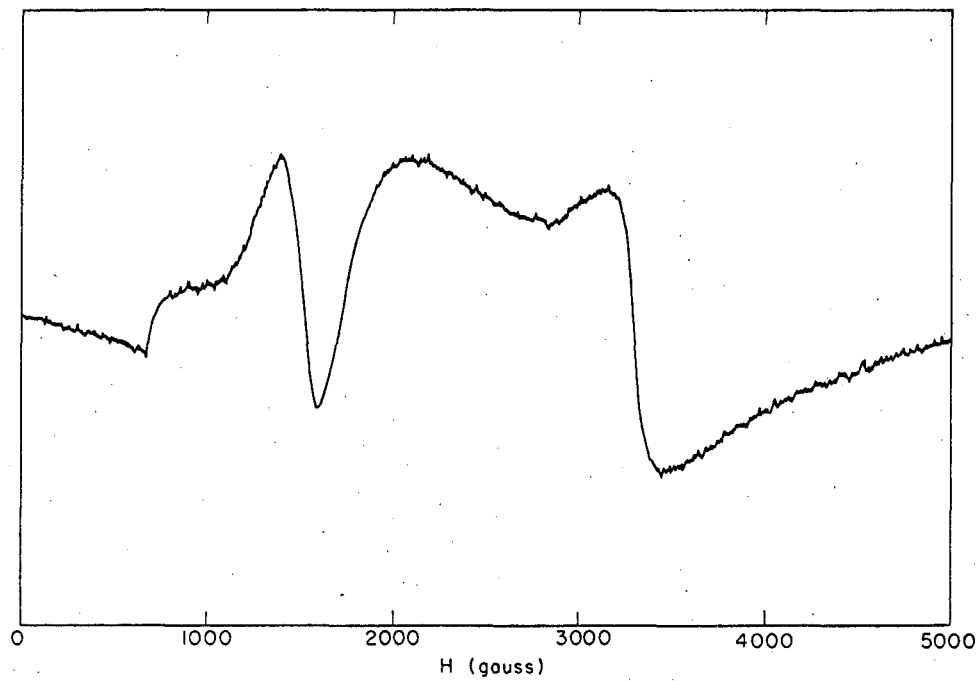

MU-36087

Fig. 20

uncertainty in the D value due to a distribution of distortions for various sites, such a broad sweep from $g_{eff} = 4.3$ to 2 could be expected. Spectra taken at different frequencies would help to resolve this situation. The site symmetry necessary for λ to be close to 1/3 could be provided by distorted water octahedra. It is also possible that there is some perchlorate complex formation,[51] perhaps of the type $Fe(H_2O)_2(ClO_4)_2^+$ type, which would give the line at $g_{eff} = 4.3$.

The S = 5/2 configuration for ferric ion offers a unique opportunity for using glass measurements to obtain information about symmetries and zero field terms in high spin complexes. In the present case, we have been able to identify the tetrachloroferrate ion in several solutions. In conjunction with low temperature studies and several frequencies, this method is capable of providing useful estimates of the signs and magnitudes of interactions in the spin Hamiltonian.

D. $Cr(H_2O)_6^{+3}$, $CrCl(H_2O)_5^{+2}$ and $CrCl_2(H_2O)_4^+$

Chromic ion in an axial field including hyperfine interaction has been used as an example by Low[4] for the development of the appropriate spin Hamiltonian. He gives the transitions expected and their complete angular dependence. Since we have observed no hyperfine structure in these experiments, the appropriate spin Hamiltonian is that used in the previous section, Eq. (26), but with S = 3/2. Once again we will use the representation in which the two variables for the zero field terms are D and λ.

For the case in which the zero field terms are small compared with the magnetic interfaction, the $\Delta M_s = 1$ transitions occur at $g_{eff} = g$ (approximately 1.94-1.99 for chromic ion) for the $M_s = \pm 1/2$ transition

and are symmetric about this point for the other two transitions. The band edges for these anisotropic transitions are found at $\pm 2D$ and at $\mp D(1-\lambda)$. There is also the "forbidden" $\Delta M_s = 3$ isotropic transition between the $M_s = \pm 3/2$ levels which would occur at $g_{eff} = 3g$ with an intensity increasing as $\lambda^2 D^2/(h\nu)^2$.

When D is the largest term in the Hamiltonian, one again starts by diagonalizing the zero field Hamiltonian and then adds the Zeeman interaction as a perturbation. This is analagous to the treatment for $S = 5/2$, but without the fortuitous occurrance of an isotropic transition for a particular value of λ. In zero field, the two doubly degenerate levels have energies of $\pm D\sqrt{1+3\lambda^2}$. Transitions between these two levels cannot be observed since D is assumed to be larger than the microwave quantum. It is possible, however, to observe transitions within each of these levels. Clearly the sign of D will make no difference in the positions of the resonances, but only in their intensities at low temperatures, so D will be taken as positive for the remainder of the discussion. Then for these levels, when the perturbation of the magnetic field is included in first order, one can calculate principal g_{eff} values as was done for ferric ion. The results are

		$\lambda=0$	$\lambda=1/3$
Upper level	g_z	3g	2.732g
	g_x	0	g
	g_y	0	0.732g
Lower level	g_z	g	0.732g
	g_x	2g	g
	g_y	2g	2.732g

where g is the isotropic g value for chromic ion and is in the range 1.94-1.99. For $\lambda = 0$ one would expect to see the onset of resonance around $g_{eff} = 6$ with increased absorption around $g_{eff} = 4$ and continuing to $g_{eff} = 2$. As the value for λ increases, the features of the spectrum could be expected to broaden. In the limit of $\lambda = 1/3$, the onset of resonance would be around $g_{eff} = 5.5$ and there would be no other prominent feature for the spectrum until the end of resonance at $g_{eff} = 1.4$. At no point would there be the convergence of g_{eff} values as in the case of ferric ion. The overall result would be that the sharpest spectrum would be for $\lambda = 0$, and even that spectrum will be spread from $g_{eff} = 6$ to $g_{eff} = 2$. In addition, chromic D values are known to be quite sensitive to stresses in crystals so that there may be a fairly large spread in the values for D and λ in a glass.

The spectrum of 0.003 F $Cr(H_2O)_6^{+3}$ in a concentrated perchloric acid glass is shown in Fig. 21. It is characterized by a sharp and fairly symmetric line at $g_{eff} = 1.97 \pm 0.03$ with a width of 54 ± 4 gauss. Spectra taken for chromic concentrations between 10^{-2} and 10^{-3} F were identical. There was significant variation in line width for the line at $g_{eff} = 2$ depending on the concentration of $HClO_4$. With the chromic ion concentration held constant at 10^{-3} F, the concentration of $HClO_4$ was varied from 10^{-3} to 5 F. The line width decreased from 250 gauss to 70 gauss when the acid concentration was increased from 10^{-3} to 1 F. Both 5 F and concentrated $HClO_4$ gave line width of about 55 gauss.

The sharpness of this spectrum and the lack of structure around $g_{eff} = 4$ indicate that we have a situation in which D is smaller than the microwave quantum as one might expect for the hexaaquo complex. Apparently the lower concentrations of $HClO_4$ allowed significant crystal

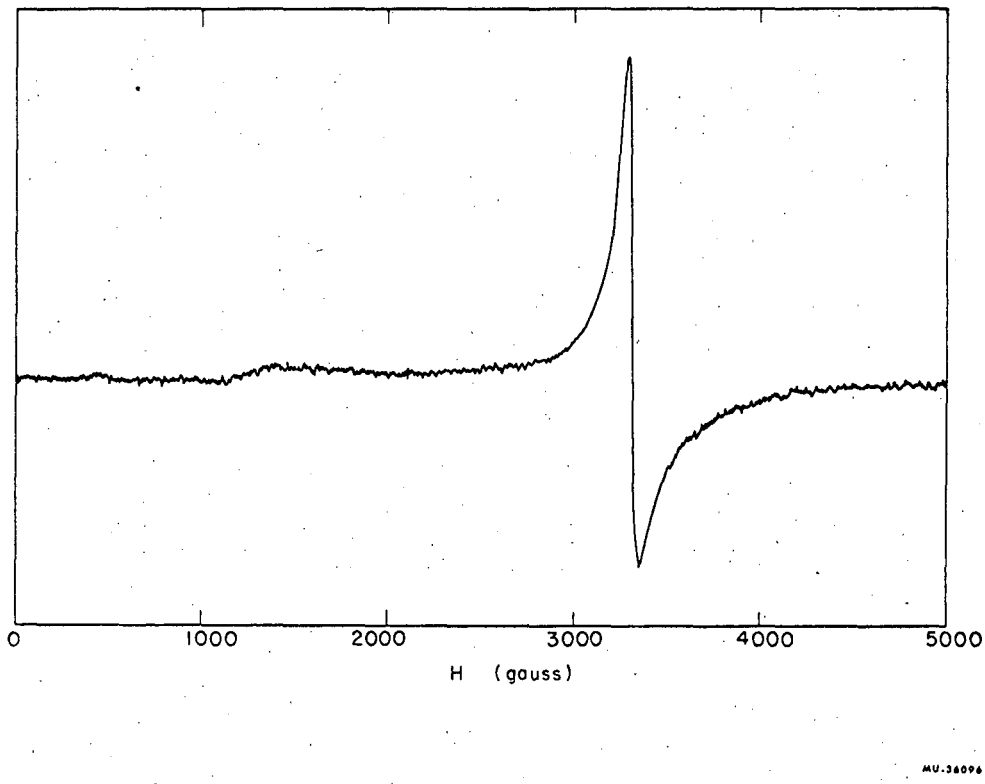

Fig. 21

formation with attendant stresses for the complex and a wider distribution of zero field splittings. Above several formal acid the spectrum changes little indicating that a better glass was formed.

The question still remains whether the line observed at $g_{eff} = 2$ is due to a superposition of all three $\Delta M_s = 1$ transitions or only the isotropic transition between the $M_s = \pm 1/2$ levels. If the line is due to the single isotropic transition, then the other two anisotropic transitions have been sufficiently broadened by stresses in the glass that their band edges cannot be seen. If this were so, one could expect the isotropic transition remaining to be insensitive to changes in the structure of the glass. This is not in accord with our observations. Assuming that the line at $g_{eff} = 2$ is composed of all three transitions, then the magnitude of D would be on the order of 10^{-3} cm^{-1} for the sharpest spectra. This can be compared with D values as low as 10^{-4} cm^{-1} for chromic ion in a cubic environment.[75] The poorer glasses would then have D values up to a factor of 10 larger, or around 10^{-2} cm^{-1}.

The spectrum of trans-$CrCl_2(H_2O)_4^+$ in a concentrated $HClO_4$ glass is shown in Fig. 22. The spectrum of the monochloro complex in a glass was identical with that in Fig. 22. The cis-dichloro complex gave spectra which differed from these only in the relative intensity of the two peaks and in the width of the peak at $g_{eff} = 2$. The spectra for all three complexes can be characterized by the onset of resonance at $g_{eff} = 6.0 \pm 0.1$ followed by a maximum at $g_{eff} = 4.3$ which gives way to almost a full derivative at $g_{eff} = 1.96 \pm 0.03$. For the monochloro and trans-dichloro complexes the width of the line at $g_{eff} = 1.96$ is 230 ± 30 gauss while the width of the same peak for the cis-dichloro complex is 410 gauss. The peak at $g_{eff} = 4.3$ has about 15% of the

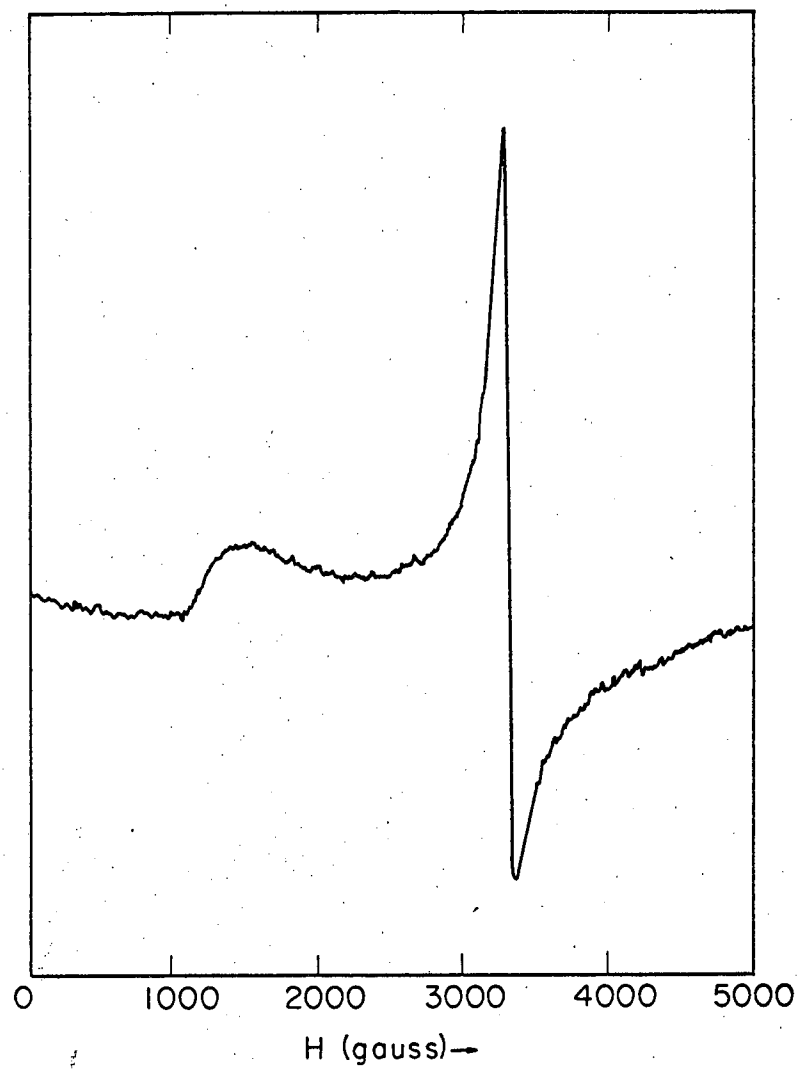

MU-36078

Fig. 22

amplitude of that at $g_{eff} = 1.96$ for the first two complexes, while for the cis complex the amplitude of the peak at $g_{eff} = 4.3$ is about 30%.

The positions and widths of the features in the spectrum are qualitatively what one would expect for complexes with a large D value. The two complexes with a four-fold axis of symmetry give spectra characteristic of a value for λ close to zero while the complex with only a two-fold axis and the possibility of a non-zero E value has a broader spectrum. The fact that the bulk of the intensity is in the line at $g_{eff} = 2$ rather than in the portion of the spectrum around $g_{eff} = 4$ is somewhat disturbing. By the arguments used for the case with $\lambda = 0$ in discussing the ferric spectra,[65] one might expect the opposite to be true. This apparent shift in intensity toward the $g_{eff} = 2$ region could be due to the zero field terms and the magnetic field interaction being of approximately the same magnitude. In that case the perturbation theory used in the two extreme cases is no longer accurate and the complete spin Hamiltonian must be diagonalized. Since in the high field approximation most of the intensity is centered around $g_{eff} = 2$ while the zero field approximation favors the $g_{eff} = 4$ region, it is reasonable that the observed spectra could be an intermediate case. That would place D in the approximate range of 0.1 to 0.5 cm^{-1} which is not unusually large for chromic complexes.[4,75]

It appears that glass spectra for chromic complexes will yield only very limited information. Semi-quantitative determinations of the size of the zero field terms are possible if several microwave frequencies are available. As far as the effects of complex symmetry on the spectrum are concerned, one can distinguish complexes of high symmetry, but not between complexes of lower symmetry.

ACKNOWLEDGEMENTS

I am indebted to Professor Rollie J. Myers for his helpful advice in this work and throughout my graduate career.

The many discussions with my colleagues and their technical assistance have been indispensable.

Particular thanks are due my wife for her continuing support and encouragement.

Fellowship aid from the National Science Foundation is gratefully acknowledged.

This research was supported by the United States Atomic Energy Commission through the Lawrence Radiation Laboratory.

REFERENCES

1. B. Bleaney, K. W. H. Stevens, Rept. Progr. Phys., 16, 108 (1953).
2. K. D. Bowers, J. Own, Rept. Progr. Phys., 18, 304 (1955).
3. J. W. Orton, Rept. Progr. Phys., 22, 204 (1959).
4. W. Low, Paramagnetic Resonance in Solids, Academic Press, New York, 1960.
5. G. E. Pake, Paramagnetic Resonance, W. A. Benjamin, New York, 1962.
6. C. P. Slichter, Principles of Magnetic Resonance, Harper and Row, New York, 1963.
7. S. A. Al'tshuler, B. M. Kozyrev, Electron Paramagnetic Resonance, Academic Press, New York, 1964.
8. J. S. Griffith, The Theory of Transition-Metal Ions, Cambridge Univ. Press, Cambridge, England 1961.
9. C. J. Ballhausen, Introduction to Ligand Field Theory, McGraw-Hill Book Co., New York, 1962.
10. A. Abragam, M. H. L. Pryce, Proc. Roy. Soc. (London), 206A, 173 (1951).
11. R. H. Sands, Phys. Rev., 99, 1222 (1955).
12. R. Neiman, D. Kivelson, J. Chem. Phys., 35, 149, 156, 162 (1961).
13. H. R. Gersmann, J. D. Swalen, J. Chem. Phys., 36, 3221 (1962).
14. Ph. Kottis, R. Lefebvre, J. Chem. Phys., 39, 393 (1963); 41, 379 (1964).
15. W. P. Griffith, J. Lewis, G. Wilkinson, J. Chem. Soc., 1959, 872.
16. I. Bernal, S. E. Harrison, J. Chem. Phys., 34, 102 (1961).
17. C. S. Naiman, J. Chem. Phys., 35, 1503 (1961).
18. H. B. Gray, C. J. Ballhausen, J. Chem. Phys., 36, 1151 (1962).
19. R. G. Hayes, "Electron Spin Resonance Line Widths of Transition Metal Ions and Complexes in Solution," Lawrence Radiation Laboratory Report UCRL-9873, September, 1961.

20. R. G. Hayes, J. Chem. Phys., 38, 2580 (1963).

21. I. Bernal, S. E. Harrison, J. Chem. Phys., 38, 2581 (1963).

22. S. I. Weissman, M. Cohn, J. Chem. Phys., 27, 1440 (1957).

23. A. G. MacDiarmid, N. F. Hall, J. Am. Chem. Soc., 76, 4222 (1954).

24. A. W. Adamson, J. P. Welker, W. B. Wright, J. Am. Chem. Soc., 73, 4786 (1951).

25. A. W. Adamson, J. P. Welker, M. Volpe, J. Am. Chem. Soc., 72, 4030 (1950).

26. R. G. Hayes, private communication.

27. J. B. Spencer, R. J. Myers, J. Am. Chem. Soc., 86, 522 (1964).

28. H. A. Kuska, M. T. Rogers, J. Chem. Phys., 40, 910 (1964).

29. A. Abragam, M. H. L. Pryce, Proce. Phys. Soc. (London), 63A, 409 (1950).

30. A. Abragam, M. H. L. Pryce, Proc. Roy. Soc. (London), 206A, 164 (1951).

31. B. Bleaney, R. P. Penrose, B. E. Plumpton, Proc. Roy. Soc. (London), 198A, 406 (1949).

32. B. Bleaney, K. D. Bowers, M. H. L. Pryce, Proc. Roy. Soc. (London), 228A, 166 (1955).

33. K. W. H. Stevens, Proc. Roy. Soc. (London), 219A, 542 (1953).

34. J. Owen, Proc. Roy. Soc. (London), 227A, 183 (1955).

35. A. H. Maki, B. R. McGarvey, J. Chem. Phys., 29, 31, 35 (1958).

36. J. Bjerrum, C. J. Ballhausen, C. K. Jorgensen, Acta Chem. Scand., 8, 1275 (1954).

37. O. G. Holmes, D. S. McClure, J. Chem. Phys., 26, 1686 (1957).

38. B. M. Kozyrev, Bull. Acad. Sci. USSR, English Transl., 21, 828 (1957).

39. S. A. Al'tshuler, K. A. Valiev, Soviet Phys. JETP, 35, 947 (1958); English Transl., 10, 661 (1959).

40. V. I. Avvakumov, Soviet Phys. JETP, 37, 1017 (1959); English Transl., 10, 723 (1960).

41. V. I. Avvakumov, N. S. Garif'yanov, B. M. Kozyrev, P. G. Fishkov, Soviet Phys. JETP, 37, 1564 (1959); English Transl., 10, 1110 (1960).

42. C. W. Merideth, "Temperature Dependence of Transverse Relaxation Time of Oxygen-17 in Aqueous Solutions Containing Cupric and Chromous Ions," Lawrence Radiation Laboratory Report, UCRL-11704, January, 1965.

43. E. Rabinowitch, W. H. Stockmayer, J. Am. Chem. Soc., 64, 335 (1942).

44. R. J. Myers, D. E. Metzler, E. H. Swift, J. Am. Chem. Soc., 72, 3767, 3772, 3776 (1950).

45. H. L. Friedman, J. Am. Chem. Soc., 74, 5 (1952).

46. G. A. Gamlen, D. O. Jordan, J. Chem. Soc., 1953, 1435.

47. G. W. Brady, M. B. Robin, J. Varimbi, Inorg. Chem., 3, 1168 (1964).

48. C. L. Standley, R. F. Kruh, J. Chem. Phys., 34, 1450 (1961).

49. H. Coll, R. V. Nauman, P. W. West, J. Am. Chem. Soc., 81, 1284 (1959).

50. R. N. Heistand, A. Clearfield, J. Am. Chem. Soc., 85, 2566 (1963).

51. J. Sutton, Nature, 169, 71 (1952).

52. B. Zaslow, R. E. Rundle, J. Phys. Chem., 61, 490 (1957).

53. N. S. Gill, J. Chem. Soc., 1961, 3512.

54. A. P. Ginsberg, M. B. Robin, Inorg. Chem., 2, 817 (1963).

55. R. J. H. Clark, T. M. Dunn, J. Chem. Soc., 1963, 1198.

56. W. E. Hatfield, R. C. Fay, C. E. Pfluger, T. S. Piper, J. Am. Chem. Soc., 85, 265 (1963).

57. B. Bleaney, R. S. Trenam, Proc. Roy. Soc. (London), 223A, 1 (1954).

58. E. Y. Wong, J. Chem. Phys., 32, 598 (1960).

59. E. G. Brock, D. Stirpe, E. I. Hormats, J. Chem. Phys., 37, 2735 (1962).

60. S. Geschwind, Phys. Rev., 121, 363 (1961).

61. J. Wakabayashi, J. Chem. Phys., 38, 1910 (1963).

62. H. S. Jarrett, J. Chem. Phys., 27, 1298 (1957).

63. J. E. Bennett, J. F. Gibson, D. J. E. Ingram, Proc. Roy. Soc. (London), 240A, 67 (1957).

64. J. S. Griffith, Proc. Roy. Soc. (London), 235A, 23 (1956).

65. T. Castner, G. S. Newell, W. C. Holton, C. P. Slichter, J. Chem. Phys., 32, 668 (1960).

66. H. H. Wickman, "Nuclear and Magnetic Resonance Studies in S-State Ions," Lawrence Radiation Laboratory Report, UCRL-11538, August 1964.

67. H. H. Wickman, M. P. Kline, D. A. Shirley, J. Chem. Phys., 42, 2113 (1965).

68. J. S. Griffith, Mol. Phys., 8, 213, 217 (1964).

69. M. Alei, Inorg. Chem., 3, 44 (1964).

70. H. Taube, H. Myers, J. Am. Chem. Soc., 76, 2103 (1954).

71. P. J. Elving, B. Zemel, J. Am. Chem. Soc., 79, 1281 (1957).

72. H. S. Gates, E. L. King, J. Am. Chem. Soc., 80, 5011 (1958).

73. E. L. King, S. M. J. M. Woods, H. S. Gates, J. Am. Chem. Soc., 80, 5015 (1958).

74. C. W. Merideth, W. D. Mathews, E. F. Orlemann, Inorg. Chem. 3, 320 (1964).

75. W. Low, Editor, Paramagnetic Resonance, Vols. I and II, Acadmic Press, New York, 1963.

76. B. R. McGarvey, J. Phys. Chem., 61, 1232 (1957).

77. B. M. Kozyrev, Bull. Acad. Sci. USSR, English Transl., 21, 828 (1957).

78. N. Edelstein, "A Study of the Kinetics of the Reaction H+ O_2 by Paramagnetic Resonance," Lawrence Radiation Laboratory Report, UCRL-10108, April 1962.

79. L. H. Brickwedde, J. Res. Nat. Bur. Std., 42, 309 (1949).

80. D. H. Levy, "The Electron Spin Resonance Spectra of Radical Anions in Liquid Ammonia," Lawrence Radiation Laboratory Report, UCRL-11864, January 1965, Appendix I.

81. H. B. Gray, I. Bernal, E. Billig, J. Am. Chem. Soc., 84, 3404 (1962).

82. P. T. Manoharan, W. C. Hamilton, Inorg. Chem., 2, 1043 (1963).

83. H. M. McConnell, J. Chem. Phys., 25, 709 (1956).

84. D. Kivelson, J. Chem. Phys., 33, 1094 (1960).

85. R. N. Rogers, G. E. Pake, J. Chem. Phys., 33, 1107 (1960).

86. D. R. Stranks, R. G. Wilkins, Chem. Revs., 57, 743 (1957).

87. D. R. Stranks, Modern Coordination Chemistry, J. Lewis and R. G. Wilkins, Eds., Interscience, New York, 1960. Chapter 2.

88. W. M. Latimer, Oxidation Potentials, Second edition, Prentice-Hall, New York, 1952. Pp. 106,129.

89. C. C. Addison, J. Lewis, Quart. Revs., 9, 115 (1955).

90. H. Abe, K. Ono, J. Phys. Soc. Japan, 11, 947 (1956).

91. E. H. Carlson, R. D. Spence, J. Chem. Phys., 24, 471 (1956).

92. Handbook of Chemistry and Physics, 36th. Ed., Chemical Rubber Publishing Co., Cleveland, 1954-5, p. 2002.

93. H. H. Glaeser, G. A. Lo, H. W. Dodgen, J. P. Hunt, Inorg. Chem., 4, 206 (1965).

94. A. F. Wells, Structural Inorganic Chemistry, 3rd. Ed., Clarendon Press, Oxford, 1962, p. 870-5.

95. L. Pauling, The Nature of the Chemical Bond, Cornell University Press, Ithaca, New York, 1948, p. 189.

96. W. L. Jolly, C. J. Hallada, "Liquid Ammonia," Lawrence Radiation Laboratory Report, UCRL-11254, February 1964, p. 9-10.

97. S. I. Sklyarenko, E. V. Smirnov, L. B. Belyaeva, E. A. Malysheva, Russ. J. Phys. Chem., 34, 921 (1960); English Transl. p. 435.

98. G. Pinevich, Kholodil. Tekh., 20, 30 (1948), reported in Chem. Abs. 43, 8813e (1949).

99. J. R. Heiks, M. K. Barnett, L. V. Jones, E. Orban, J. Phys. Chem., 58, 488 (1954).

100. H. S. Harned, B. B. Owen, The Physical Chemistry of Electrolyte Solutions, 3rd. Ed., Reinhold, New York, 1958, p. 713.

101. A. I. Rivkind, Russ. J. Phys. Chem., 35, 2099 (1961); English Transl. p. 1031.

102. R. R. Richards, N. W. Gregory, J. Phys. Chem., 69, 239 (1965).

103. L. A. Woodward, M. J. Taylor, J. Chem. Soc., 1960, 4473.

104. T. B. Swanson, V. W. Laurie, J. Phys. Chem., 69, 244 (1965).

FIGURE CAPTIONS

1. Solution spectrum of 10^{-2} F $Cr(CN)_5NO^{-3}$ in H_2O.
2. Low field half of spectrum in Fig. 1 with x35 increase in gain.
3. Solution spectrum of $Cr(CN)_5NO^{-3}$ after partial exchange with $C^{13}N^-$.
4. Low field part of spectrum in Fig. 3 with x45 increase in gain.
5. Solution spectrum of $Cr(CN)_5NO^{-3}$ with 55% $C^{13}N^-$.
6. Low field part of solution spectrum of $Cr(CN)_5NO^{-3}$ after partial exchange with $C^{13}N^-$ in solution with added acid.
7. Glass spectrum of $Cr(CN)_5NO^{-3}$ in water-methanol.
8. Glass spectrum of $Cr(CN)_5NO^{-3}$ with 55% $C^{13}N^-$ in water-methanol.
9. Temperature dependence of rate constant for axial CN^- exchange with $Cr(CN)_5NO^{-3}$.
10. Temperature dependence of rate constant for equatorial CN^- exchange with $Cr(CN)_5NO^{-3}$.
11. Glass spectrum of 5.2×10^{-3} F $Cu(H_2O)_6^{+2}$ in 5.26 F $HClO_4$.
12. Solution spectrum of 5×10^{-2} F $Cu(D_2O)_6^{+2}$ in 96% D_2O at 0°C.
13. Glass spectrum of 5×10^{-2} F $Cu(NH_3)_6^{+2}$ in ammonia-THF at -190°C.
14. Solution spectrum of 3×10^{-2} F $Cu(NH_3)_6^{+2}$ in liquid ammonia at -83°C. Dots are for a Lorentzian and dashes for a Gaussian line shape.
15. Spectrum of 3×10^{-2} F $Cu(NH_3)_6^{+2}$ in frozen ammonia at -92°C.
16. Variation of corrected line width with temperature for cupric ion in aqueous solutions. Solid circles are for 0.1 F $Cu(H_2O)_6^{+2}$ in 0.1 F $HClO_4$. Squares are for 0.1 F $Cu(D_2O)_6^{+2}$ in 96% D_2O. Open circles are for 0.05 F $Cu(H_2O)_6^{+2}$ in 5.26 F $HClO_4$, the high field hyperfine component.
17. Variation of corrected line width with temperature for cupric ion

in liquid ammonia. Solid circles are for the high field hyperfine component. Open circles are for the low field hyperfine component. Squares are the difference between the two as explained in the text.

18. Glass spectrum of 1×10^{-2} F $FeCl_3 \cdot 6H_2O$ in 12 F HCl.
19. Glass spectrum of 5×10^{-2} F $FeCl_3 \cdot 6H_2O$ in 10 F $HClO_4$.
20. Glass spectrum of 1×10^{-2} F $Fe(ClO_4)_3 \cdot 6H_2O$ in 10 F $HClO_4$.
21. Glass spectrum of 3×10^{-3} F $Cr(ClO_4)_3 \cdot 6H_2O$ in 70% $HClO_4$.
22. Glass spectrum of 1×10^{-2} F trans-$CrCl_2(H_2O)_4^+$ in 70% $HClO_4$.